Title
Spatiotemporal Manipulation of Hindbrain Development and Cancer Induction in Live Zebrafish via Optical Tools

Author
Feng, Zhiping

Publication Date
2016

Peer reviewed|Thesis/dissertation

UNIVERSITY OF CALIFORNIA

Los Angeles

Spatiotemporal Manipulation of Hindbrain Development and Cancer Induction in Live Zebrafish via Optical Tools

A dissertation submitted in partial satisfaction of the
requirements for the degree Doctor of Philosophy
in Molecular, Cellular, and Integrative Physiology

by

Zhiping Feng

2016

ABSTRACT OF THE DISSERTATION

Spatiotemporal Manipulation of
Hindbrain Development and Cancer Induction
in Live Zebrafish via Optical Tools

by

Zhiping Feng

Doctor of Philosophy
in Molecular, Cellular, and Integrative Physiology
University of California, Los Angeles, 2016
Professor Shimon Weiss, Chair

Living organisms are made of cells that are capable of responding to external signals by modifying their internal state and subsequently their extracellular context. Understanding the spatio-temporal dynamics of these complex interaction networks in biological systems is the subject of a field known as systems biology. To investigate these interactions (a necessary step before understanding or modeling them), one needs to develop means to control or interfere spatially and temporally with these processes and to monitor their responses on a fast timescale and with single-cell resolution. Among all the great tools to precisely perturb the dynamics of biological networks, light activation has been witnessed as an extremely powerful, non-invasive methodology, providing an accurate control over biomolecules' activity at an unprecedented resolution. This dissertation exemplifies the advantages of using optical tools to investigate complex bioprocesses with studies in two different fields which are developmental biology and

cancer biology. In the first project, we show how photo-isomerization of the 13-cis retinoic acid to the trans-isomer (and vice versa) could be used in studying retinoic acid's role in hindbrain development during zebrafish embryogenesis. The second project employs photon uncaging to induce oncogenic expression, and models tumor evolution from single cells in the zebrafish. Developing and validating these tools in these two projects greatly facilities our understanding of several biological networks. Photo-isomerization of retinoic acid between all-trans and cis form helps illuminate retinoic acid's unique spatial distribution and function on hindbrain development in a developing zebrafish embryo. And this again clarifies the long-standing controversy of retinoic acid acting as a morphogen in patterning vertebrate embryo. Photo-uncaging of caged cyclofen proves to be a novel and powerful tool to non-invasively manipulate tumor-associated gene expression. The work shown here could shed new light on cancer initiation and growth, and provide new tools for target validation and testing of novel anti-cancer drugs.

The dissertation of Zhiping Feng is approved.

Nancy L. Wayne

Lily Wu

Alvaro Sagasti

Shimon Weiss, Committee Chair

University of California, Los Angeles

2016

This dissertation is dedicated to

My family for always supporting and believing in me with unconditional love;

To dear friends that were, are and will be shaping me;

and last but not least,

To this beautiful universe that I eternally admire to appreciate.

TABLE OF CONTENTS

LIST OF FIGURES

Chapter One

Chapter Two

Chapter Three

ACKNOWLEDGMENTS

Although it appears as prior pages, I begin lastly to write this section, still holding my breath in awe. I am indebted to so many great and brilliant people without whom I shall have not led myself here, and of course shall have not manifested this dissertation. In the very first place, I have to state my deep and sincere gratefulness to my advisors, Dr. Shimon Weiss and Dr. David Bensimon. They offered me with enormous, altruistic and invaluable mentorship, which has guided me through my PhD journey and their mentorship will indubitably presents as a permanent emblem of my future growth. Being the first and only one working with the live animal in Weiss lab has been quite a challenge, yet an honor. As my primary advisor, Shimon always shows his constant support, both academically and financially to carrying my work on. Shimon is so considerate and is the one who has been striving together with me through all the hardships. Having David as my co-advisor is an amazing gift. Although our conversations occur often times across continents, I could always feel David's enthusiasm and precious insight in improving the project and me as a whole.

I want to thank my other committee members, Dr. Alvaro Sagasti, Dr. Lily Wu and Dr. Nancy L. Wayne. I appreciate their help serving in my committee board and providing valuable advice and guidance along the way. In particular, Lily helped me a lot on qualification exam preparation; Alvaro offered many suggestions for my projects, especially at the beginning phase of the cancer project. Besides, Alvaro's kind introduction of other zebrafish labs has greatly expanded my networks in the community. Nancy provided a lot of critics, advice and discussions at several of my public presentations, and assisted a lot with polishing this dissertation. I must thank my other collaborators, Dr. Jullien Ludovic, Dr. Michel Volovitch, Dr. Sophie Vriz and Dr. Shuo Lin for their intellectual contribution and technical assistances. Thanks also goes to David Traver lab for kindly providing a ubi:cre-ert fish line.

I also have to state my deep gratefulness to the whole Weiss lab. The past six years have been extremely fun and fruitful. In particular, Dr. Yuval Ebenstein helped take me into the lab and supervised my research when I was still an exchange undergraduate student. Working with Yuval is one of my best memories of exploring science. I must also specially thank Dr. Jianqing(Jack) Li for his constant support and encouragement along the years. Thanks go to Dr. Jianmin Xu, Dr. Xavier Michalet, Dr. Gopal Iyer, Dr. Sarah Weitz, Dr. KyungWon Park, Dr. Eitan Lerner, Dr. Antonio Ingargiola, Dr. Soohong Kim, SangYoon Chung, Yazan Alhadid, Xiyu Yi, Yung Kuo, Robert Boutelle and Romy Yanagisawa for their kind support, helpful conversions and long-lasting friendship. I also would like to thank my three undergraduate students, Cong Han, Alex Aronson and Suzy Nam for their help and assistance on experiments. The Paris stay was so fruitful and memorable. I am grateful for the help from and collaboration with Dr. Lijun Xu, Dr. Bertrand Ducos, Dr. Deepak Sinha, Dr. Tal Markus and Weiting Zhang. Lin lab has served my second training station through the years. I greatly appreciate those helps of all kinds kindly provided by Dr. Haigen Huang, Dr. Chengjian (Jerry) Zhao, Dr. Hong Jiang, Dr. Yao Zu, Dr. Jason Ear and Haishan Zhao. Special thanks go out to Dr. Laurent Bentolila and Dr. Matthew J. Schibler for their training and assistance on confocal microscopic imaging. I definitely thank Linda Dong, the manager at UCLA fish core facility for her assistance with fish maintenance.

My warmest and heartfelt thanks must also go to my closest friends through my stay at UCLA. Ting Liu, Dr. Jie Li, Rui Li, Wenyuan Wang, Jason Chang and Yuchao (Jessica) Gu. The company and encouragement from these brilliant people make my foreign life so colorful and memorable. In particular, I genuinely thank Jessica for her patience in science, life and waiting for me. I am able to be a proud bruin largely because of the well-established UCLA Cross-discilinary Scholars in Science and Technology (CSST) program. I thank two of the program leaders, Dr. Ren Sun and Dr. Yibin Wang for their kind guidance and assistances in scientific research and from many other aspects. Lastly, I deeply appreciate UCLA Molecular, Cellular and Integrative Physiology Interdepartmental program that I am so honored to join. Hereby, I would also like to state my appreciation to Dr. James Tidball and Dr. Mark Frye for their tremendous efforts in founding and maintaining MCIP as one of the most prestigious doctoral programs in the world.

Chapter one includes a refined excerpt from the following published paper on which I am the first author.
Feng Z, Zhang W, Xu J, Gauron C, Ducos B, Vriz S, Volovitch M, Jullien L, Weiss S, Bensimon D. (2013) Optical control and study of biological processes at the single-cell level in a live organism. *Rep Prog Phys*. 76(7):072601

Chapter two includes the following publication to which I am a co-first author, and unpublished results and discussion on retinoic acid early sequestration. Xu L contributed to the developmental response data (Figure 4), *in situ* hybridization and RT-PCR data (Figure 6, 7, 8). Le Saux T contributed to the capillary electrophoresis analysis data (Figure 5). Sinha D helped with laser setup on local uncaging. Gauron C helped with Keada mRNA injection at one-cell stage.
Xu L*, **Feng Z***, Sinha D, Ducos B, Ebenstein Y, Tadmor AD, Gauron C, Le Saux T, Lin S, Weiss S, Vriz S, Jullien L, Bensimon D. (2012) Spatiotemporal manipulation of retinoic acid activity in zebrafish hindbrain development via photo-isomerization. *Development* 139(18): 3355-62 (***co-first author**)

All contents in chapter three are unpublished and have been summarized in a manuscript for journal publication.

Supporting funding for the work includes China Scholarship Council (CSC) Fellowship, Partner University Fund (PUF) grant between ENS and UCLA, Jennifer S. Buchwald Graduate Fellowship from UCLA Physiology department, Dean M. Willard Chair Fund in Chemistry and Dissertation Year Fellowship at UCLA.

VITA

EDUCATION:

University of California-Los Angeles, Los Angeles, CA Expected March 2016
PhD candidate in Molecular and Cellular Integrative Physiology
École Normale Supérieure, Paris, France September-December 2011
Visiting Scholar at Statistics Physics Laboratory, ENS
Nankai University, Tianjin, P.R. China June 2010
B.S. in Pharmacy

PUBLICATIONS:

1. **Feng Z** et al., Optical initiation of cancer from single cells in zebrafish. *In Manuscript*
2. **Feng Z**, Zhang W, Xu J, Gauron C, Ducos B, Vriz S, Volovitch M, Jullien L, Weiss S, Bensimon D. (2013) Optical control and study of biological processes at the single-cell level in a live organism. *Rep Prog Phys*. 76(7):072601
3. Xu L*, **Feng Z***, Sinha D, Ducos B, Ebenstein Y, Tadmor AD, Gauron C, Le Saux T, Lin S, Weiss S, Vriz S, Jullien L, Bensimon D. (2012) Spatiotemporal manipulation of retinoic acid activity in zebrafish hindbrain development via photo-isomerization. *Development* 139(18): 3355-62 (***co-first author**)
4. Zhu Y, **Feng Z**, Xu C, Niu M, Zhu H, Hua T (2009) Effect of alkaloids from *Magnolia Officinalis* on isolated guinea-pig tracheal smooth muscle, *Chinese Traditional and Herbal Drugs*.

CONFERENCES:

The 8th Annual Zebrafish Disease Models Conference
Boston, MA August 24-27, 2015
- Poster Presentation "*Optical Control of Tumor Initiation from Single Cells in Zebrafish*"

11th International Conference on Zebrafish Development and Genetics
Madison, WI. June 24-28, 2014
- Poster Presentation "*Optical Control of Tumor Initiation from Single Cells in Zebrafish*"
- Panelist on "*Plenary Session and Workshop for Undergraduate Researchers*"

EMBO-ICAM-PGG Conference on Single Cell Physiology
Paris, France July 23-28, 2012
- Poster Presentation "*Spatiotemporal manipulation of retinoic acid activity in zebrafish hindbrain development via photo-isomerization*"

MCIP Annual Retreat
Arcadia, CA February 11, 2012
- Oral Presentation "*Spatiotemporal manipulation of retinoic acid activity in zebrafish hindbrain development*"

UCLA-CSST Program Closing Reception

Los Angeles, CA September 4, 2009

- Selected Oral Presentation "*Study of retinoic acid pathway in hindbrain development by two-photon excitation*"

HONORS AND AWARDS:

UCLA Dissertation Year Fellowship (Los Angeles) 2015

Chinese-American Engineers and Scientists Association of Southern California (CESASC) Scholarship (Los Angeles) 2014

Chinese Scholarship Council Fellowship (Los Angeles & China) 2010-2014

Buchwald Fellowship in Physiology (Los Angeles) 2010

National Scholarship (Tianjin, China)……..……..……..2007

LEADERSHIP EXPERIENCE:

Co-founder and inaugural president, " UCLA Chinese-American Students and Scholars Seminar (UCLA-C3S http://www.uclac3s.org)" 2014-present

Publicity Chair, 2nd and 3rd Leadership, Excellence, Aspiration, and Platform (LEAP http://www.leapcareer.org) Career Development Forum. (Los Angeles, CA) 2013-2014

Co-founder, Chinese Peer Biomedical Seminar Club, UCLA 2011-2014

CHAPTER ONE:

INTRODUCTION TO OPTICAL CONTROL IN STUDYING BIOLOGICAL PROCESSES IN LIVE ORGANISMS.

1.1 ABSTRACT

Living organisms are made of cells that are capable of responding to external signals by modifying their internal state and subsequently their extracellular context. Revealing and understanding the spatio-temporal dynamics of these complex interaction networks is the subject of a field known as systems biology. To investigate these interactions (a necessary step before understanding or modeling them), one needs to develop means to control or interfere spatially and temporally with these processes and to monitor their responses on a fast timescale (< minute) and with single-cell resolution. Therefore, enormous efforts have been taken, in the past several decades, in developing such tools for precise spatio-temporal perturbations and observations. In this chapter, a non-exhaustive list of examples are described of exploring cellular interactions and developmental pathways that could benefit from these new approaches, especially recent techniques to photo-control the activity of biomolecules, which allow for local perturbations of physiological processes.

1.2 WHEN OPTICAL TOOLS MEET COMPLEX BIOLOGICAL SYSTEMS

In order to modulate regulation networks at play in cellular and physiological processes, one needs to understand who the players are, i.e. which molecules control which processes and how they might interact. Cells are essentially composed of DNA, RNA, proteins, lipids and sugars. DNA is a long linear double-helical hetero-polymer of deoxyribonucleotides containing the bases: Adenine, Guanine, Cytosine and Thymine (A, G, C, T) that serves as the repository of genetic information in the cell. RNAs are smaller mediating single chain heteropolymers of

ribonucleotides A, G, C and U (uridine-monophosphate) copied (transcribed) from the DNA template, exhibiting a defined 3D structure and used for a variety of purposes in the cell.

One of their important roles, as transient copies of genes (or messenger mRNA), is to serve as template for the synthesis of amino-acid chains (proteins) by ribosomes: each amino-acid corresponding to a definite codon (a sub-set of three specific bases) on the mRNA. In the ribosome complex comprising about 70 different proteins, ribosomal rRNA is the catalyst for the formation of proteins (translation) from the successive docking on the mRNA of a matching transfer tRNA (i.e. one displaying the appropriate anti-codon and loaded with the corresponding amino-acid). Non-coding RNAs (ncRNAs) are RNA molecules (some of them only a few tens of nucleotides long) that participate in the control of a great variety of cellular processes (transcription, translation, mRNA splicing, chromatin remodeling, etc.).

Proteins are hetero-polymers of (mostly) 20 different amino-acids displaying a specific 3D structure related to their function in the cell as structural, regulatory or catalytic (enzymatic) agents. Finally lipids are amphiphilic molecules composing the many membranes used by the cell as reaction compartments (such as in mitochondria, golgi, endosomes, outer membrane, etc.) and playing important roles as signaling molecules on their own. When discussing intra and inter-cellular regulation networks, one usually considers protein-mediated regulation, since much less is known on the mechanisms of regulation by ncRNA. In the context of the central dogma: DNA $\Rightarrow$ mRNA $\Rightarrow$ protein, protein regulation is assumed to intervene mainly in the first step (transcription) by controlling the level of expression of the corresponding gene. In conventional scenario, property dynamics of regulating protein such as concentration, degradation or

modification, such as phosphorylation and isomerization, are considered in interpreting bioprocess regulative networks. Protein production could generally explain many features of cellular regulation such as the existence of bistable states and lateral inhibition between neighboring cells, a recurrent motif in many developmental pathways[1]. However, for many networks investigated experimentally as well as obtained by *in silico* evolution studies[2], the function is often achieved not via the control of production but rather through the control of protein degradation and modification. Comprehensive understanding in complexity of biological regulatory networks would be greatly benefited from tools that can achieve physiological perturbation at high spatiotemporal level. Photon, given its ability of non-invasive penetration, high tunability at spatiotemporal level, has become an emerging powerful tool to perturb and study complicated biological systems. In my dissertation work (see following chapters), I demonstrate how the optical tools I have developed could be employed to understand important questions in these complicated biological networks. Specifically, two examples in my project, namely retinoic acid's signaling pathway in hindbrain patterning and cancer initiation are investigated, and therefore are listed here for discussion.

1.2.1 Illuminating retinoic acid's role in hindbrain patterning

The development of methods that allow interfering locally with the protein's interaction network may help shed new light on biological dynamical systems. These methods may have even greater relevance for the study (via local perturbations) of the developmental networks involving diffusible molecules, or known as morphogens. Ever since the pioneering work of A.Turing[3], it has been known that patterns can be generated by the interaction between morphogens. However it has been difficult to test the validity of these models, in particular because of the lack of means

to perturb the morphogen fields. For example in the famed "French Flag model" [4], the differentiation state of cells along a morphogen gradient is supposed to be triggered by the local morphogen concentration: differentiation into a "blue" state occurring at a high concentration of morphogen, into a "white" state at a lower concentration, while the "red" state is the default (in absence of morphogen, Fig. 1). Lacking a means to locally perturb the supposed gradient of morphogen it has been difficult to test the validity of this model in various developmental situations.

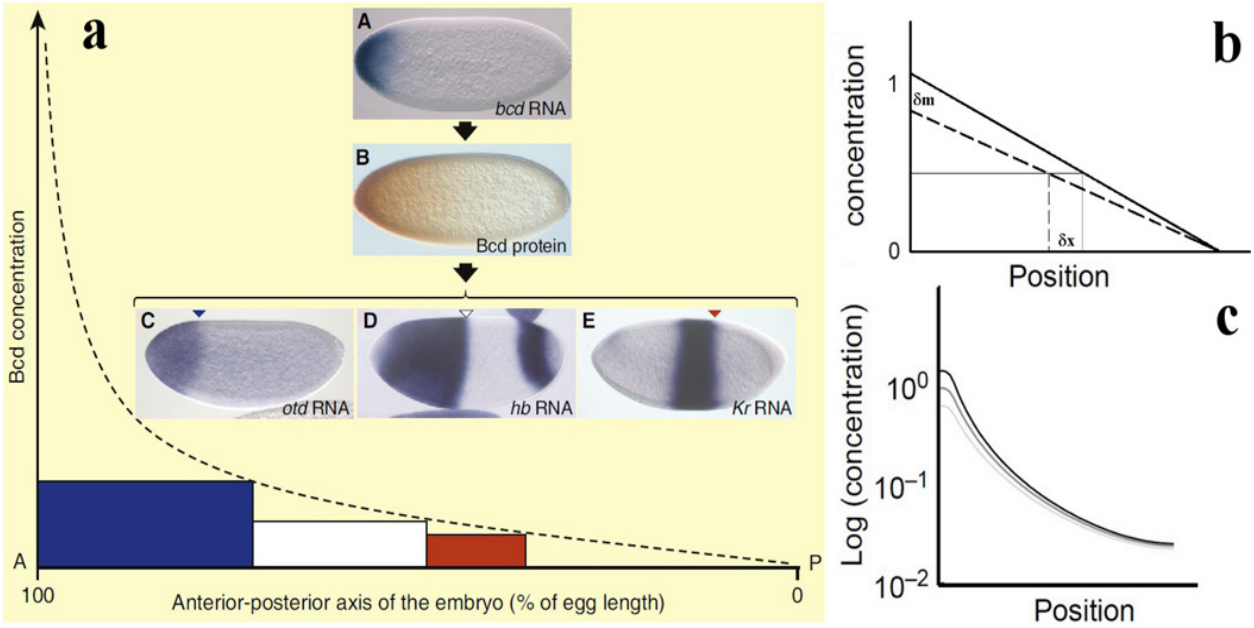

Figure 1. French-flag model explains gene expression network. (a) The French-flag model as a possible explanation of the action of Bicoid (a morphogen) on differentiation in the fly embryo: genes such as orthodenticle (otd), hunchback (hb) and Kruppel (Kr) are expressed in well and robustly determined regions of the fly embryo, ¨ which may be defined by the local bicoid concentration, reproduced from [5], Copyright 2010, with permission from Elsevier. (b) A linear concentration gradient does not yield robustly defined boundaries between domains of gene expression. (c) Uniform but non-linear degradation of a morphogen diffusing from a single point source does yield a robust gradient (independent of the boundary condition), reproduced from [6], Copyright 2003, with permission from Elsevier.

There are many more developmental issues that are still very much open problems and for which both detailed models and the investigation of the response to local perturbations with the tools described below could yield much needed information. In my project, I employ one of these optical tools to reveal the role of a controversial morphogen, retinoic acid in hindbrain patterning during early embryogenesis (see chapter two).

Retinoic acid is an important retinol derivative that regulates various intercellular signaling pathways [7]. In particular, retinoic acid plays a crucial role in early embryonic development, ensuring normal embryogenesis in a wide range of species [8-10]. Both excess and deficiency of retinoic acid during embryogenesis result in severe teratogenic phenotypes. Although retinoic acid has been found extremely indispensible in embryogenesis along the past decades, the question of how exactly retinoic acid organizes such complicated regulatory networks has not been fully answered. Especially, retinoic acid has been considered as a morphogen by some researchers, but doubts stay [11-13]. In addition, the unique spatial-temporal distribution of retinoic acid during embryogenesis has been extensively documented. However, most of the observations [14-16] rely on the activities of enzymes that synthesize or degrade retinoic acid, which consequently do not directly measure or perturb the molecule itself. Retinoic acid's tiny existence in live organisms as well as its simple chemical structure holds challenging barriers to standard biological probes. Some researches have tried perturbing retinoic acid *in vivo* by implanting retinoic acid beads into the tissues [17, 18]. While this approach does allow one to spatially manipulate retinoic acid's distribution in a live organism, it is not able to quantitatively control the release of the molecule. In face of these challenges and the photosensitive nature of retinoic acid isoforms, we come up with an optical technique that enables quantitative

perturbation of retinoic acid's activity at a high temporal-spatial level in the live zebrafish embryos (see chapter two). This novel approach provides a more reliable tool to delineate retinoic acid's morphogenic role in hindbrain development, and could be used in investigating many other signaling pathways involving retinoic acid in live organisms.

1.2.2 Cancer initiation under light

Cancer, also known as malignant neoplasm, is widely considered a genetic disease. Genetic and epigenetic mutations of proto-oncogenes, tumor suppressor genes and genes involved in DNA repair, in many cases, are able to alter a cell's biological capabilities, causing a cell to be cancerous. Those alternations make cancer cells to carry abnormal traits including sustaining proliferative signaling, resisting cell death, avoiding immune destruction and so on [19]. Most current cancer therapies are designed on the basis of our recognition of these hallmarks in a cancer cell. However, our understanding of cancer is mostly, if not completely based on investigations with cancer cells that have become already clinically evident. A long-standing and fundamental question in cancer biology asks that how exactly a normal somatic cell could turn itself into a cancer cell. Even it has been found that oncogenic mutations could cause cancer in some cases, no clear answers explain why those mutations fail to induce cancer in many other cases. In the cancer origin model [20] first proposed by Nowell in 1976, cancer is believed to be a process of repetitive clonal selection and expansion. An initial normal somatic cell gains sequential oncogenic mutations and becomes a cancer cell. Different cells in a cancer could then possess dramatically different genomic properties after serial clonal expansions. Although other cancer models such as the cancer stem model [21] have also been proposed and investigated in recent years, few research has been able to answer what key factors are involved to keep cells

from developing into cancer upon oncogenic shocks. Many theories believe some factors such as intercellular microenvironment and stem cell homeostasis [22, 23] play critical role in determining a cell's fate upon oncogenic mutations. Yet, few studies come up with solid evidence for this question by far. The knowledge of interpreting this mystery is the key to cancer prevention as well as to developing novel cancer therapies. In order to answer the question, one has to look into the origin of cancer, at the very early stage of cancer initiation.

The most common and widely used technique to examine how tumor cells act in cellular context is tumor xenograft [24], in which exogenous tumor cells are transplanted into certain tissues of a immune-deficient recipient. Although it has been shown as a quite useful and successful tool to study cancer, there are many profound drawbacks if one relies on this technique to study cancer initiation. First, in tumor xenograft, transplanted cells are exogenous and already cancerous, and have completely altered cellular properties. Second, tumor xenograft usually requires the receipt to carry immune deficiency to avoid rejection response. However, people diagnosed with cancer are rarely immune-deficient, or immune-suppressed, at least in the beginning phage. Lastly, cancer is generally believed to arise from a very limited number of cells, but it is extremely challenging to manipulate cancer development from only small number of transformed cells in tumor xenograft model. Another alternative invites the use of genetically engineered cancer models [25]. Transgenic models solve the problems of immune-deficient background and ensure tumorigenic progression develops in an unaltered, endogenous environment. Even so, one major concern still presents because most transgenic models are not able to manipulate particular cells at a small scale. Here in my dissertation (chapter three), I have developed a novel optical tool to solve all the above issues and have established an animal model for understanding cancer

initiation. I have demonstrated how the optical tool can be used to control the expression of a specific oncogene at high spatial and temporal level in live zebrafish embryos.

1.3 PHOTO-ACTIVABLE MOLECULES FOR THE CONTROL OF PHYSIOLOGICAL PROCESSES

The biological networks described above serve only two examples of various biological systems that need high spatiotemporal perturbation and therefore could benefit from investigations with novel optical tools. In the past years, different methods have been developed to study complex biological networks, such as the massively parallel analyses. These analytical tools, comprising 2D electrophoresis associated to mass spectrometry for the study of protein interaction networks, DNA chips for the study of mRNA expression patterns and next generation (shot-gun) DNA sequencing are powerful [26]. However, these only correlate biological states to instantaneous molecular compositions. Hence the picture that emerges from these methods is purely static. The topology of the network at the molecular level can be deduced from these high-throughput methods but not the reactive fluxes running through it. To get this dynamic information requires the use of non-invasive methods that are able to investigate *in vivo* the mechanisms and measure the rate constants associated to the network edges [27]. To obtain this dynamic information without perturbing the system, a first approach relies on recording and analyzing the fluctuations in fluorescence of a reporter molecule serving as a proxy for the fluctuations in concentration of a molecule labeled with the reporter. Thus Fluorescence Correlation Spectroscopy (FCS) [28, 29], which measures the fluctuations in fluorescence originating from a diffraction limited (focal) illumination volume has been applied to analyze various phenomena in living cells [30].

A second approach to address the mechanisms and rate constants of networks *in vivo* relies on the modulation or sudden variation of some control parameters followed by an analysis of the temporal response of the perturbed system. The most common parameters affecting chemical reactions are temperature, pressure, and concentrations [31]. Although the response to temperature jumps has been considered in view of the versatility of this parameter [32-35], the effects of temperature *in vivo* are pleiotropic which limits the interpretation of the results. Therefore the control of the concentration of some species is still the favorite method to perturb a living system and analyze the dynamics of its response. A first approach consists in altering the intracellular concentration of a biologically active compound by modifying its extracellular concentration or its flux. In particular this strategy has been successfully implemented by temporally modulating the external media of cells [36-38], and by incubating or feeding living organisms with the active molecule [39]. However, this approach has known limitations since the change in intracellular concentration will occur on a time-scale limited by the time required for the compound to be absorbed in the organism under study and to cross the membrane of cells. Pipettes and syringes are also rather intrusive means to affect the concentration of biomolecules and are associated to low spatio-temporal resolution. Activating the intracellular release of a desired compound from an inactive precursor has thus emerged as an attractive alternative to this approach.

1.3.1 Light activation

The use of UV-Visible (UV-Vis) light is the preferred non-invasive method to intra-cellularly release a bio-active molecule and thus perturb the associated network in living systems[40] even

though ultrasounds [41], X- [42]or gamma-rays [43] have also been proposed. Light is a biologically non-invasive trigger with a variety of desired features:

- its wavelength can be used to control its absorption by a precursor molecule leading to a variety of relevant photochemical reactions;
- light can be used to address single cells in a cell-culture but also single cells in a transparent tissue and an organism;
- light is notably appropriate for exciting fluorescent probes, which have gained wide acceptance as read-outs of the response of the system following its perturbation (see above).
- light is compatible with conventional and novel high-resolution microcopy methods (see above).
- finally, light actuation is compatible with new photonic methods readily available to biologists such as photoacoustic microscopy which have been recently developed to image well beyond the penetration limit of conventional microscopy [44, 45].

Photo-activation can be achieved upon one- or multi-photon absorption. In the case of the organic chromophores widely used in the present context, one-photon activation (typically at 365 nm) is associated with a significant absorption cross sections ($\sigma = 10^{-21} - 10^{-20}$ m^2/molecule are obtained for molar absorption ε in the 10^3-10^4 $M^{-1}cm^{-1}$ range), which allows for the use of readily available light sources for photo-activation. However, biological media significantly absorb and diffuse light in the UV-Vis range. Hence one-photon activation has been mostly restricted to transparent or thin biological samples. An alternative photo-activation approach relies on multi-photon infrared (IR) excitation [46]. Absorption cross sections are significantly

smaller than with one-photon excitation, which necessitates the use of pulsed IR laser sources. Despite this constraint, multi-photon excitation possesses significant advantages. In particular, in addition to the improved transparency of biological samples to IR light (which is less-damaging than UV-Vis light), it restricts the photo-activation to the focal point of the laser beam: the three-dimensional resolution thus achieved is higher than with one-photon excitation which activates all the molecules along the beam path.

Since the energies of photons in the UV-Vis wavelength range (~100 k_BT at 298 K) are comparable to the energies of intramolecular chemical bonds (~200 k_BT at 298 K), light absorption can considerably alter the molecular reactivity. Two different types of photo-induced reactions have been used to photo-activate biologically inactive precursors in order to pilot some biological functions (Fig. 2). In the first type (uncaging), the photon energy leads to the rupture of an internal bond in a precursor molecule, thus releasing the biologically active substrate. In the second type of reaction (photo-isomerization), the photon energy allows the precursor to change its shape by reorganizing its chemical bonds, which may alter its biological activity.

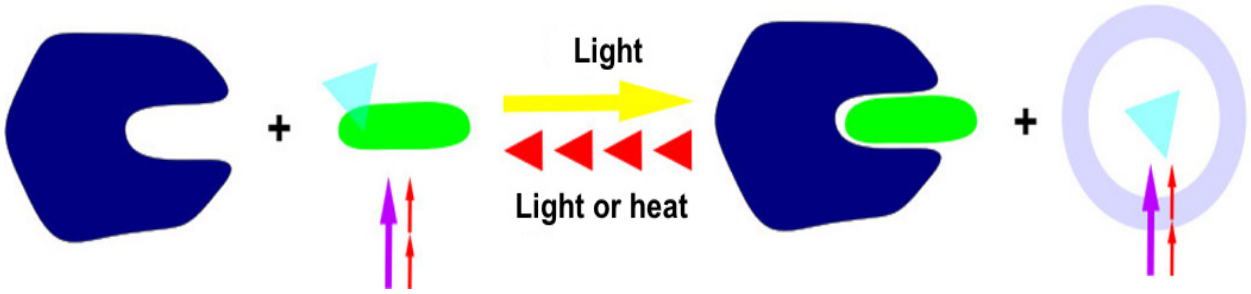

Figure 2. The main strategies for the control by light of some biological functions. Following activation with one- or two-photon excitation (arrows), the photo-activatable precursor (green shape) yields its biologically active state which interacts with the biological system (pictured as a deep blue shape). Depending on the type of light-induced reaction, that activation can be irreversible (e.g. in uncaging) or reversible (in the case of photo-isomerization). Upon uncaging, photo-activation may release a fluorescent co-product, which can be used to quantify the amount of photo-released substrate.

1.3.2 Light activation via uncaging

Caging groups are photolabile-protecting moieties that can be cleaved upon light absorption. They were originally introduced in the context of organic synthesis, where they are used to selectively regenerate functional groups temporarily protected in polyfunctional molecules, for example during photolitography of DNA chips [47, 48]. This selectivity and the non-invasive character of light are biologically attractive features. Caged molecules have been used to study the dynamics of several biological processes (e.g. neurotransmission) with high spatio-temporal resolution [49-52]. To be relevant in such experiments, the caging group must fulfill various photophysical and photochemical requirements (such as absence of biological effect due to the illumination only). In addition non-photophysical issues must be addressed such as access of the caged molecules to the biological targets (cellular permeability) and absence of any poisonous activity. This large number of engineering constraints has led to the introduction of new types of photolabile protecting groups. Present challenges in the field of caging groups concern:

- improving the uncaging action cross sections with one- and two-photon absorption;
- driving the uncaging reaction with absorption in the visible range [53, 54];
- quantifying the amount of uncaging (e.g. by means of fluorescence reporting) [55, 56];
- developing orthogonal photo-activation reactions for two different substrates using two wavelengths with one-photon [57, 58] and two-photon [59] excitation.

Various strategies can be used to control biological functions by means of a caging group [60]. The first approach relies on directly caging the biomolecule of interest (e.g. ATP, neuro-transmitters, etc.). Such a goal can be achieved by chemical derivatization (Fig. 3a). However this derivatization may lack selectivity towards highly polyfunctional biomolecules, such as proteins. In this case, this drawback can be overcome by relying on protein ligation, which allows for the selective introduction of non-native (photo-cleavable) segments in proteins (Fig. 3b) [61, 62]. However, it is then necessary to introduce this caged protein into the targeted cells. This invasive step relying on a permeabilizing agent such as a syringe, electroporation perturbs the system, often significantly. Consequently it weakens the use of this approach in a live organism and weakens the case of photo-activation as a non-invasive trigger.

An attractive alternative consists in designing caged precursors (e.g. non-natural caged amino-acids) and engineering cells/organisms that express the appropriate enzymatic machinery (the

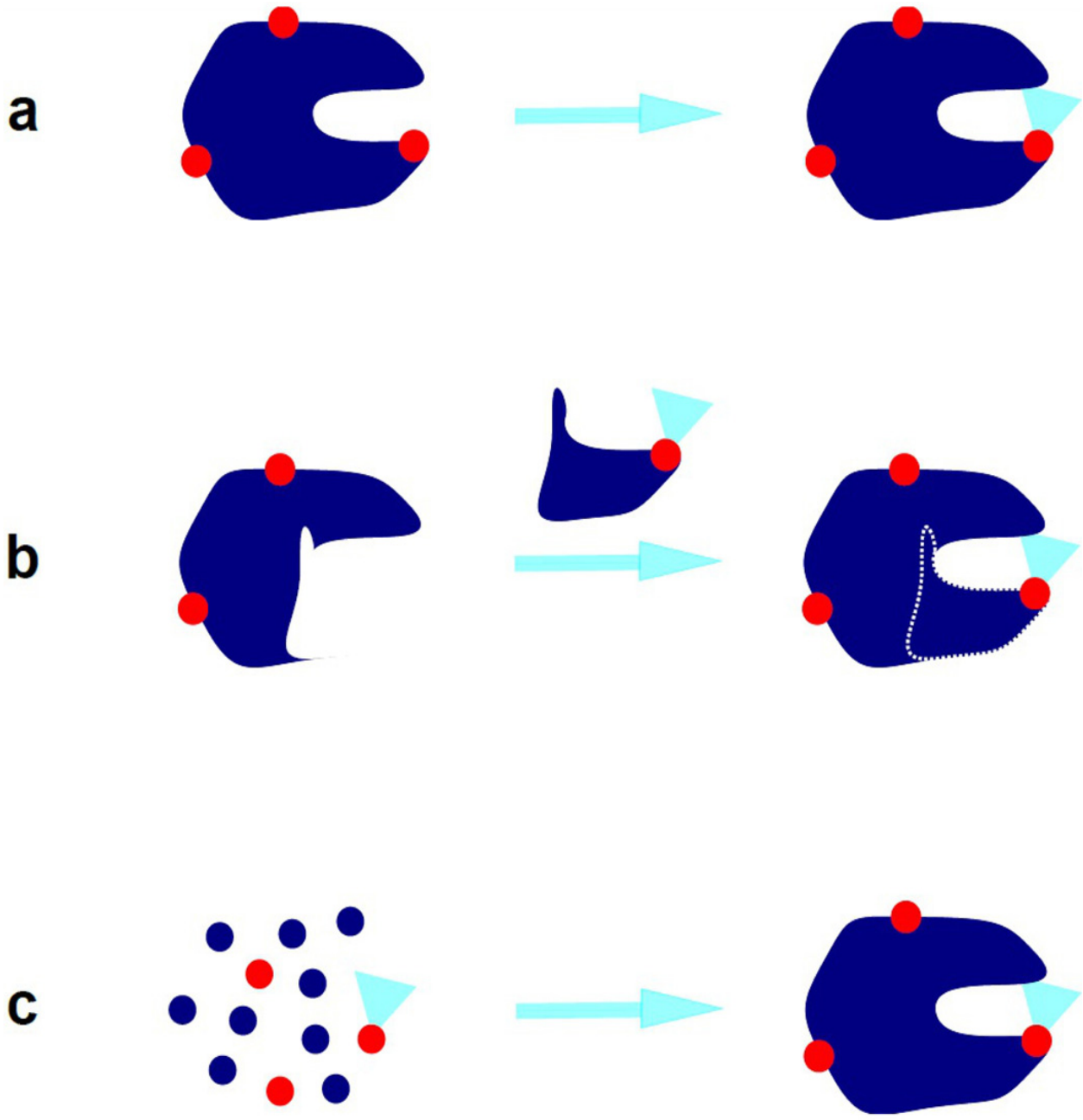

Figure 3. Strategies for caging biomolecules. (a) Direct derivatization: the caging group (blue triangle) has to selectively react with the targeted functional group (red disc); (b) protein ligation: the caging group (blue triangle) is first introduced in a chemically synthesized peptide at the targeted position (red disc). The latter is subsequently introduced within the protein of interest; (c) endogenous incorporation of caged amino-acids. Caged non-endogenous amino-acids are integrated within the protein of interest during its synthesis in living cells.

tRNA synthetase which links the caged precursor to its cognate tRNA). The ribosomal machinery can then integrate the caged precursors in proteins during their synthesis (Fig. 3c). This approach elegantly addresses both issues of selectivity and cell permeation, even though the introduction of a non-natural amino-acid (hitch-hiking on the tRNA machinery) affects the synthesis of all proteins in the cell. Nonetheless the method remains rather demanding and has been restricted so far to the synthesis of a few caged proteins in engineered cells [63-66].

The second approach relies on caging a small biomolecule (ATP, neurotransmitter, retinoic acid, etc.) such as to alter its biological activity. One should however note that it is not always possible to rationally design the position of the caging group on the biomolecule when structural information on the biomolecule's target site is lacking. This approach has however several advantages:

- selective caging is chemically easier for a "small" molecule than for a protein.
- small caged precursors are often sufficiently cell-permeable so that they simply diffuse into the intra-cellular environment where they can be subsequently photo-activated.
- in view of the large diversity of possible cellular effectors known to interact specifically with their target protein, various biological functions can be photo-controlled.

Thus both endogenous and exogenous substrates have been caged with the purpose of photocontrolling some enzymes [67] or the expression of some genes in cells as well as in living organisms [68-73]. And in chapter three, a very dexterous example of light uncaging has been demonstrated in studying cancer initiation in live zebrafish.

1.3.3 Light activation via photo-isomerization

Photochromism designates the property of a molecule or a material to change its absorption spectrum (typically by photo-isomerization) when submitted to an illumination. This property has found numerous applications in various fields (e.g. sunglasses or optical data storage) [74-77]. In contrast to the photo-cleavage of a covalent bond (uncaging), which is seldom encountered in endogenous biological systems, photo-isomerization is an extremely prevalent phenomenon in Biology. In particular it is responsible for controlling important light-driven processes such as conversion of light energy to chemical energy in bacteria or vision in vertebrates, which involve the retinal-containing opsin proteins [78] or light-driven regulations in microorganisms [79, 80]. Such photochromic platforms have been subsequently introduced in microbes engineered to control gene expression by light [81]. Photo-isomerization, in our hands, has also been used to control the activity of retinoic acid [82] (also see chapter two), whose trans-isoform is a morphogen crucial in the initial stages of development of vertebrates.

In neurophysiology, neuron photoactivation has been traditionally performed by means of caged compounds [83]. Photo-activable proteins, including channelrhodopsin-2 and halorhodopsin, have been recently expressed in neurons to enable photo-control of action potential firing. Alternatively synthetic small photochromic molecules have been implemented to photo-control native receptors [84] or the transport through ion channels. In that instance the photo-isomerization of small molecules covalently (or non-covalently) bound to the channel [85-87] was used to selectively block (or unblock) it leading to light-driven control of action potential firing and synaptic events. These developments have triggered the emergence of the new field of optogenetics, which uses light to control and study neuronal networks [88, 89].

1.4 OPTOGENETICS: LET THERE BE LIGHT

In 2009, Miesenböck defined the optogenetic field as a set of methods to manipulate (actuate) or record (sense) physiological processes at the cellular level [90]. These methods involve DNA-encoded light responsive proteins. They have been used extensively *ex vivo* (in cell cultures or in organ slices), and were recently transferred into live animals. The current methods of gene delivery (transient or permanent) only broadly restrict the spatial and temporal extent of experimental interventions (making use of specific regulatory devices, including photo-chemically inducible ones, see previous section). The use of light, sometimes combined with mosaic distribution of the affected cells, enables one to reach single-cell resolution. These new approaches allow one to revisit or directly address long-standing problems in the study of development, tissue homeostasis, neural network operation and signal integration among others.

1.4.1 Physiological Sensors

The translation of physiological signals into fluorescent ones benefits from the advantages of fluorescent proteins: high spatial and temporal resolution, very good sensitivity, versatility and spectroscopic modulation. An ideal fluorescent sensor should be non-toxic, highly specific, and sensitive with a high signal-to-noise ratio and allowing simple ratiometric image analysis. Sensor design relies on our current knowledge of the physiological traits to be monitored, and the spectroscopic properties of light-sensitive proteins, among which Fluorescent proteins (FPs) play a central role.

The growing number of natural and mutant forms of fluorescent proteins (FPs), including the prototypical Green Fluorescent Protein, GFP, offers a large range of colors and properties [91], and it is worth noting that FPs are largely insensitive to fusion with other polypeptides (except if these are specifically designed to this aim, see below). In addition, photo-activable, photo-switchable, and blinking FPs are now available. FPs have been developed to sense physiological processes using different strategies. In the most direct set-up, the signal directly comes from the FP, and information is drawn from changes in spectral properties (due for instance to sensitivity to the physico-chemical environment) or changes in sub-cellular localization (in the case of fusion proteins). Another possibility is to build permuted FPs (in which the N-terminal and C-terminal have been interchanged and connected by a short spacer), which can get back their original properties under specific physico-chemical constrains. The recorded signal may also arise from Fluorescence Resonance Energy Transfer (FRET), either intramolecular as in the Ca^{2+} sensor Cameleons [92], or intermolecular as successfully used to monitor kinase activity[93]. In recent years, proteins derived from 7-transmembrane rhodopsins have enlarged this optogenetic tool-box [94].

1.4.1.1 Direct fluorescence and translocation sensors Among the key questions recently addressed thanks to optogenetic tools, cell lineage is an issue that has attracted attention for more than a century: in a developing organism, where does a particular cell come from? Where is it going, and what will it become? In 2007, the groups of Litchman and Sanes devised a new strategy for the mosaic expression of multiple FP genes via combinatorial site-specific recombination. In classical set-ups, a site- specific recombinase can turn on the expression of an engineered gene by removing a stop cassette of DNA flanked by a pair of cognate recombination

sites. The new strategy, called Brainbow, took advantage of the discovery of variant recombination sites, allowing different and mutually exclusive outcomes in a series of FP genes with appropriately arranged pairs of recombination sites. With such a scheme, they were able to follow individual neurons in the mouse brain by means of stochastic marking of individual cells with 90 different colors in a single experiment [95]. This strategy was further expanded to fish [96], fly [97-99] and Arabidopsis [100]. Not only were cells identified, but individual axons in bundles, or closely packed synapses, could also be distinguished by this method. The same kind of multicolor clonal analysis was recently applied to shed light on the relative contribution of distinct precursor cell populations on heart morphogenesis [101].

Another important issue in life science concerns tissue homeostasis. Cellular proliferation and death are key cell behaviors to understand organ development or renewal, and failures in these processes are at the root of most diseases [102, 103]. Being able to monitor the progression of the cell cycle *in vivo* is a key to understanding its coordination with other aspects of cell behavior in many physiological processes. The group of Miyawaki first achieved this in 2008 [104]. Their sensor named Fucci (Fluorescent Ubiquitination-based Cell-Cycle Indicator) relies on the cell-cycle-dependent proteolysis of two oscillating proteins, Cdt1 and Geminin, to specifically mark the G1/S transition in living cells. By fusing red and green FPs to portions of Cdt1 and Geminin, respectively, this method colors up cell cycle progression. The nuclei of cells in G1 (and G0) phase appear red, those of cells in S/G2/M appear green and those during the transition G1 to S turn yellow, clearly marking cells that have initiated DNA replication. Since then, this sensor has been introduced in transgenic animals [105, 106] and allows studying cell cycle behavior *in vivo* in a wide range of processes (development, stem cell, tumor growth).

Apoptosis (or programmed cell death) is involved in tissue development and homeostasis. Failure of apoptosis is one of the main contributions to tumor development and autoimmune diseases. Apoptosis is a multi-step, multi-pathway program with a series of common effectors (caspases) corresponding to cysteine-dependent aspartate-specific proteases working in cascade [107]. Most of the apoptotic sensors exploit the caspase-3 protease activity on its specific cleavage sequence, to report either a direct fluorescence signal [108], a FRET signal [109] or a change in sub-cellular localization of the fluorescence signal [110].

Proper cell function and homeostasis requires the coordination of mRNA and protein synthesis with cell cycle progression. Major efforts have been made to improve the temporal and spatial resolution in order to allow for the visualization of the location of a given gene in the nucleus, the synthesis and trafficking of its mRNA in the cell and the production of the corresponding protein. Over the last 10 years, the laboratory of R.Singer has developed FP tools to monitor all these events in real time and in single cells (see [111] for review). This approach provided direct evidence for chromatin remodeling at the minute time scale and for cell-to-cell heterogeneity in a population [112]. This powerful approach has yet to be transferred in live animals

1.4.1.2 Environmentally sensitive chromophores The spectral properties of certain chromophores may be affected by their environment (e.g. pH). In such cases measuring the ratio of fluorescent emission/adsorption at two different wavelengths allows for the use of these chromophores as sensitive probes of their environment. Even though fluorescent proteins (FPs) can be sensitive to chloride [113, 114], metal ions [115] and redox potential [116, 117], one of their first and most common use is as pH-sensitive sensors. This use relies on the properties of

the natural GFP chromophore. Wild-type GFP normally exists as a mixed population of neutral phenols and anionic pheno-lates, with adsorption peaks at respectively 400 and 480nm [118, 119]. Since, the proportion of the anionic phenolate form increases upon a rise in pH, GFP can in principle be used to monitor pH changes in living cells. Extensive mutagenesis has further provided several optimized sensors for pH; amongst them pHluorin [120] has been used to study vesicular trafficking (exocytosis, endocytosis) during various physiological processes [121]. These measures are particularly interesting since the pH is a reliable gauge of a cell metabolic state and a good indicator of the different sub-cellular compartments.

1.4.1.3 FP modified with conformationally sensitive domain Another large group of sensors is based on fusion proteins including a domain prone to conformational change under the specific condition to be monitored, and a FP which chromophore properties will be modified as a result of this conformational change. Sensors to monitor Calcium ions (Ca^{2+}) will be detailed here, given its physiological significance.

Calcium ions impact nearly every aspect of cellular life [122]. In particular, an increase in Calcium is observed in excited neurons [123] and the measurement of Ca^{2+} can reflect action potential in neural cells. For these reasons Calcium sensors are the most investigated physiological sensors: over the past ten years more than ten different Calcium sensors have been proposed[124]. Each new one offers a better signal-to-noise ratio, a faster or easier measurement and an enhanced fluorescent brightness. Most of them rely on the conformational change of calmodulin upon Ca^{2+} fixation. Some sensors are based on FRET while others on the fluorescence of a circularly permutated EGFP (cpEGFP) [125]. This last one represents the newest family of Calcium sensors named G-CaMP. The cpEGFP has been linked to calmodulin

and a small domain of a myosin light chain kinase. In absence of calcium, the GFP barrel is open and its fluorescence quenched. The fixation of calcium on calmodulin induces a conformational change, allowing the barrel to close and the chromophore to fluoresce. These sensors have been successfully used as an indirect readout of electrical activity [126] and allow better understanding the setting up of spinal central pattern generator during development [127]. In conjunction with light-sheet illumination microscopy [128], these sensors have recently been used to monitor in real time the activity of thousands of neurons in a zebrafish brain [129, 130]

1.4.1.4 Opsin derived sensors Recently, a direct sensor for the visualization of action potentials has been developed [131]. This breakthrough in the study of the dynamics of complex neural circuits has been achieved thanks to the use of rhodopsin. Rhodopsins are a group of light-sensitive membrane-bound proteins that bind to retinal, which forms the chromophore. They are present in all kingdoms and transform light signal into an electrical signal. The group of Adam Cohen bet on the fact that the Archaerhodopsin 3 (Arch), which is a light-driven outward proton pump, could be run in reverse, i.e. that a membrane potential could modify its optical properties. This device works! Upon optimization by mutagenesis (mutation D95N) these authors have obtained a very efficient tool able to optically record action potentials [131] with a signal/noise similar to direct electrical recording and a $\sim$ 1 msec response time. They suggested that this first FP sensor based on opsin protein could open the way to other physiological sensors based on the large family of microbial opsin proteins.

1.4.2 Physiological actuators

The actuators transduce optical signals into physiological ones and thus make cellular function controllable with light. Until recently optogenetic actuators were mainly used in the field of neuroscience [132-134], partly due to the easy optical access to sliced organs, still an appropriate level of analysis. These tools are now available in freely moving animals, from worms and flies to mice. The first results where obtained with engineered neuronal receptors and channels either gated by photo-uncaged ligands, or controlled by cysteine-conjugated photo-switchable tethered ligands (SPARKS and LiGluR for instance, reviewed in [133]). However, these methods suffered from the requirement for the delivery of a synthetic chemical. The microbial opsin family (seen above in the context of sensors) corresponds to a very large group of proteins that opened a new landscape for optogenetic actuators [94]. Among these channelrhodopsins and halorhodopsins have been used as voltage actuators [94, 135]. Channelrhodopsin responding to blue light conducts cations and depolarizes neurons upon illumination, leading to neuron activation. Conversely, halorhodopsins conduct chloride ions into the cytoplasm upon yellow light illumination, leading to hyperpolarization and inhibition of neuronal activity [136]. Since the first use of these tools *in vivo* to control neuronal activity [135], significant efforts have gone into screening natural opsins and generating a variety of chimeric rhodopsin versions with different dynamical response and light sensitivity [94, 136]. In the last five years, freely moving animals in which the neuronal activity of specific cells is controllable by light has provided truly novel insights in our knowledge of neuronal connectivity and circuitry, cognition and behavior [137].

More recently, these tools have also been used in the field of developmental biology, allowing the precise mapping and control of the cardiac pacemaker [138-140] or the automated control of embryonic stem cell differentiation [141]. Furthermore, recent modifications of opsins via chimeric molecules (collectively termed optoXRs) allow to photo-control specific biochemical events such as Gs, Gq or Gi signaling [142, 143]. This opens a new era for optogenetics in biology.

CHAPTER TWO:

SPATIONTEMPORAL MANIPLATION OF RETIONIC ACID ACTIVITY IN ZEBRAFISH HINDBRAIN DEVELOPMENT VIA PHOTO-ISOMERIZATION

2.1 ABSTRACT

All-trans retinoic acid (RA) is a key player in many developmental pathways. Most methods used to study its effects in development involve continuous all-trans RA activation by incubation in a solution of all-trans RA or by implanting all-trans RA-soaked beads at desired locations in the embryo. Here we show that the UV-driven photo-isomerization of 13-cis RA to the trans-isomer (and vice versa) can be used to non-invasively and quantitatively control the concentration of all-trans RA in a developing embryo in time and space. This facilitates the global or local perturbation of developmental pathways with a pulse of all-trans RA of known concentration or its inactivation by UV illumination. In zebrafish embryos in which endogenous synthesis of all-trans RA is impaired, incubation for as little as 5 minutes in 1nM all-trans RA (a pulse) or 5nM 13-cis RA followed by 1-minute UV illumination is sufficient to rescue the development of the hindbrain if performed no later than bud stage. However, the rescue of hindbrain development is impaired if the embryo is illuminated (no later than bud stage) for 1 minute with UV light (to isomerize, i.e. deactivate, all-trans RA) subsequent to this all-trans RA pulse. This suggests that all-trans RA is sequestered in embryos that have been transiently exposed to it. Using 13-cis RA isomerization with UV light, we further show that local illumination at bud stage of the head region (but not the tail) is sufficient to rescue hindbrain formation in embryos whose all-trans RA synthetic pathway has been impaired.

2.2 INTRODUCTION

All-trans retinoic acid (RA) is a major player in early embryogenesis [144-146]. It has been shown to be required for the proper development of the anteroposterior axis [147], to be implicated in left-right asymmetry [148-150] and to act as a morphogen during hindbrain development [151] and somitogenesis [152, 153], as well as heart and appendage regeneration [154, 155]. All-trans RA and its 13-cis isomer have also been used in various cancer therapies [156, 157]. RA is synthesized [145] by retinaldehyde dehydrogenase (Raldh) from retinal, which is obtained from retinol (vitamin A). It exists in various isoforms. All-trans RA, the major active isomer, binds to the retinoic acid receptor (RAR). Another isomer, 9-cis RA, targets mainly the retinoic X receptor (RXR), which is capable of binding many other ligands, termed retinoids [145]. RAR and RXR form dimeric complexes that are capable of regulating the expression of hundreds of RA-responsive genes, some of them directly by binding to a regulatory element upstream of the gene. In developing embryos of zebrafish [158] and chicken [159], HPLC analysis has found evidence mostly for the trans-isomer. Other isomers, in particular 13-cis RA, have only been found in 10-day-old fish embryos.

Because of its involvement in so many developmental pathways, much effort has been devoted to control RA activity in developing embryos. The usual approach is to block endogenous RA synthesis and look for rescue of the investigated pathway when externally supplying all-trans RA. To impede RA synthesis, Raldh mutant lines or drugs (such as diethyl-aminobenzaldehyde, DEAB) that block Raldh can be used. To rescue normal development all-trans RA is usually dispensed continuously, either globally [160] by adding it at a known concentration to the

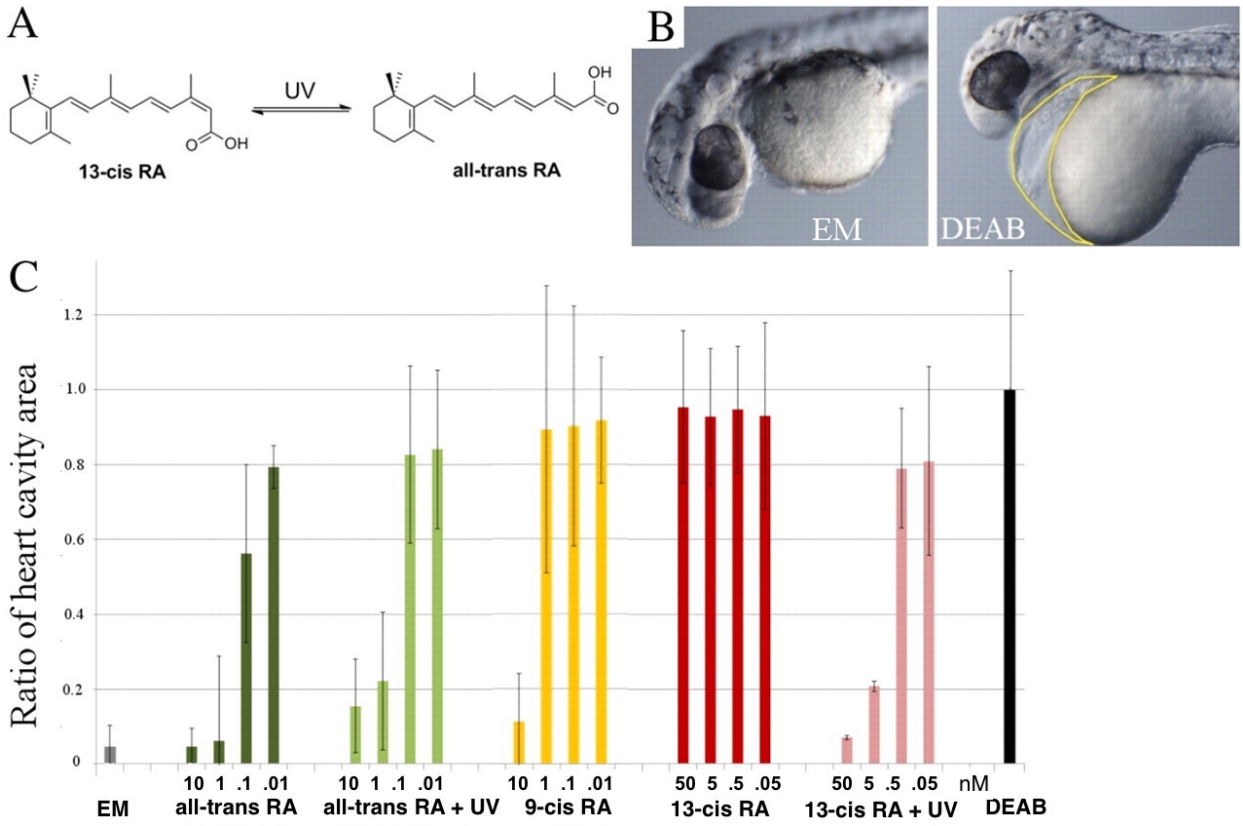

Figure 4. Developmental response to various concentrations of different RA isomers. (A) Isomerization reaction of 13-cis RA into all-trans RA (and vice versa). (B) Typical phenotype of a zebrafish embryo incubated in embryo medium (EM) and in DEAB. Note the enlarged heart cavity (area enclosed by yellow line). (C) Developmental response of embryos incubated in DEAB to transient (5-minute) incubation in various concentrations of all-trans RA, 9-cis RA and 13-cis RA, subjected or not to UV illumination and fixed in 4% paraformaldehyde at 33hpf. Since the heart cavity is enlarged in DEAB, we used the ratio of its transverse area (as enclosed by the yellow line in B) to the value in DEAB as a means to quantify the rescue (which is maximal when the ratio is minimal). Note that rescue of heart development requires ~1nM all-trans RA, 10nM 9-cis RA or 5nM 13-cis RA plus UV illumination (1 minute). No rescue is observed in up to 50nM 13-cis RA. The number of embryos used for each condition is ~20. Error bars indicate s.d.

embryo medium or locally through the implantation of beads soaked in all-trans RA [151], which generates an unknown gradient of RA. However, to better investigate these issues it is essential

to control the concentration, timing and location of all-trans RA, which is difficult using current techniques.

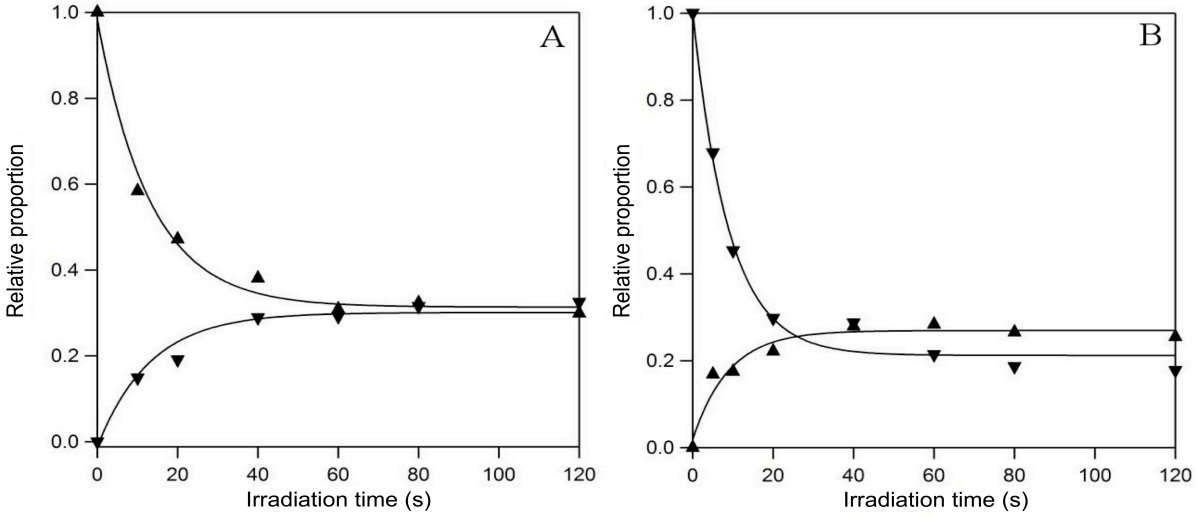

Figure 5. UV isomerization of all-trans RA to 13-cis RA and vice-versa. UV irradiation at 365nm of 25mM solutions of all-trans RA (A) and 13-cis RA (B) in acetonitrile:EM 1:1 (v/v) at 25°C. The photo-conversion extent extracted from the capillary electrophoresis electropherograms of the irradiated solution is plotted as a function of time. Up-pointing triangles, all-trans RA; down-pointing triangles, 13-cis RA; lines, exponential fits. Notice that illumination of an all-trans RA solution leads to an exponential decay of its concentration and the simultaneous formation of 13-cis RA within a characteristic time 13±2 s. Conversely, illumination of a 13-cis RA solution leads to an exponential decay of the concentration of 13-cis RA and increase of all-trans RA within a characteristic time 9±2 s. Beyond 50 s, the solution composition does not vary anymore on a 100 s timescale. In addition, it does not depend on the nature of the initial stereoisomers: all-trans RA and 13-cis RA coexist in similar relative proportions (0.25±0.05), the remaining initial amount being transformed in other RA stereoisomers [161].

To achieve local spatiotemporal control of all-trans RA activation, we have previously used photoactivation of caged all-trans RA [161]. However, owing to the poor water solubility of the caged compound, the concentration of the released all-trans RA is ill defined. Here we propose an alternative method to precisely control RA concentration, timing and location by UV illumination (at 365nm) and isomerization of 13-cis RA or all-trans RA. These stereoisomers exhibit widely different levels of biological activity [162]. Thus, illuminating the biologically

inactive 13-cis RA form generates at steady state ~20-25% of the biologically active all-trans RA (in addition to 30-35% 9-cis and 20-25% 13-cis RA stereoisomers [161]). Conversely, illumination of the active all-trans RA reduces its concentration by a factor of four to five. This approach for controlling all-trans RA (and 9-cis RA) concentration *in vivo* is non-invasive, simple, quantitative, precise in both space and time and reproducible.

Before investigating the developmental response to a local activation (or deactivation) of all-trans RA, it is important to verify that uniform global activation/deactivation at a given time of a controlled concentration of all-trans RA in an embryo is feasible and results in well-characterized perturbations to its development. An experiment in which an embryo at a given developmental stage is transiently exposed to all-trans RA (either directly or through photoactivation) differs in principle from the more common experiments in which an embryo is exposed beyond a certain stage to a constant concentration of all-trans RA. In the case of transient exposure, all-trans RA might diffuse out of the embryo and may therefore not necessarily affect its development.

We show here that in zebrafish embryos whose endogenous RA synthetic pathway has been blocked by DEAB, a global transient exposure (pulse) to 1 nM all-trans RA (either directly or via the isomerization of 13-cis RA) reproduces the previously characterized rescue of hindbrain formation (indicated by rhombomere 3 and 5 patterning) by continuous exposure to all-trans RA, suggesting that all-trans RA is sequestered in embryos that have been exposed to it. We show that isomerization of all-trans RA (if performed no later than bud stage) is enough to impair this rescue, suggesting that the critical window for hindbrain rescue by all-trans RA is at the end of gastrulation. We then use our approach to evaluate the concentration of endogenous all-trans RA

at a given developmental stage. Finally, we show that activation of all-trans RA at the end of gastrulation, via the photo-isomerization of 13-cis RA, in the precursor cells of the head rescues hindbrain development, but fails to rescue it if activated in the precursors of the tail region, implying that the concentration of all-trans RA can be controlled, and have its effect, locally.

2.3 MATERIALS AND METHODS

2.3.1 Fish lines and maintenance

Fish were raised and bred according to standard methods [163]. A transgenic line mp311+/+GFP was obtained from a large-scale enhancer trap screen (S.L., unpublished) using a Tol2 vector [164] containing a 249bp zebrafish gata2 minimal promoter [165] linked to a GFP reporter gene. *In situ* hybridization shows that the expression pattern and RA response of this transgene are similar to those of krox20 (see Fig. 6), a known marker of rhombomeres 3 and 5. Hence, in some experiments we used this transgenic line to observe and analyze the development of these rhombomeres. The embryos were incubated at 28°C. Developmental stages were determined as hours post-fertilization (hpf).

2.3.2 Whole-mount *in situ* hybridization and RT-qPCR

Single whole-mount *in situ* hybridization with digoxigenin-labeled riboprobes was performed at the 1- to 2-somite stage as described previously [166], and double *in situ* hybridization with fluorescein-labeled probes was as described [167]. Riboprobes (gift of P. Charnay, IBENS) were synthesized from template plasmids: krox20, hoxb1a [168] and vhnf1 [169]. Total RNA was extracted using Trizol (Invitrogen) and the RNeasy Mini Kit (Qiagen) at the 1- to 2-somite stage

from embryos incubated from sphere stage in 10 μM DEAB. Some of these embryos were also transiently incubated (5 minutes) at 90% epiboly in 1nM all-trans RA, 1nM or 5nM 13-cis RA and in some cases subsequently UV illuminated for 1 minute. cDNA was synthesized from these pools of total RNA (extracted from 30- 40 embryos) using the Superscript II Reverse Transcription System for RTqPCR (Invitrogen), and RT-qPCR was performed using these cDNAs with TaqMan Universal PCR Master Mix and TaqMan Gene Expression Assay: Dr03144482_m1(vhnf1) and Dr03124995_m1(hoxb1a) (Applied Biosystems). The difference (ΔCt) in the number of amplification cycles between these genes (in various conditions) and a reference gene (β-actin) was measured in triplicate PCR assays. The fold increase (f.i.) in expression with respect to incubation in DEAB (which inhibits the expression of vhnf1 and hoxb1a) was computed as: $f.i.=< 2^{\Delta Ct}/2^{\Delta Ct(DEAB)} >$ where the average is taken over five different experiments.

2.3.3 Drug treatments

Wild type and mp311+/+GFP embryos were incubated in 10 μM DEAB, 0.01-10nM all-trans RA, 0.01-10nM 9 cis-RA or 0.05-50nM 13 cis-RA (all Sigma-Aldrich; all from a 10mM stock in DMSO). Dilutions were made with embryo medium (EM), which was either Volvic water [170] or double-distilled water supplemented with 5mM NaCl, 0.17mM KCl, 0.33mM CaCl2, 0.33mM MgSO4. Incubations were carried out in 10 ml plastic Petri dishes. All-trans RA, 9 cis-RA and 13 cisRA treatments were carried out in the dark. Transient RA incubations were performed by transferring DEAB-incubated embryos into RA solution in EM for a set time (usually 5 minutes), followed by washing in EM and then back into DEAB solution. As controls, siblings were kept in EM.

2.3.4 UV illumination

2.3.4.1 UV isomerization

We used capillary electrophoresis (CE) to investigate the course of the photo-isomerization of all-trans RA into 13-cis RA and vice-versa under the UV illumination conditions used in our experiments on zebrafish embryos. Starting from a 25μM solution of a pure retinoic acid stereoisomer (either all-trans RA or 13-cis RA), we measured the concentrations of all-trans RA and 13-cis RA as a function of the illumination duration by integrating their corresponding CE peaks.

2.3.4.2 Global illumination with UV lamp

Global one-photon illumination experiments were performed at room temperature with a benchtop UV lamp (Fisher VL-6-L) at 365 nm. This lamp has a strong line at 365 nm accompanied by a Gaussian spectral dispersion around 350 nm with a 40 nm width at half maximum, delivering on the illuminated sample a typical photon flux [161] of ~4.3104 Einstein/($s \cdot m^2$). This UV lamp was placed on top of a Petri dish containing the embryos. We checked that, when illuminated for up to 4 minutes under such conditions, the embryos developed normally. To inactivate all-trans RA (by isomerization into cis-isomers) the embryos previously incubated transiently in all-trans RA were illuminated for 1 minute with the UV lamp. Similarly, to activate all-trans RA (by photo-isomerization of 13-cis RA) the embryos previously incubated in 13-cis RA were illuminated for 1 minute with the UV lamp. Following illumination, all embryos were incubated at 28°C in 10 μM DEAB solution.

2.3.4.3 Local illumination with UV laser

A 40 0.8 NA water-immersion objective (Olympus) was used to image the embryos on a CCD camera (Andor Luca) and locate the focal spot of the UV laser. For the UV illumination (375

nm, CW, from Crystal Laser) a beam of 1 mm diameter was coupled to the microscope without expansion. The incident UV power at the sample (~5 μW) was measured with a NOVA II power meter (Laser Measurement Instruments). For local 13-cis RA isomerization, embryos were kept in 10 μM DEAB from 4hpf, and were exposed to 5nM 13-cis RA for 5 minutes at the 75% epiboly stage. They were dechorionated and gently mounted in an array of agarose wells [171]. They were orientated properly as shown in Fig. 14A with extended length tips, and were then illuminated with the UV laser at the 80-90% epiboly stage for 20 seconds in selected regions of the gastrula that give rise to the anterior or posterior part of the embryo. To demonstrate the localization of the UV illumination, embryos were injected at the one-cell stage with mRNA encoding the photoactivatable protein Kaede (used as a label of photoactivation) and illuminated with the UV laser as described. Following UV photoactivation Kaede fluoresces in red, allowing identification of the illuminated regions at later developmental stages (see Fig.15).

2.3.5 Real-time GFP monitoring and data analysis

To monitor the development of rhombomeres 3 and 5 in different conditions, embryos under various treatments were dechorionated and gently mounted in an array of agarose wells [171]. All the embryos that orientated properly were imaged overnight at the Imaging Core Facility of the California NanoSystems Institute (CNSI) using a time-lapse confocal microscope (STED, Leica). To ensure proper development of the embryos, their temperature was kept at ~28°C with a heating mat. To measure the GFP intensity from rhombomeres 3 and 5, the fluorescence from all the stacks of confocal images was added together. The ratio of the rhombomere fluorescence was then calculated after background subtraction and intensity averaging.

2.3.6 Capillary electrophoresis analysis following RA isomerization

Electrophoretic measurements were performed with a PACE/MDQ (Beckman Coulter) capillary electrophoresis system [172]. Migrations were performed at 20 kV in bare fused silica capillaries (Polymicro, Phoenix, AZ, USA), 50μm internal diameter 50cm, filled with running buffer (30 mM $Na_2B_4O_7$ and 20mM α-cyclodextrin containing 10% acetonitrile) at 25°C. The analytes were detected by UV absorbance at 350nm. In view of the similarity of the absorption spectra of the two analyzed retinoic acids at that wavelength, we assimilated the corrected areas of the peaks to the amounts of the corresponding retinoic acids.

2.3.7 *In-vitro* fertilization

Sperms from male transgenic fish mp311+/+GFP were cryopreserved following procedures described as reported [173]. Sperms were properly stored in liquid nitrogen for long-term use. Before fertilization, female mp311+/+ GFP fish were set together with and chased by male counterparts for 10 minutes, and then anesthetized by 0.4% tricaine solution. Female fish were first carefully dried by softly wiping with tissue paper. Then unfertilized eggs of good quality were gently squeezed out from female belly onto a clean, dry 55mm×16mm petri dish (Sigma-Aldrich). For a short all-trans RA pulse before fertilization, 100uL 5nM all trans RA in 10uM DEAB with Hank's Balanced Salt Solution (HBSS, Thermo Fisher) was dropped onto around 300 eggs for two minutes. Eggs in the other group were instead immersed in 100uL 10uM DEAB with HBSS for two minutes. Meanwhile, sperm vials were taken out from liquid nitrogen and thawed briefly in 33°C water bath for 6 seconds. Thawed sperms were immediately injected and mixed with eggs. 750uL E3 fish medium was added to mix, and the mixture was left for 5 minutes before they were transferred into 100mm × 20mm petri dish filled up with 10uM DEAB,

and maintained at 28°C. After 30 minutes, fertilized eggs without pre-pulse of all-trans RA were incubated in 5nM all-trans RA for 2 minutes. After 3hours, infertile eggs in all groups were selected and discarded. Hindbrain developments were assessed by quantifying ratio of rhombomere 5 over rhombomere 3 the next day.

2.4 RESULTS

2.4.1 A transient exposure to RA rescues zebrafish development

It has been shown [160, 174] that zebrafish embryos incubated in 5-10μM DEAB, an inhibitor of Raldh, the enzyme responsible for all-trans RA synthesis, from 5hpf exhibit abnormal development affecting organs such as the anteroposterior axis, brain and heart. These severe phenotypes (Fig. 4B) can however be rescued with addition to the embryo medium before the end of gastrulation of 1-10nM all-trans RA [160, 174]. In order to test whether a short transient pulse of all-trans RA could also rescue the development of embryos incubated in DEAB, we investigated the rescue of zebrafish embryos incubated at 90% epiboly for 5 minutes in increasing external concentrations (0.01-50nM) of all-trans RA, 9-cis RA and 13-cis RA. To quantify the rescue we measured the area of the heart cavity that is expanded in the absence of RA (Fig. 4B) [153]. A normal heart cavity is indeed observed when embryos are transiently incubated in as little as 1nM all-trans RA (Fig. 4C). This rescue was also observed in embryos transiently incubated in 9-cis RA but required 10-fold higher concentrations and was not observed in 13-cis RA even at concentrations as high as 50nM. Hence, possible endogenous isomerization of cis-RA into all-trans RA is negligible at the developmental stages studied here. However, rescue was observed in the presence of 5nM 13-cis RA if the embryos were exposed

for 1 minute to UV light, thereby isomerizing 20-25% of 13-cis RA to all-trans RA (Fig. 4A; Fig. 5). When isomerizing with UV light we chose to tune the initial concentration of 13-cis RA rather than the illumination time to control the final concentration of all-trans RA. Indeed, the isomerization reaction proceeds quickly to photostationary state (~10 seconds) [161] (Fig. 5) and it is therefore more difficult to tune the final concentration via the illumination time.

2.4.2 Rescue of hindbrain development upon transient exposure to all-trans RA

The rescue of zebrafish development by all-trans RA has been particularly studied in the context of the hindbrain where its absence affects the development of the more posterior rhombomeres. We have studied quantitatively the effect of a short pulse of all-trans RA, either through a transient (5 minute) incubation in all-trans RA or via UV illumination of 13-cis RA, on the rescue of hindbrain development in embryos incubated in DEAB. We performed *in situ* hybridization against RA-responsive genes that are expressed in early development of the hindbrain [krox20 (egr2 – Zebrafish Information Network), vhnf1 (hnf1ba – Zebrafish Information Network), hoxb1a] and are known to differ in expression in DEAB-treated embryos versus normally developing controls [160]. A short pulse of 1nM all-trans RA given at 90% epiboly is sufficient to rescue the known normal expression pattern of these RA-responsive genes, as identified by *in situ* hybridization (Fig. 6, Fig. 7).

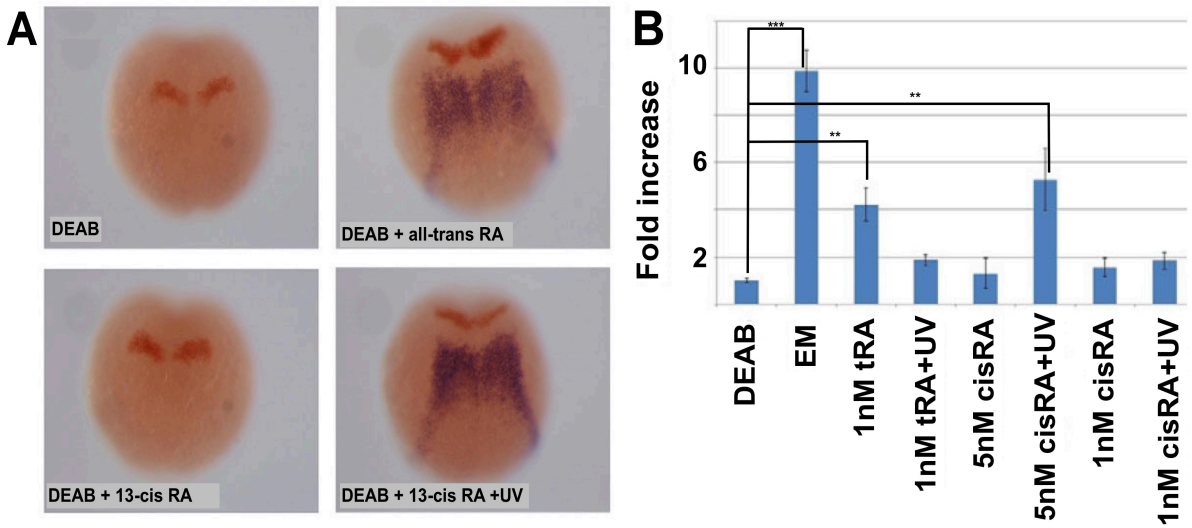

Figure 6. Response of vhnf1 to transient exposure to all-trans RA and 13-cis RA. Zebrafish embryos were incubated from sphere stage in 10 μM DEAB (except for the control incubated in embryo medium, EM), exposed at 90% epiboly for 5 minutes to various concentrations of all-trans RA (tRA) and 13-cis RA (cisRA) and UV illuminated (for 1 minute) or not. (A) *In situ* hybridization at the 1- to 2-somite stage for vhnf1 (blue) and krox20 (red) in embryos incubated in DEAB and 5nM 13-cis RA (no vhnf1 is visible) or DEAB plus 1nM all-trans RA and DEAB plus 5nM 13-cis RA plus 1-minute UV illumination (rescue of vhnf1 expression is visible). (B) Quantification of the expression of vhnf1 by RT-qPCR in various conditions. Note that the expression of vhnf1 in 1nM all-trans RA is similar to that in 5nM 13-cis RA plus UV. Also, the expression of vhnf1 is similar in 1nM all-trans RA plus UV and 1nM 13-cis RA plus UV, as expected because in both cases the concentration of all-trans RA after UV illumination is the same. Error bars indicate s.e.m. from five experiments (for each experiment, RT-qPCR for the various genes was performed in triplicate, ***$p<0.001$, ** $p<0.01$).

To better quantify this rescue we used RT-qPCR to estimate the change in expression levels of two RA-responsive genes, the expression of which is blocked in presence of DEAB: vhnf1 and hoxb1a. Partial quantitative (~50%) rescue of the expression levels of these genes was observed following a pulse of 1nM all-trans RA, either through transient incubation in all-trans RA or via transient incubation in 5nM 13-cis RA followed by UV illumination for 1 minute (Fig. 6, Fig. 7). Note that 1-minute UV illumination of 1nM all-trans RA or 1nM 13-cis RA yields similar, but

much reduced, rescue of these genes (~15%). This is to be expected because UV illumination of all-trans RA or 13-cis RA yields a similar final concentration of the active all-trans RA isomer, at ~20-25% of the initial concentration (Fig. 5) [161].

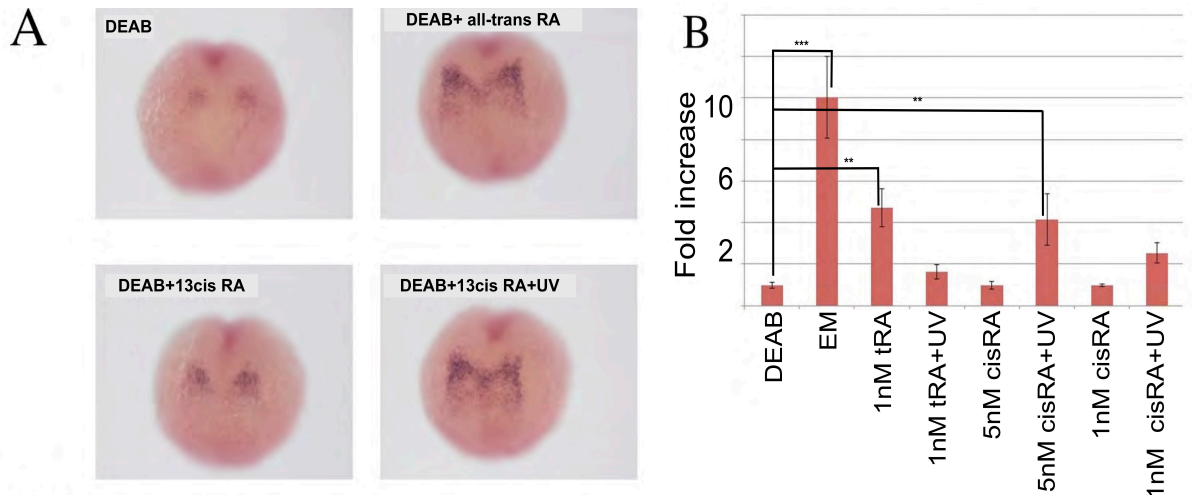

Figure 7. Response of hoxb1a to transient exposure to all-trans RA. Quantification of the response of hoxb1a to various transient exposures to all-trans RA (tRA) and 13-cis RA (cisRA). The embryos were incubated from sphere stage in 10mM DEAB (except for the control incubated in embryo medium, EM), exposed at 90% epiboly for 5 minutes to various concentrations of all-trans RA and 13-cis RA and UV illuminated (for 1 minute) or not. (A) *In situ* hybridization at the 1- to 2-somite stage against hoxb1a1 (blue) for embryos incubated in DEAB with or without 5nM 13-cis RA, DEAB + 1nM all-trans RA and DEAB + 5nM 13-cis RA + 1 minute UV illumination (rescue of hoxb1a expression is visible). (B) Quantification of the expression of hoxb1a by RT-qPCR in various conditions. Note that the expression of hoxb1a in 1nM all-trans RA is similar to the expression in 5nM 13-cis RA + UV. Note further that the expression of hoxb1a is similar in 1nM all-trans RA and 13-cis RA after UV illumination, as expected since in each case the concentration of all-trans RA after illumination is the same. Error bars are statistical errors on the mean from five experiments (each RT-qPCR assay was performed in triplicate, ***$p<0.001$, **$p<0.01$).

To further investigate the possible rescue of hindbrain development upon exposure to an all-trans RA pulse, we used a transgenic zebrafish line expressing GFP in rhombomere (r) 3 and r5 of the

hindbrain only (see Materials and methods). We first verified that the GFP response to all-trans RA in these embryos was similar to that of RA-responsive genes by performing *in situ* hybridization of GFP and krox20 (a known RA-responsive gene expressed in r3 and r5). The expression patterns of GFP and krox20 are similar whether the embryos are grown in normal conditions or incubated in DEAB (Fig. 8).

The advantage of this line is that one can monitor in living embryos the expression pattern of GFP and thus observe in real time the response of DEAB-treated embryos to pulses of all-trans RA. The rate of GFP fluorescence increase in r5 in embryos past the 6-somite stage varied in different conditions. It is maximal (similar to r3) in normal conditions (embryo medium), minimal in DEAB and rescued in embryos exposed to 5nM 13-cis RA and UV illuminated for 1 minute (Fig. 9A). To quantify the response to all-trans RA we have thus used the ratio (Rf) of GFP expression (fluorescence) in r5 versus r3 measured in 24hpf embryos. For normally developing embryos Rf=1.25±0.05, whereas for embryos incubated in DEAB Rf=0.25±0.05 (Fig. 9B). In agreement with our previous observations, transient exposure of the embryos at 90% epiboly to 1nM all-trans RA (or to 5nM 13- cis RA followed by 1-minute UV illumination) is enough to partially rescue the expression of genes in r5 (Rf=1.00±0.05).

2.4.3 Short exposure to all-trans RA before bud stage rescues hindbrain development

In the experiments described above the embryos were transiently exposed to all-trans RA at 90% epiboly, a stage that has been shown to be critical for proper rescue of the hindbrain [152, 174]. To test whether the timing of exposure was critical, we exposed embryos incubated in DEAB at various developmental stages for 5 minutes to 1nM all-trans RA. To quantify the rescue, we

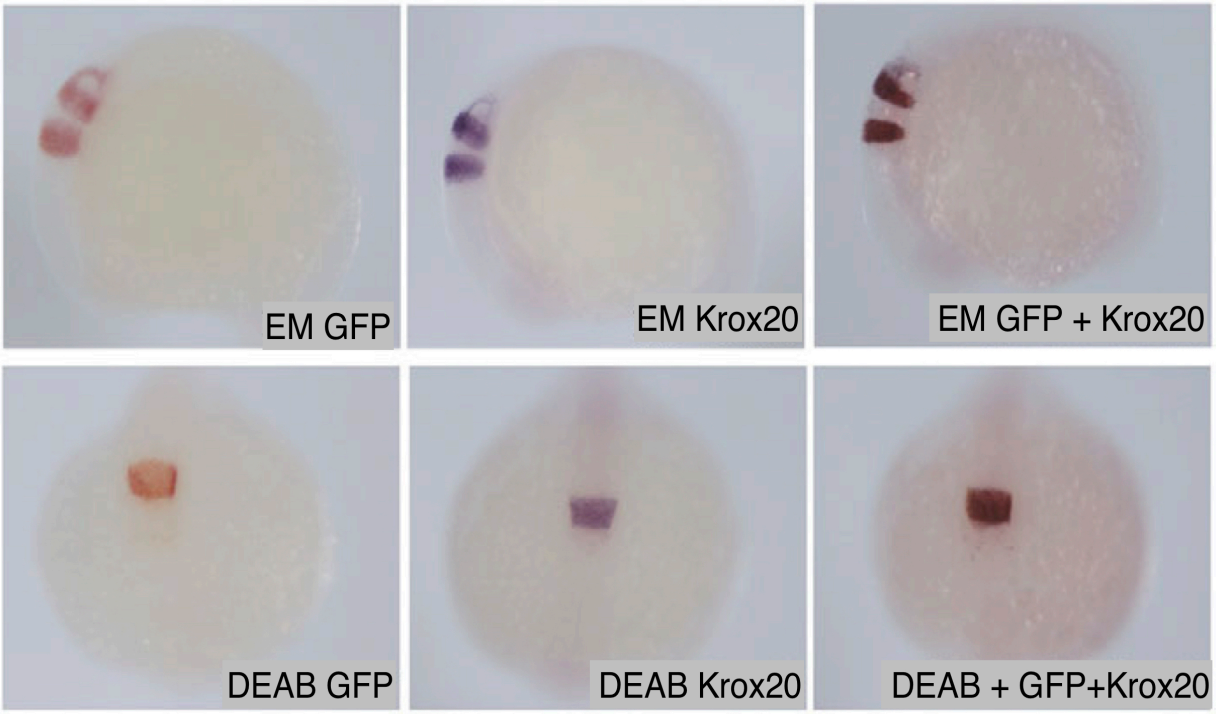

Figure 8. Response of the GFP transgenic embryos to DEAB and RA treatments. GFP expression in r3 and r5 in transgenic zebrafish embryos incubated in EM or 10μM DEAB (from sphere stage). (Top row) *In situ* hybridization of embryos grown in EM at the 12- to 14-somite stage for GFP (red), krox20 (a known marker of r3 and r5, blue) and both GFP and krox20. Side view. (Bottom row) *In situ* hybridization of embryos grown in DEAB for GFP, krox20 and both GFP and krox20. Dorsal view. GFP expression reproduces the response of krox20. Since GFP allows the monitoring of live embryos, we have used it to quantify their response to all-trans RA.

measured Rf at 24hpf. Although rescue is maximal at 90% epiboly, partial rescue is also observed in embryos incubated for 5 minutes in all-trans RA as early as sphere stage (Rf1), but not in embryos transiently exposed to all-trans RA at 3 somites (Rf0.2) (Fig. 10). Surprisingly, the length of exposure to all-trans RA does not seem to affect the rescue. Embryos incubated at sphere stage in 0.2nM all-trans RA for 5, 10, 25 and 40 minutes exhibited similar levels of GFP rescue (Rf0.55) (Fig. 11). This suggests that rapid equilibrium is achieved with the external

concentration of all-trans RA. Notice, however, that after exposure RA is retained for hours, even though the embryos are incubated in a DEAB solution lacking any RA.

2.4.5 Short UV illumination of all-trans RA prevents rescue of hindbrain development

The previous experiments implied that although all-trans RA can rapidly enter the embryo, it does not diffuse out, suggesting that all-trans RA might be sequestered until required for proper development at later stages. Since UV illumination can partially isomerize all-trans RA to its inactive cis-isomers, we tested this hypothesis by attempting to hinder hindbrain rescue by illuminating for 1 minute with UV light a DEAB-treated embryo transiently exposed at sphere stage to 1nM all-trans RA, thereby photoisomerizing at different (later) stages ~75-80% of the stored all-trans RA. As surmised if photo-isomerization is performed no later than bud stage, rescue of r5 is incomplete (Rf0.5) and corresponds to the level observed when all-trans RA is isomerized immediately after incubation at sphere stage (Fig. 12). However, if photo-isomerization is attempted at the 3-somite stage, r5 is rescued as it would in the absence of UV illumination (i.e. in the presence of 1nM all-trans RA; Rf=0.85±0.05). These observations were validated (data not shown) by *in situ* hybridization of genes (krox20, vhnf1) known to be involved in early hindbrain development [160, 174].

We have furthermore used our approach to estimate the concentration of all-trans RA at a given developmental stage: 75% epiboly. We compared the rescue of r5 when an embryo is transferred into a DEAB solution at 75% epiboly (with and without subsequent UV illumination) with that of an embryo incubated from an early stage (blastula) in DEAB and exposed at 75% epiboly to a pulse of all-trans RA of various concentrations. From this comparison (Fig. 13), we deduced that

the concentration of all-trans RA in the embryo at 75% epiboly is ~0.05nM. These results demonstrate that quantitative control of all-trans RA concentration and activity can be achieved

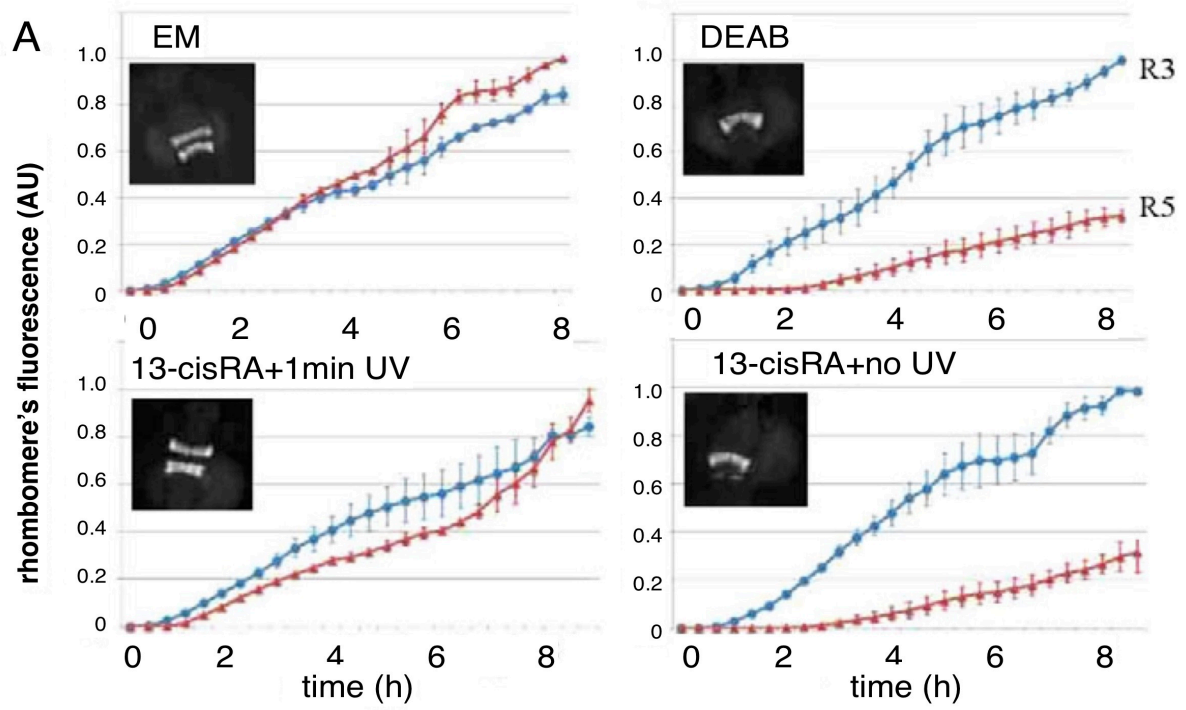

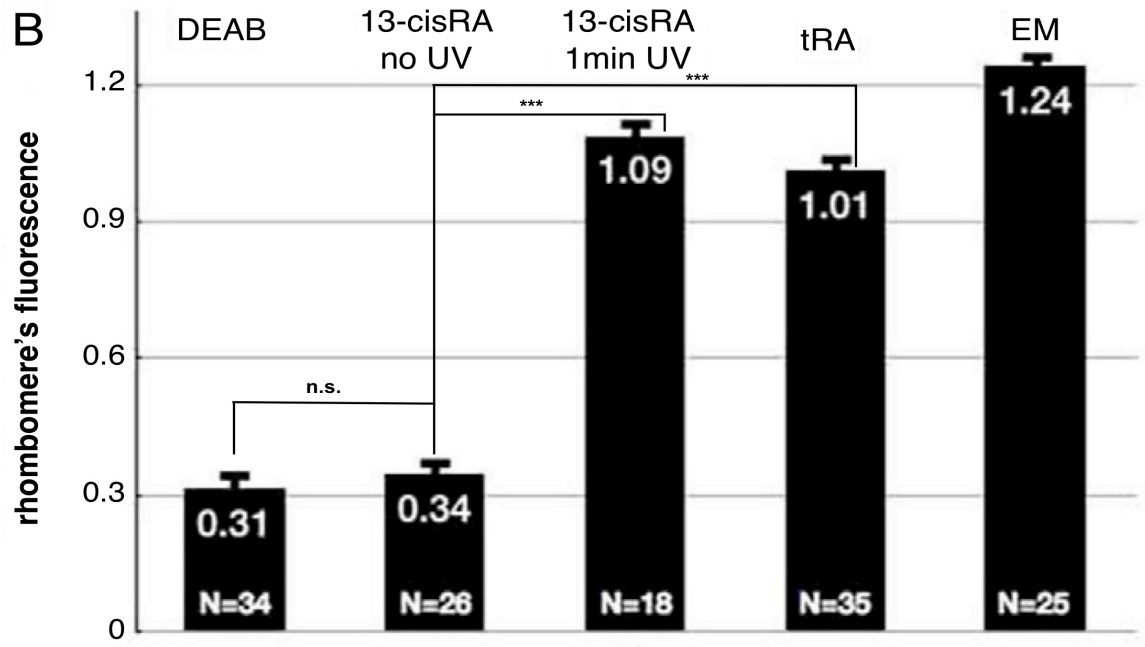

Figure 9. Quantification of RA response in the GFP transgenic line. (A) Dynamics of the total expression of GFP in r3 and r5 in transgenic zebrafish embryos incubated from sphere stage in 10μM DEAB (except for the control incubated in embryo medium, EM). Some of the embryos were exposed at 90% epiboly for 5 minutes to 13-cis RA (cisRA) and illuminated (or not) for 1 minute with a UV lamp. GFP fluorescence can be detected at ~6 somites, which defines the time origin in these data. From the almost linear increase with time of the fluorescence in r3 and r5, we deduce that the ratio of fluorescence of r5 to r3 is a good proxy for the response to all-trans RA. Error bars indicate s.d. from the dynamics measured in three different embryos for each condition. Insets show typical fluorescent images of the embryos at 24hpf. (B) To quantify the response of the embryos to all-trans RA exposure we measured the ratio of total fluorescence in r5 versus r3 in 24-hpf embryos. It is minimal in DEAB and in the presence of 5nM 13-cis RA, but is almost normal (maximal) in embryos transiently incubated in 1nM all-trans RA (tRA) or 5nM 13-cis RA plus 1-minute UV illumination. Error bars indicate s.e.m. (***$p<0.001$, n.s. not significant).

by UV-induced isomerization: all-trans RA can be activated by photo-isomerization of 13-cis RA as well as it can be deactivated by its own photoisomerization. We note, however, that because UV-induced isomerization yields a steady state of RA isomers [161] (Fig. 5), one cannot deactivate the all-trans RA generated from photo-isomerization of cis-isomers.

2.4.6 Rescue of hindbrain development by local activation of RA

Local release has been achieved by implanting beads soaked with all-trans RA in various tissues, in particular in the posterior part of the brain to investigate the rescue of development in DEAB-treated embryos [151]. These experiments led White et al. to suggest that all-trans RA is a bona fide morphogen, an anteroposterior gradient (in conjunction with similar gradients of Fgf8 and Cyp26) of which determines the proper location and development of the rhombomeres. Even though much can be, and indeed has been, learned from such experiments, the high concentration of all-trans RA in the beads (between 10μM and 1mM) and the lack of control of the all-trans RA gradient hinder the test of the elaborate models proposed for the action of all-trans RA during the development of this (and other) organs (e.g. during somitogenesis [144]). Although

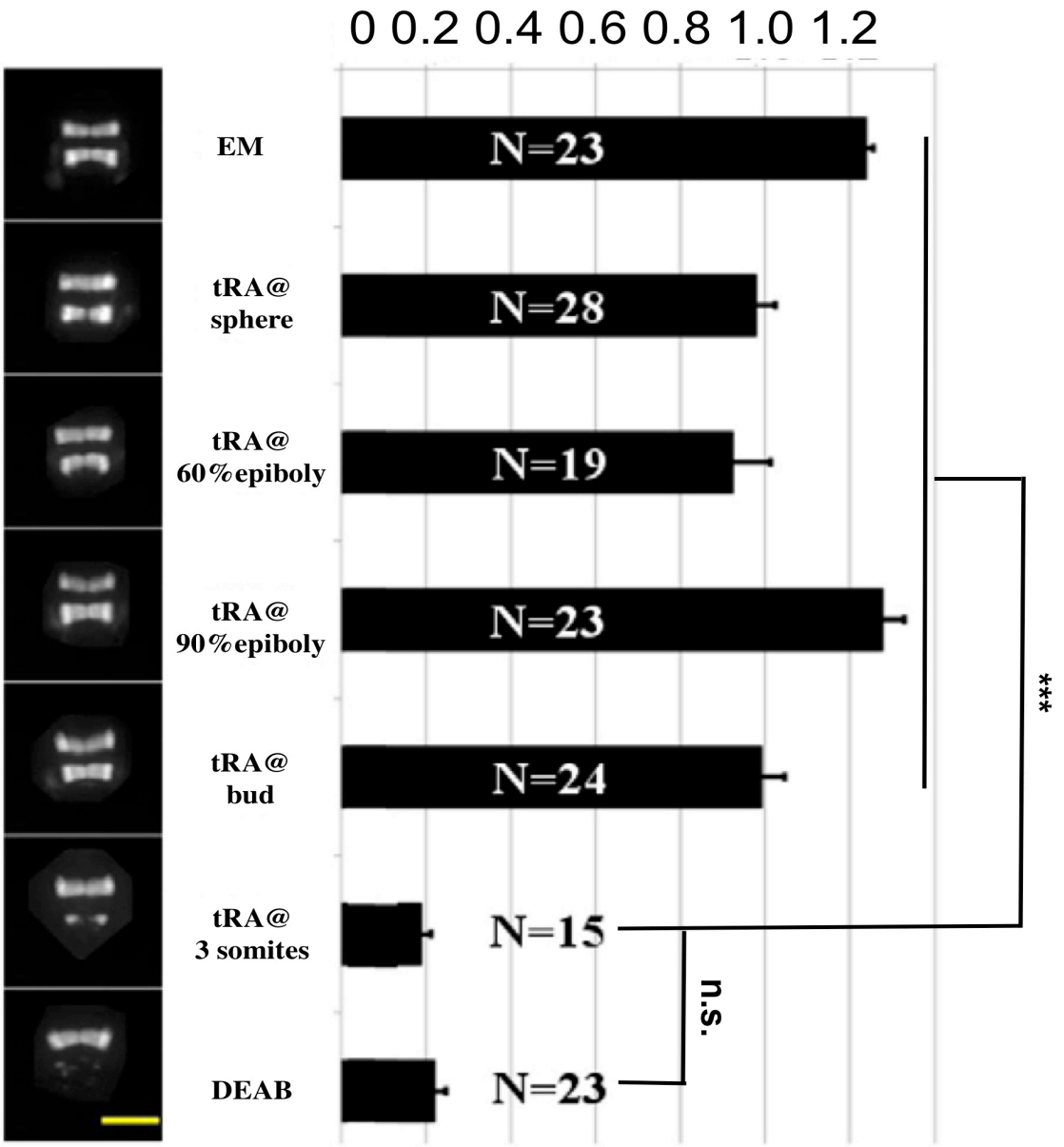

Figure 10. Rescue of hindbrain upon an all-trans RA pulse at various developmental stages. Rescue of hindbrain development in zebrafish embryos expressing GFP in r3 and r5, continuously incubated in 10µM DEAB from sphere stage (4hpf) and exposed for 5 minutes to 1nM all-trans RA (tRA) at various developmental stages (except for the control incubated in embryo medium, EM). On the left are shown typical patterns of GFP expression at 24hpf. On the right is shown the average ratio of total fluorescence in r5 versus r3. Note that exposure to all-trans RA until bud stage yields an almost normal pattern of hindbrain development, whereas exposure to all-trans RA at the 3-somite stage (11hpf) does not rescue normal development of r5. Error bars indicate s.e.m. Scale bar: 200µm (***$p<0.001$, n.s. not significant).

our purpose here is not to test these models, we show below that our approach for all-trans RA control via UV photo-isomerization offers a means to locally activate (or deactivate) all-trans RA at specific times and locations during embryogenesis. Zebrafish embryos were incubated from sphere stage in 10 μM DEAB and exposed at 75% epiboly for 5 minutes to 13-cis RA (5nM). They were then returned to a DEAB solution and individually placed in separate wells of an array in agarose [171]. They were then illuminated at 80-90% epiboly for 20 seconds with a focused UV laser beam (375 nm) in selected regions of the gastrula where precursors of the head or tail are located. The UV illumination locally isomerizes 13-cis RA into all-trans RA. To test for all-trans RA activity we then looked for the rescue of GFP expression in r5 at 24hpf in the transgenic line described above. The rescue of r5 (Rf0.9) upon global UV illumination is similar to the rescue observed upon local UV laser illumination in the precursor of the head region (Fig. 14). A much less substantial rescue (Rf0.35) is observed upon laser illumination in the precursor of the tail region, possibly owing to light scattering that might isomerize some 13-cis RA in the head region. These results imply that all-trans RA is sequestered locally before being used as a possible morphogen as implicated in the development of the hindbrain. As a control, other embryos were injected at the one-cell stage with mRNA encoding Kaede [91] and similarly illuminated with the UV laser beam (the fluorescence of Kaede then switches from green to red). Although the green fluorescence of Kaede interferes with the GFP fluorescence of r3 and r5 and thus cannot be used in conjunction with GFP, the fluorescence of the photoactivated Kaede allows us to verify at later stages that the head or tail regions have indeed been UV illuminated (Fig. 15).

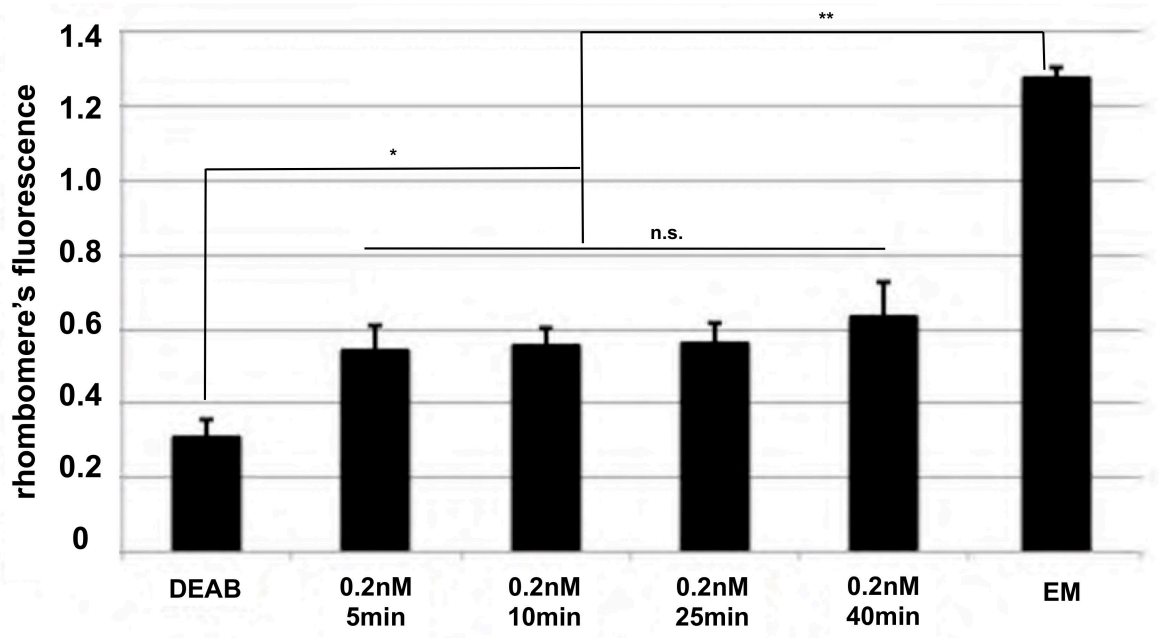

Figure 11. Response to transient all-trans RA exposure for varied times. Ratio of GFP fluorescence in r5 versus r3 at 24hpf in transgenic embryos incubated in EM or 10mM DEAB from sphere stage and transiently incubated in 0.2nM all-trans RA for various times (5, 10, 25 and 40 minutes). The partial rescues of GFP expression in r5 are similar in all cases (** $p<0.01$, * $p< 0.05$, n.s. not significant).

2.4.7 A short pulse of all-trans retinoic acid after, but not before fertilization could rescue hindbrain development.

In our investigation, surprisingly we found that an early all-trans RA pulse at sphere stage (4hpf) as low as 1nM exhibited significant rescue on hindbrain development. As reported in others' work [174, 175], zebrafish embryos begin to synthesize endogenous all-trans RA only after 5hpf. This implies an interesting mechanism of all-trans RA sequestration by the embryo after a short exposure to a low dose of all-trans RA. We further asked whether sequestrated all-trans RA could be replaced if those embryos were later exposed to all-trans RA solution with much lower

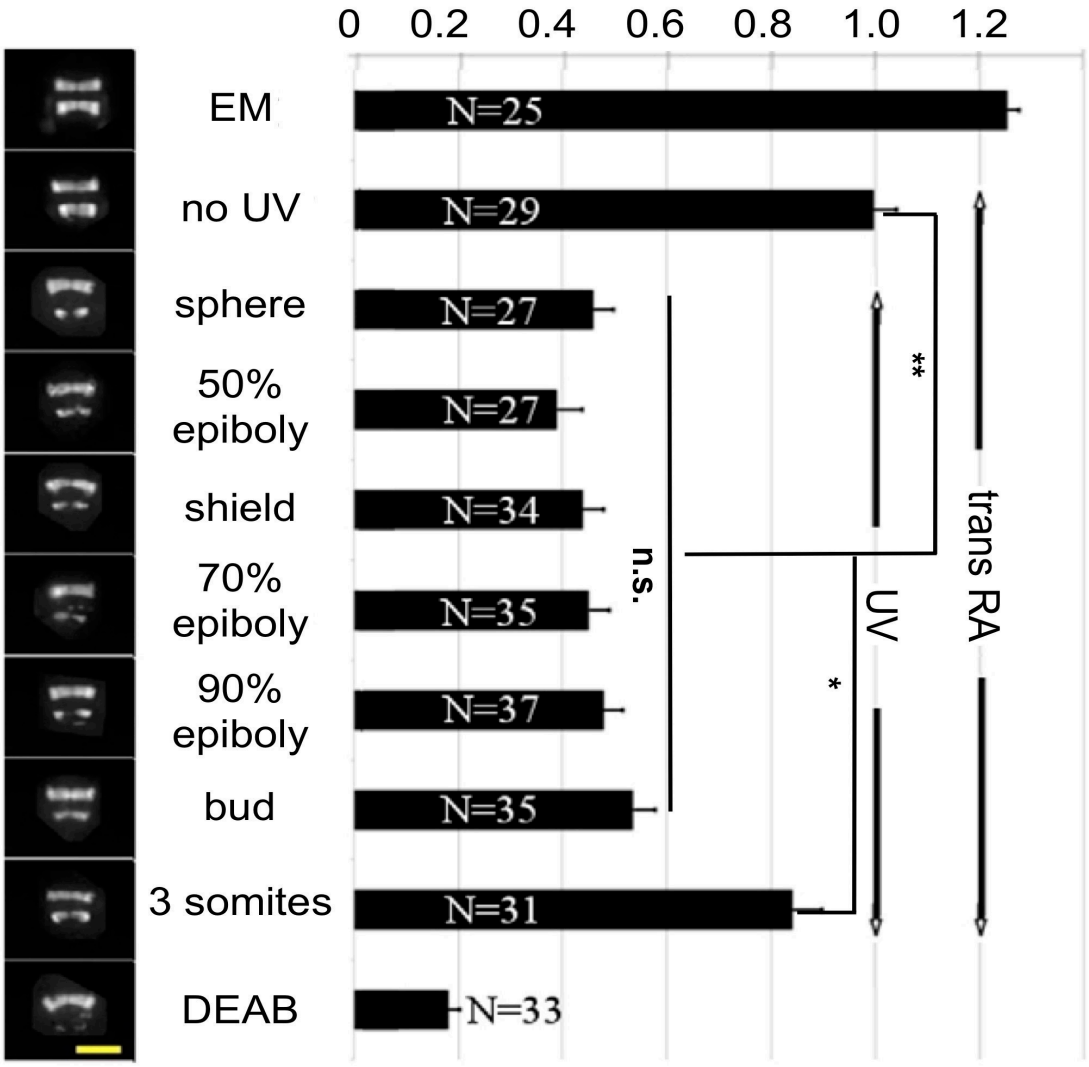

Figure 12. Partial abortive rescue of hindbrain upon UV illumination of all-trans RA. Hindbrain development in zebrafish embryos expressing GFP in r3 and r5, continuously incubated in 10µM DEAB from sphere stage (4 hpf) and exposed for 5 minutes to 1nM all-trans RA (tRA) at sphere followed at various developmental stages by UV illumination for 1 minute (which isomerizes, i.e. deactivates, ~80% of all-trans RA). On the left are shown typical patterns of GFP expression at 24hpf. On the right is shown the average ratio of total fluorescence in r5 versus r3. Note that UV illumination of the embryos until bud stage prevents full rescue of r5. Fuller rescue of hindbrain development by all-trans RA is however possible if UV illumination is performed at the 3-somite stage. Error bars indicate s.e.m. Scale bar: 200µm (** $p<0.01$, * $p< 0.05$, n.s. not significant).

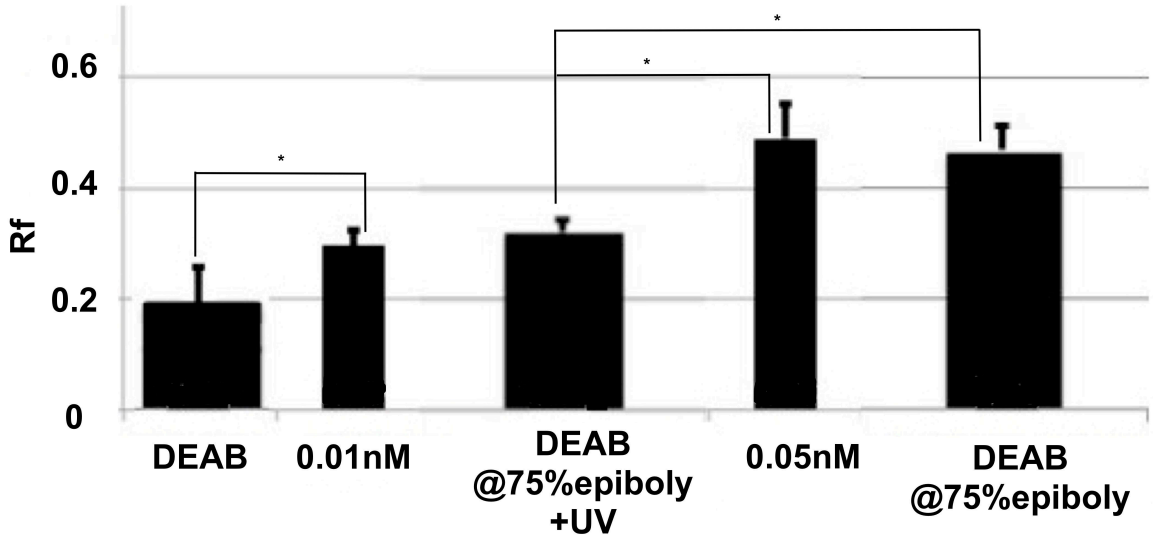

Figure 13. Estimating the all-trans RA concentration at 75% epiboly. To estimate the concentration of all-trans RA at 75% epiboly, we incubated embryos from that stage on in DEAB and illuminated (or not) the embryos for 1 minute with UV light. We then compared the response of these embryos (the ratio of GFP fluorescence in r5 versus r3 at 24hpf, Rf) to the response observed in embryos incubated in DEAB from sphere stage and exposed at 75% epiboly to a pulse of all-trans RA of various concentrations. Since UV illumination inactivates about 80% of the endogenous all-trans RA, we deduce from this comparison that the endogenous all-trans RA concentration at that stage is ~0.05nM, which is reduced upon UV illumination to ~0.01nM all-trans RA consistent with the result of rescue by transient incubation at 75% epiboly of an embryo incubated in DEAB from sphere stage in these concentrations of all-trans RA (* $p<0.05$).

concentration. 2nM or 0.2nM all-trans RA was administered at sphere stage for 5minutes and transferred to E3 medium. Half an hour later, embryos pre-incubated in 2nM all-trans RA were exposed to another 0.2nM all-trans RA pulse for 5min, 10min, 20min, 40min, and 60min respectively. According to our observation, all-trans RA pulses later at lower concentration, were not able to deter hindbrain rescue (Fig.16A), indicating a very strong binding and sequestration of prior all-trans RA pulse, which otherwise could not be disassociated by a following lower all-trans RA pulse. Based on what we had observed, we proposed a "valve" model (Fig. 16 B) that might explain how a pulse of all-trans RA could be sequestered. The channel for all-trans RA

only substantively opens when concentration of all-trans RA outside surpasses the concentration inside. The next big quest is to search for the all-trans RA sequestering co-factor(s). More surprisingly, we found an early pulse of all-trans RA even at one-cell stage demonstrated similar hindbrain rescue to what a pulse did at sphere stage (Fig.17 A). Hindbrain rescue by extremely early pulse suggested that the sequestering co-factor(s) were readily available even at one-cell stage. Arguably one would expect various biomolecules like cellular retinoic acid bind proteins (CRABP) are not synthesized yet at one-cell stage [176, 177]. Essential sequestering factors must be accessible from the very beginning after the egg is fertilized. One may also hypothesize that these perplexing sequestering co-factor(s) could exist in the egg even before fertilization. To investigate whether the egg is able to sequester all-trans RA pulse before fertilization, we performed *in vitro* fertilization experiments in which a 2-minute pulse of 5nM all-trans RA was introduced to unfertilized eggs before they were mixed with sperms. For the post fertilization pulse, a 2-minute pulse of 5nM all-trans RA was given to fertilized eggs 30 minutes later (see materials and methods).

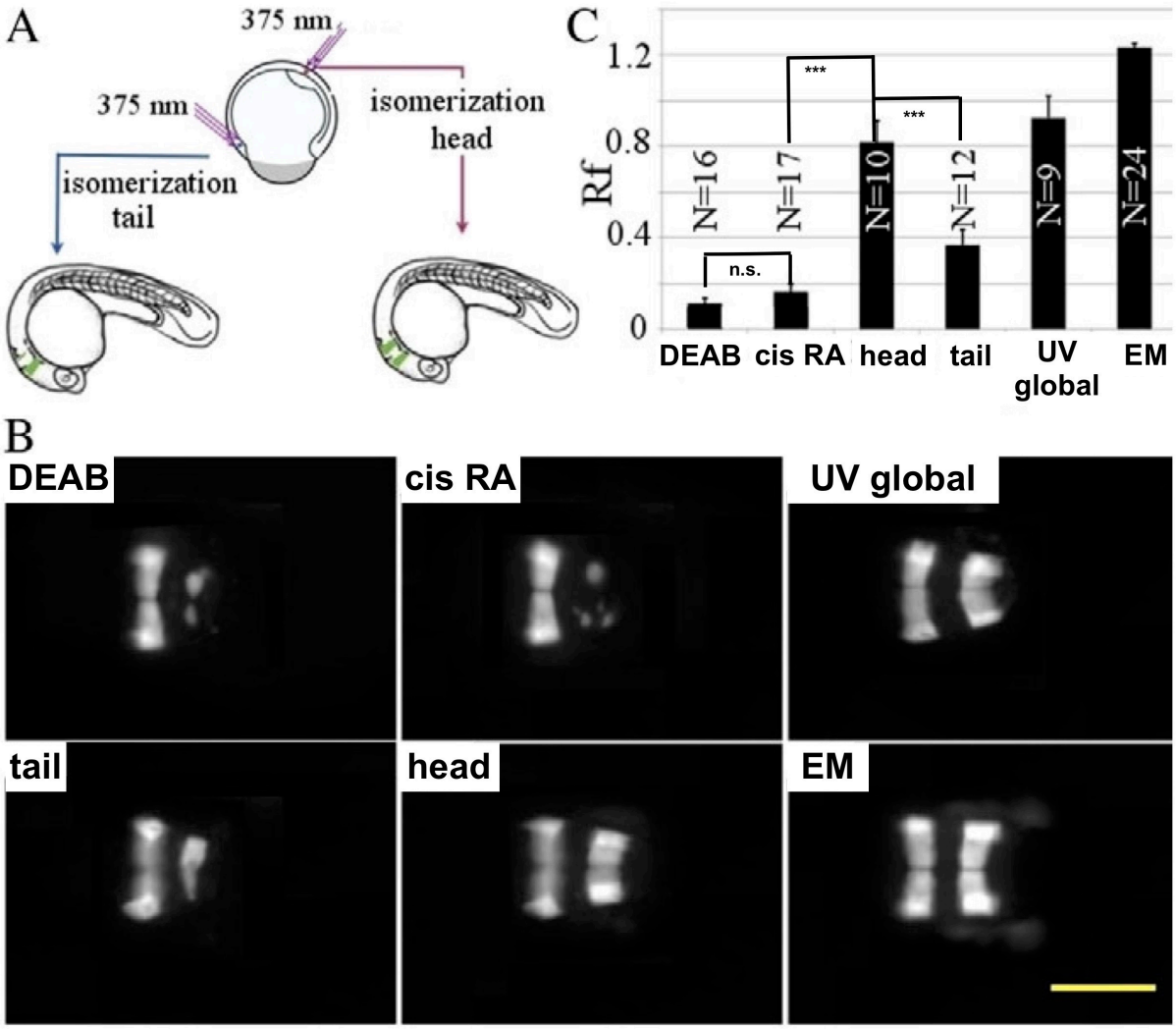

Figure 14. Local activation of RA via isomerization. Local activation of all-trans RA in zebrafish embryos at 80-90% epiboly (incubated from 4hpf in 10 μM DEAB) by UV laser illumination at 375 nm following a 5- minute 13-cis RA (cisRA) pulse (5nM) at 75% epiboly. (A) Schematics describing how embryos were illuminated in localized areas during embryogenesis (see Materials and methods for details). (B) Representative images of embryos incubated in EM (control), in EM plus DEAB, subjected to a 13-cis RA pulse and global UV illumination or to local UV laser-induced isomerization in the tail or head regions. (C) Quantification of the average ratio (Rf) of total fluorescence in r5 versus r3 for the different conditions in B. Error bars indicate s.e.m. Scale bar: 200 μm (*** $p<0.001$, n.s. not significant).

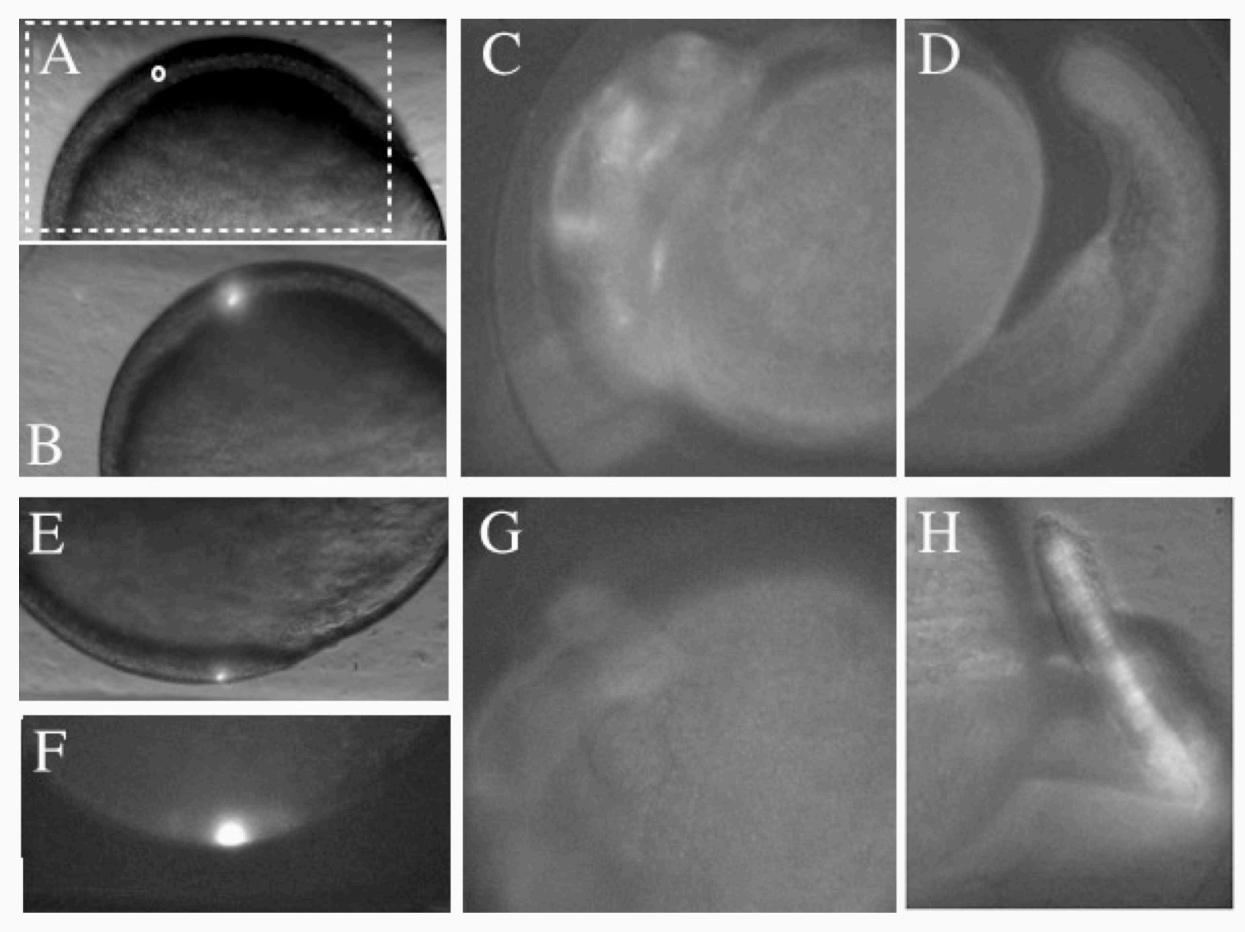

Figure 15. Local labeling with photo-activation of Kaede. Local illumination with a UV laser at ~80% epiboly in the precursor of the head region. To confirm the localization of the UV laser illumination we used the photoconversion of Kaede (from green to red fluorescence) to track the fate of the illuminated region. The mRNA encoding Kaede [178] was injected at the one-cell stage. (A) Embryo overview. The boxed region indicating the anterior part of the embryo corresponds to the area shown in B,C. The region indicated by the small circle was selected for UV irradiation. (B) Twenty seconds of UV irradiation (bright spot) in the circled region in A. (C,D) At 24hpf, red fluorescence from diffused Kaede was observed in the head (C), but not in the tail (D). (E) UV irradiation for 20 seconds in a region (bright spot) that develops into the tail. (F) Corresponding red fluorescent image immediately after photo-conversion. (G,H) At 24hpf, red fluorescence was observed in the tail (H) but not in the head (G).

All treated embryos were incubated in 10uM DEAB except the E3 control. Rf was measured for different groups 24 hours later. The results showed that a 5nM all-trans RA pulse before fertilization failed to rescue hindbrain development (a low Rf value similar to DEAB group).

However, the same pulse after fertilization resulted in a much higher Rf (Fig. 17B). These results imply that possible all-trans RA sequestering co-factor(s) are not available before fertilization, and they are not likely to be CRABPs as we had considered. More and deeper investigations are required to further probe what exactly sequesters all-trans RA at an early stage.

2.5 DISSCUSION

We have described a method for the quantitative, temporal and local control of RA activity in a developing embryo. This method relies on photo-isomerization of an inactive isomer of RA (13-cis RA) to yield ~20% and ~30% of the active all-trans and 9-cis RA isomers. By transient incubation of the embryos in all-trans RA versus 9-cis RA, we observed that the all-trans RA isomer could rescue the developmental defects observed in a zebrafish embryo incubated in DEAB (an inhibitor of RA synthesis) at concentrations 10-fold lower than 9-cis RA. We deduce that, in the experiments reported here, the main effect of 13-cis RA isomerization is to yield ~20% of the active all-trans RA isomer. This conclusion is supported by RT-qPCR results showing that the expression levels of RA-responsive genes (vhnf1, hoxb1a) were equal when equal concentrations of all-trans RA and 13-cis RA were UV illuminated (they yield similar distributions of isomers). When only 13-cis RA was illuminated we had to use a 5-fold higher concentration to observe equal expression of the studied genes as when using all-trans RA. Our results (RT-qPCR on all-trans RA-responsive genes and the GFP intensity ratio in r5 versus r3) show that UV isomerization of 13-cis RA is similar to a transient (5-minute) incubation in all-trans RA at one-fifth of the concentration. This is expected because ~20% of 13-cis RA is isomerized into all-trans RA upon UV illumination. Surprisingly, however, the embryo can be

partially rescued by such a pulse of all-trans RA if it is given as early as sphere stage (but no later than bud stage).

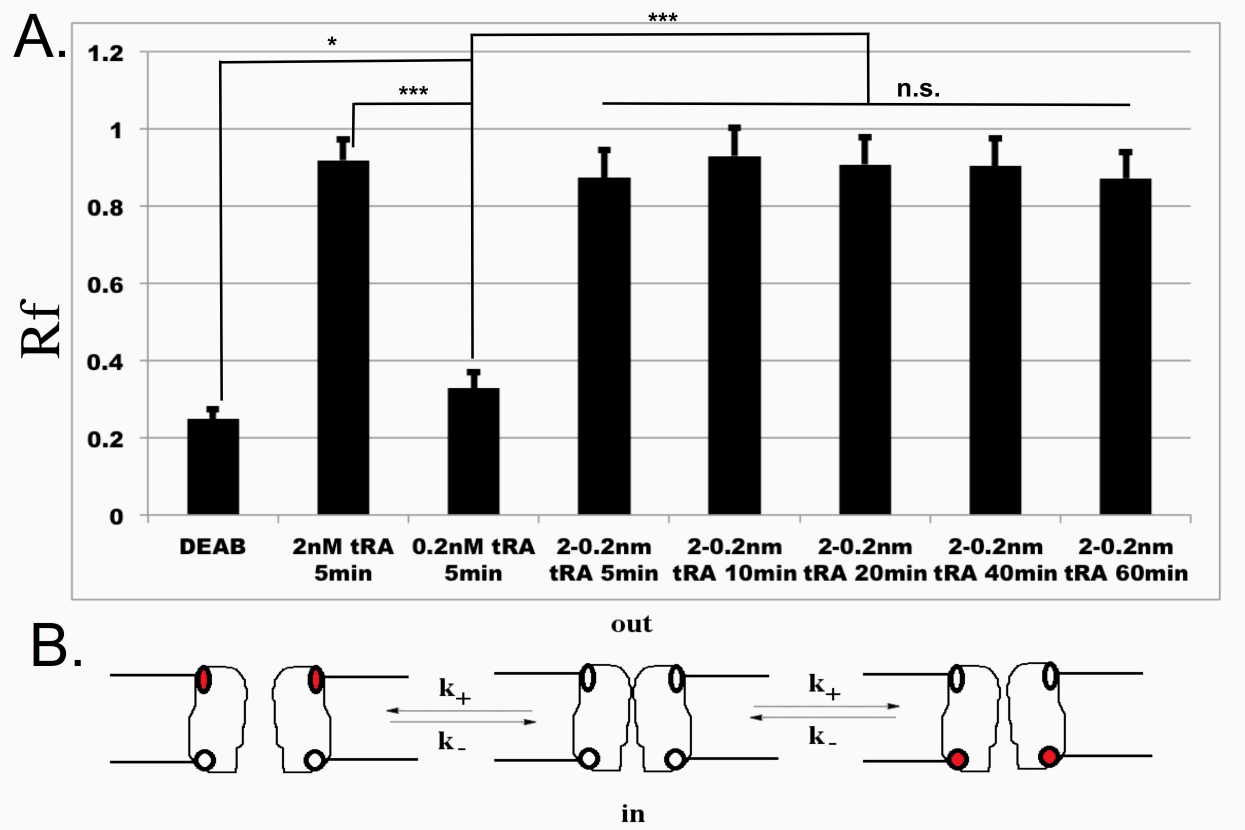

Figure 16. A "valve" model for all-trans RA early sequestration. (A) Average ratio (Rf) of r5 versus r3 quantified by GFP intensity in different conditions. A lower 0.2nM all-trans RA pulse did not decrease hindbrain rescue caused by a higher 2nM all-trans RA pulse at sphere stage. (B) A "valve" model explains that an unspecified RA channel only opens when it detects a higher concentration of RA outside (*** $p<0.001$, * $p< 0.05$, n.s. not significant).

Because after 5 minutes of incubation in all-trans RA (or 13-cis RA) the embryo is put back into a DEAB solution, one might have expected the internalized RA to diffuse out on a similar time-scale. This, however, is not the case as implied by two lines of evidence. First, the embryo is rescued by such pulses of all-trans RA, which is believed to be required at the end of gastrulation [152]. Second, if, between the exposure to all-trans RA (at sphere) and the end of gastrulation,

the embryo is UV illuminated then only very partial rescue is observed (as would be expected from a decrease in the internal concentration of all-trans RA due to isomerization). We deduce that RA is sequestered in the embryo in the time interval (a few hours) between exposure and the end of gastrulation. Sequestration per se is not surprising, as many proteins are known to bind intracellular all-trans RA with sub-nanomolar affinities (e.g. CRABP [179]). Extracellular all-trans RA-binding proteins have also been described [180, 181]. However, these proteins have much lower affinities for cis-isomers. Their presence would therefore not explain why 13-cis RA could be activated hours after a 5-minute incubation. Binding to these proteins would equally fail to explain why equilibrium with an external concentration of all-trans RA is reached within 5 minutes, whereas the RA can be retained for hours after the embryos are transferred into a solution lacking any RA. More surprisingly, a short pulse of all-trans RA at one cell stage could partially rescue DEAB phenotypes as well. In contrast, attempt of introducing the same pulse before egg fertilization fails to deliver the same rescue effects. All these intriguing observations imply that possible all-trans RA sequestering molecule(s) become available even at one-cell stage, but not before fertilization. Further investigations are needed to pin down the exact co-factors as well as the mechanisms involved.

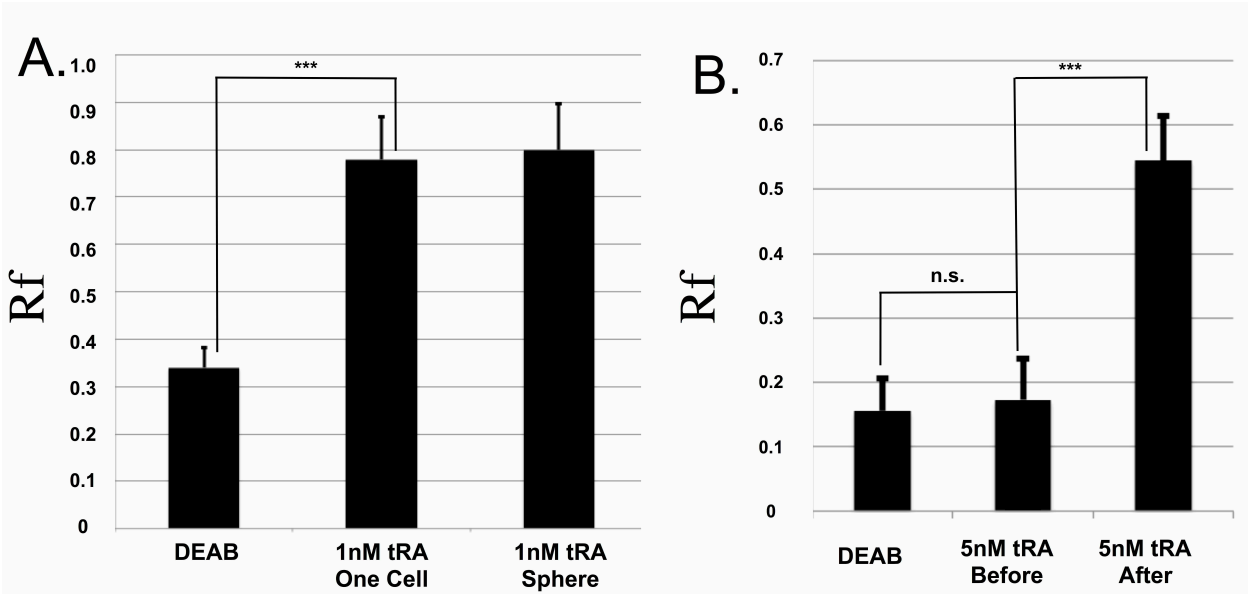

Figure 17. Hindbrain rescue caused by all-trans RA pulse at one cell stage, but not before fertilization. (A) 1nM tRA pulse at one cell stage and sphere stage showed the same rescue effects. (B) A 5nM tRA pulse after fertilization, but not before fertilization, rendered partial rescue of hindbrain development (*** $p<0.001$, n.s. not significant).

Beyond the role possibly played by all-trans RA sequestration in normal development, our results suggest that spatiotemporal control of all-trans RA concentration is possible via its photoisomerization. This was demonstrated by the rescue of hindbrain patterning upon photo-isomerization of 13-cis RA in the head and to a lesser extent in the tail region. This should open the way for a detailed investigation of various developmental models in which all-trans RA is known to play an important role, such as hindbrain patterning and somitogenesis. The local release of a known concentration of all-trans RA at a specific location in the embryo and at a specific time during the developmental program will allow more precise characterization of the response to test the relevant models of development [162, 182]. There are a few caveats to these investigations though: because all-trans RA is sequestered and regulated in the embryo, it is better to conduct these types of studies in embryos devoid of endogenous all-trans RA (e.g. those treated with DEAB) so that the local perturbations achieved by photo-isomerization of 13-cis RA

(or all-trans RA) are not modulated by an ill-defined, local, endogenous all-trans RA response (such as the compensatory release or sequestration of endogenous all-trans RA); moreover, because photo-isomerization of 13-cis or all-trans RA also generates 9-cis RA, one should keep in mind and investigate separately the possibly synergistic role of 9-cis RA, a natural ligand of RXR.

2.6 STATEMENT

Most of the work above was published in the paper "*Spatiotemporal manipulation of retinoic acid activity in zebrafish hindbrain development via photo-isomerization*" [82]. This work was performed within the Laboratoire International Associé between CNRS-ENS and CNSI-UCLA and was supported by an Agence Nationale de la Recherche (ANR) Proteophane grant (to D.B. and L.J.); a Partner University Fund (PUF) grant (to D.B. and S.W.); and a European Associated Laboratory NanoBio Sciences (LEA-NaBi) fellowship (to D.S.); Z.F. was partly supported by a Jennifer S. Buchwald Graduate Fellowship from UCLA Physiology department and a China Scholarship Council (CSC) Fellowship. We thank M. Volovitch and P. Charnay for valuable conversations; the Rosa and Charnay laboratories for *in situ* hybridization protocols; Haigen Huang for help with *in vitro* fertilization; UCLA zebrafish Core Facility for help with the maintenance of zebrafish lines; and anonymous referees for useful suggestions.

CHAPTER THREE:

OPTICAL CONTROL OF CANCER INDUCTION IN SINGLE CELLS IN ZEBRAFISH

3.1 ABSTRACT

Although cancer initiation and evolution have been extensively studied, they are not, as of yet, fully understood. Several models have attempted to answer how cancer arises from individual transformed cells. However, current probes of cancer development are restricted to the collective properties of many thousands of cells. In particular, two outstanding questions, the effectiveness of oncogenic transformation and the role of the local microenvironment on cancer initiation, require the study of the fates of individual cells and their progenies. To address these challenges, we have developed a technology that allows for the control of protein activity and gene expression in a small group of cells through light activation. In this work, we utilize this method to activate a typical oncogene, K-RasG12V, in a small number of cells in a live zebrafish and investigate the effects of these changes on tumorigenesis under varied genetic backgrounds. We successfully demonstrate the spatiotemporal control of oncogene expression in live zebrafish. Furthermore, we investigate different tumorigenic phenotypes by transiently or permanently activating human K-RasG12V at varied developmental stages. We believe that our studies could shed new light on cancer initiation and growth and provide new tools for target validation and testing of novel anti-cancer drugs.

3.2 INTRODUCTION

The initiation of cancer is believed to be a rare event, taking place at the level of individual cells[20, 183, 184]. Commonly considered as a genetic disease, cancer is attributed to accumulative somatic mutations and epigenetic changes. Those alternations at genetic level

contain substitution, insertion and deletion of bases, rearrangements and changes in copy numbers of DNA segments[185, 186], and inheritable epigenetic changes in lineage such as DNA methylation, histone modifications and small noncoding microRNAs[187]. The complexity of tumor conditions magnifies as tumor progresses, acquiring further genetic variabilities from a single cell of origin. Current understanding of cancer genomes categorizes two subsets of somatic mutations-"driver mutation" and "passenger mutation". While "driver mutation", in most cases, involves critical "cancer genes" that are able to drive transformed cells to expand and proliferate more than surrounding normal cells; "passenger mutation" usually doesn't confer significant advantages for transformed cells in terms of growth and proliferation. However, it remains largely unknown[188] why and how certain genetic transformations in a single cell or small number of cells eventually advance to tumor, but others, in contrast, are usually extruded or suppressed. The occurrences of cancer in an individual subject are widely due to interactive environment, life style and certainly to the genetic predisposition carried in one's fertilized egg. Even so, how much and exactly how each of those factors contributes to cancer initiation, from cellular perspective particularly, remains largely unclear and open to discussion[189-191]. One recent controversial paper claims that cancer might be simply due to "bad luck" of random mutations from stem cell division[191], of which the numbers on the other hand, have essentially been pre-destined among species. In other words, this means cancer is not preventable in many cases. All those fierce debates and discussions provide worthy creditable insights, yet, desperately urge deeper understanding on triggering events of cancer initiation and progression. Now assorted approaches enable us to investigate characteristic shifts of a formed tumor at genetic and molecular level. Cytogenetic and copy number study, as well as second generation DNA sequencing empower us to precisely pin down the genetic transformations within solid

tumor cells[192]. Additionally, over the course of past decades, numerous cancer models[193-196] have been developed to help investigate cancer cell behavior and more importantly, develop treatments for cancer progression and relapse. Nonetheless, tumor initiation is organ- and species-specific[197]. Examinations of tumors at late stages of cancer development are not able to shed light on the initiation and early statistical "history" of cancer cells. Current approaches show limits in ability to develop therapies aimed at preventing cancer initiation. The idea of understanding tumor evolutionary process in the very initial stage has been emerging over last decades[184, 198]. Specifically, two key unresolved questions of cancer development, namely the roles and effectiveness of mutations in proto-oncogenes and/or tumor suppressor genes in cancer initiation and the role of the local microenvironment on cancer initiation require a defined look at the level of individual cells. Yet current probes of cancer development are mostly restricted to the collective properties of many thousands of cells after tumor already forms. Several attempts were reported in very recent years that investigated the interaction between single transformed cells with surrounding normal epithelial cells and immune cells[199, 200]. However, these investigations were limited to specific cell types and more critically, they did not mimic true tumorigenic initiation in physiological scenario where only a single transformed cell starts to develop tumor within a solid tissue. Here in our work, we develop a sophisticated tool that is able to optically control tumor initiation in a live zebrafish embryo without limitation to specific cell/tissue types. The approach relies on the well-known use of tamoxifen to release proteins fused to the tamoxifen specific receptor (ERT)[201] and sequestered in the absence of ligand by cytoplasmic chaperones. This technique has been used for more than two decades in a variety of *in-vitro* and *in-vivo* contexts to induce recombination of desired gene constructs by a fusion between the ERT and a Cre-recombinase. And it has effectively shown the introduction of

somatic mutations at a chosen time and/or in a given tissue[202]. In our study, we combine this knowledge with the introduction of a caged analog of tamoxifen (caged-cyclofen), which is more stable upon photo-activation and has similar activity towards the ERT receptor. Upon illumination of UV light, cyclofen is released in the illuminated cell(s) in a zebrafish. Its binding to the ERT receptor releases the fused protein from its chaperone complex, thereby effectively turning on its activity. To induce oncogenic expression *in vivo*, we genetically modify two widely used systems of gene expression control: Gal4/UAS and Cre/Loxp recombination (see results section). Zebrafish have been used as cancer models and platform of anti-cancer drug screening only since recent decades[203-207], and they rapidly gain interest and popularity among researchers because they offers (i) optical transparency, making them ideal for optical imaging (ii) relative ease for preparing transgenic animals; (iii) high genome similarity to their human counterpart, especially regarding some genes associated with human diseases[208]; (iv) the ability to acquire data with good statistics (a single mating pair may lay hundreds of eggs thus making it possible to carry out statistically significant studies on many similar individuals); (v) the possibility for setting up high throughput screening aimed at elucidating molecular mechanisms of tumor suppression. Here in our work, we demonstrate the success of inducing oncogenic expression of a mutated human k-RasG12V gene, in both transient and permanent manner, in developing embryos by photons. We find a short activation of k-RasG12V in the early developmental stage results in a gradual decrease of oncogene expression and rarely causes tumor formation. In contrast, periodic activation is able to maintain k-RasG12V expression and indeed increases probability of tumor incidence. In addition, oncogenic activation from the very beginning at one-cell stage greatly promotes tumorigenesis. On the other hand, permanent activation of k-RasG12V could substantially advance tumorigenesis during early embryogenesis.

Furthermore, we delineate the correlation between tumorigenic rate and numbers of transformed cells in an individual fish, which confirms that higher expression of oncogene k-RasG12V lead to tumorigenesis at a higher rate. Lastly, we show that our technique is able to precisely activate and label k-RasG12V expression in a small group of cells without limit to specific cell types. Overall, we present here a novel methodology to initiate tumor from small number of cells in a zebrafish at a very high spatiotemporal level. With this powerful tool, one will be able to study cancer initiation from the very beginning stage. Future research facilitated with this tool will help examine controversial cancer evolutionary theories from both conventional[20, 183, 209, 210] and recent[191, 211] studies. The work opens up a new basis for understanding cancer initiation and growth and will eventually serve as a platform for testing novel anti-cancer drugs.

3.3 MATERIALS AND METHODS

3.3.1 Plasmid design and cloning

A 564bp DNA sequence of human k-RasG12V was slightly modified to prefer expression pattern in the zebrafish (see below for a full sequence). Plasmids carrying pUC57 vector contains cre, K-RasG12V and loxp-Eosfp-stop-loxp-kRasG12V-T2A-mTFP respectively, and were ordered from Eurogentec. Uas:kRasG12V-T2A-CFP,ubi:Eosfp plasmid was cloned by inserting k-RASG12V into a PT24uasfgf8alT2ACFPUbiEosf vector kindly provided by Dr. Michel Volovitch (ENS), using KpnI and FspAI digestive sites. Similarly, we made the uas:cre, ubi:Eosfp plasmid. Ubi:loxp-Eosfp -stop-loxp- kRasG12V-T2A-mTFP plasmid was cloned by replacing Eosfp with loxp-Eosfp-stop-loxp-kRasG12V-T2A-mTFP sequene, using BamHI and EcoRV digestive sites.

Full sequence of the modified human k-RasG12V:

atgactgaatataaacttgtggtggttggagctGTTggcgttggcaagagtgccttgacaatccagctgattcagaatcattttgtgg
acgaatatgatccaacaatcgaggattcctacaggaagcaagtggtgattgatggagaaacctgtctcttggatattctcgacacag
caggtcaagaggagtacagtgcaatgagggaccagtacatgaggactggggagggctttctttgtgtgtttgccatcaataatacta
aatcatttgaagatattcaccattatagagaacaaattaaaagagttaaggactctgaagatgtgcctatggtcctcgtgggaaataa
atgtgatttgccttcaagaacagtggacacaaaacaggctcaggacttggcaagaagttatggtattccttttattgaaacatcagca
aagacaagacagggtgttgatgatgccttctatacattggttagagaaatccgaaaacataaagaaaagatgagcaaagatggtaa
aaagaagaaaaagaagtcaaagacaaagtgtgtgattatg

3.3.2 Fish line and maintenance

Three established fish lines: ubi:gal4-ert; ubi:cre-ert and $P53^{-/-}$ were kindly provided by Dr. Sophie Vriz (fish line not published, College de France), Dr. David Traver [212] (UCSD) and Dr. Shuo Lin [204] (UCLA). Stable, double transgenic ubi:gal4-ert, P53-/-; ubi:cre-ert, P53-/- fish lines were obtained by crossing lines and screening resultant F1 fish with PCR genotyping. About 100 mosaic fish injected with ubi:loxp-Eosfp-stop-loxp-kRasG12V-T2A-mTFP plasmid were mated and resultant F1 fish were screened by both Eosfp expression and PCR genotyping. UCLA Zebrafish Core Facility provided regular maintenance of all zebrafish lines. The overall health status of fish in the facility is monitored under the supervision of UCLA veterinary advice. Veterinary protocol has been approved by UCLA Institutional Animal Care and Use Committee (ARC# 2001-074-33).

3.3.3 Drug treatments and UV uncaging

Jullien lab (ENS) synthesized and kindly provided the native cyclofen and caged cyclofen in powder form (Fig. 18b). Compounds were stored in a brown sealed box and mailed from Paris to Los Angeles via regular package. For long-term storage, both the native and caged cyclofen were carefully covered with aluminum foil and kept at -80°C. Stock of 2mM cyclofen and 4mM caged cyclofen in DMSO were also prepared and kept at -80°C in darkness. To induce k-RasG12V expression, embryos were incubated in 1, 2, 10uM native cyclofen or 4, 10uM caged cyclofen and then left for either 2 hours or over night before they were again transferred to the E3 medium. Periodic induction of kRasG12V expression was carried out by treating gal4-ert embryos injected with uas:kRasG12V-T2A-CFP;ubi:Eosf plasmid with 2uM cyclofen for 24 hours every five days until two-month post fertilization. For whole embryo uncaging, a benchtop UV lamp (Fisher VL-6-L) was used. This lamp has a strong emission peak at 365 nm accompanied by a Gaussian spectral dispersion around 350 nm with a 40 nm width at half maximum, delivering on the illuminated sample a typical photon flux of ~4.3104 Einstein/($s \cdot m^2$). Injected embryos pre-treated with caged cyclofen were put in a 60mm ×15mm petri dishe and were illuminated by the benchtop UV lamp for 2 minutes at room temperature. Illuminated fish were covered with aluminum foil and taken to 28°C incubator. Localized uncaging was achieved on a Nikon microscope equipped with an adjustable iris and a lumencor LED light engine with a UV light peaking at 396nm. The maximum relative spectral power of the UV light was 27mW/nm. Uncaging region was controlled by iris to reach a circular area of 120um in diameter. Uncaging was performed for 2 minutes at the maximum power of the UV light on each embryo. After uncaging, embryos were transferred to a 12-well plate with E3 medium and incubated in total darkness.

3.3.4 RT-PCR and *in-situ* hybridization

Expression of kRasG12V mRNA was profiled on embryos ageing from one-day post fertilization to two-week post fertilization. In each time point, five to seven injected embryos were collected for total mRNA extraction. Total mRNA was extracted and purified as previously described [213], and then stored in -80°C till all mRNA samples were prepared. SuperScript® III First-Strand Synthesis System (Invitrogen) was used to synthesize and purify total cDNA. Fast SYBR Green Master Mix (Thermo Fisher Scientific) was used for qPCR. Primer sets used for Eos and kRasG12V cDNA detection were: Eos forward (GCA ACA AAG CCA TGT GAA TAT GA), Eos reverse (CAA ACT TTC CCG CCA ATG GTC CA), kRasG12V forward (AAC CAA TGT ATA GAA GGC ATC AT), kRasG12V reverse (TAA ATG TGA TTT GCC TTC AAG AA). The difference (ΔCt) in the number of amplification cycles between kRasG12V and Eosfp (used as a reference gene) was measured in triplicate PCR assays. The ratio of kRasG12V to Eosfp in expression was quantified as: $2^{-\Delta Ct}$. Single whole-mount *in situ* hybridization with digoxigenin-labeled riboprobes was performed at 2 day post-fertilization as described previously [166]. Riboprobe for kRasG12V was synthesized from uas:kRasG12V-T2A-CFP plasmid.

3.3.5 Microinjection and microscopic imaging

Exogenous genes were incorporated into embryos at one-cell stage using transposon system [214]. DNA constructs (final concentration 25ng/ul) were mixed with tol2 mRNA (final concentration 100ng/ul), and mixed solutions were micro-injected into single cells of embryos at one-cell stage, following protocol described earlier [215]. After injection, embryos were incubated in E3 medium at 28°C. Fluorescent imaging was performed on a Nikon Eclipse Ti microscope accessorized with a C-HGFI Intensilight Fiber illuminator, and confocal imaging

was acquired on a Leica SP5-STED microscope. Embryos and adult zebrafish were anesthetized first in tricaine (Sigma-Aldrich), and laid in a small liquid drop on a cover slide for imaging. Fluorescence intensity of individual image was quantified with ImageJ64 after subtracting background signal.

3.3.6 Histological analysis

10 day-post fertilization embryos and adult zebrafish were first anesthetized with tricaine. Selected tissues bearing tumor or tissues from control were dissected. Then embryos or dissected tissues were fixed in 4% paraformaldehyde overnight at 4°C prior to rinse by 70% ethanol. Fixation and decalcification were processed as previously reported [216]. Fixed and decalcified fish were sent to UCLA Translational Pathology Core Laboratory (TPCL) for sectioning and H&E staining. Stained slides were imaged with a Leica LMD (Laser Micro Dissection) 7000 Microscope.

3.4 RESULTS

3.4.1 Expression of an oncogene, human kRasG12V, was optically controlled in live zebrafish embryos

The main motivation of this work attempts to develop an optical method to induce cancer in a live zebrafish, at a high spatiotemporal resolution. This technique derives from a previous method that involves fusing a specific protein to estrogen like receptor (ERT) [201]. As shown in Fig. 18a, a protein of interest fused with ERT is unable to enter nucleus to regulate gene expression due to the binding with large cytoplasmic chaperones. However, the protein complex

could be re-activated in presence of small ligands like tamoxifen because of their higher binding affinity to ERT. A caged analog of tamoxifen (caged-cyclofen, Fig. 18b), which is more stable upon photo-activation and which has similar activity towards the ERT receptor, was employed to activate the fused protein.

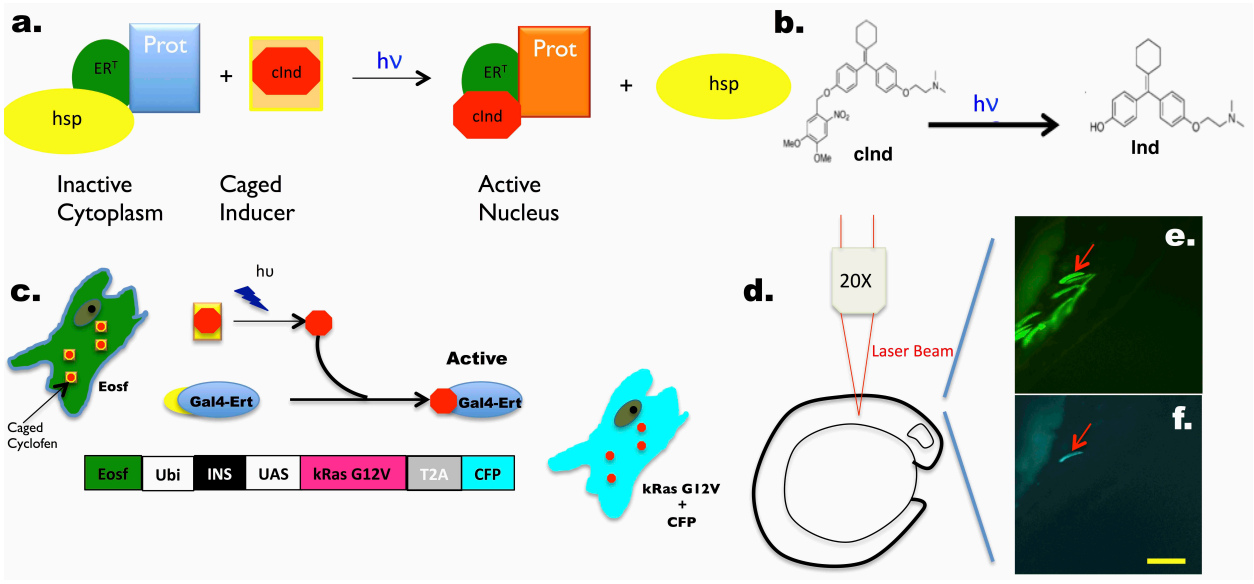

Figure 18. Schematic principle of photo-control over specific oncogene expression. (**a.**) A protein (Prot) of interest could be genetically fused with estrogen like receptor (ER^T) and becomes inactive by forming a complex together with large heat shock protein (hsp) in the cytoplasm. However, the complex can be re-activated by certain chemical inducers such as cyclofen. (**b.**) Caged inducer (cId) is chemically synthesized and could be uncaged by light of proper wavelength. (**c.**) In a live transgenic zebrafish expressing Gal4-ER^T, injection of a plasmid construct containing Ubi:Eosf;UAS:K-RasG12V-T2A-CFP and uncaging caged cyclofen results in activation of K-RasG12V and CFP. (**d.,e.,f.**) High spatial resolution can be obtained at single cells level through two-photon uncaging in a developing zebrafish embryo. After cyclofen uncaging, a muscle fiber cell carrying oncogenic construct expressed CFP (**f.**), while other cells without uncaging expressed Eosf only (**e.**). Scale bar: 100um.

Upon illumination with UV light, the ester bond in caged cyclofen breaks and releases its active form (Fig. 18b). Then the binding of uncaged cyclofen to the ERT receptor subsequently releases

the fused protein from its chaperone complex, thereby effectively turning on its activity. If the protein is active in the nucleus (such as transcription factors, DNA recombinases, etc.), its translocation there will turn on or off the targeted genes (Fig. 18c). The advantage of adopting optical tool offers accurate control at sub-cellular level. An example showed success of activating kRASG12V in a specific cell (Fig.18 e, f) upon UV ucaging in a mosaically injected embryo. To test how much expression of kRasG12V is required to induce tumorigenesis in the zebrafish, we created two systems to control kRasG12V expression optically. One allowed transient expression of kRas oncogene (Fig. 19a), and the other enabled permanent kRasG12V expression after cyclofen activation (Fig. 19b, c). To transiently activate kRasG12V, we injected uas:kRasG12V-T2A-CFP plasmid together with tol2 mRNA into Gal4-ert embryo at one-cell stage. Introducing cyclofen or caged cyclofen uncaging activated Gal4-ert protein, thus subsequently turned on kRasG12V expression. However, expression gradually diminished once the active cyclofen was removed, rendering an ideal on-off control of kRasG12V expression. The other two approaches (Fig. 19b, c) relied on Cre/Loxp recombination system. Either uas:cre and ubi:loxp-Eosfp-stop-loxp-kRasG12V-T2A-mTFP plasmids were co-injected into Gal4-ert embryo (Fig. 19b), or ubi:loxp-Eosfp-stop-loxp-kRasG12V-T2A-mTFP plasmid was injected into Cre-ert embryo at one-cell stage. Adding cyclofen permanently edited the incorporated genome so that expression of kRasG12V was turned on lastingly. These two systems could be distinguished as pulse function (Fig. 19d) and step function (Fig. 19e) in controlling kRasG12V expression.

After injection, healthy and good-shaped embryos were selected and transferred to fresh E3 medium the next day. Compared to uninjected gal4-ert embryo (Fig. 20a1, a2), positively

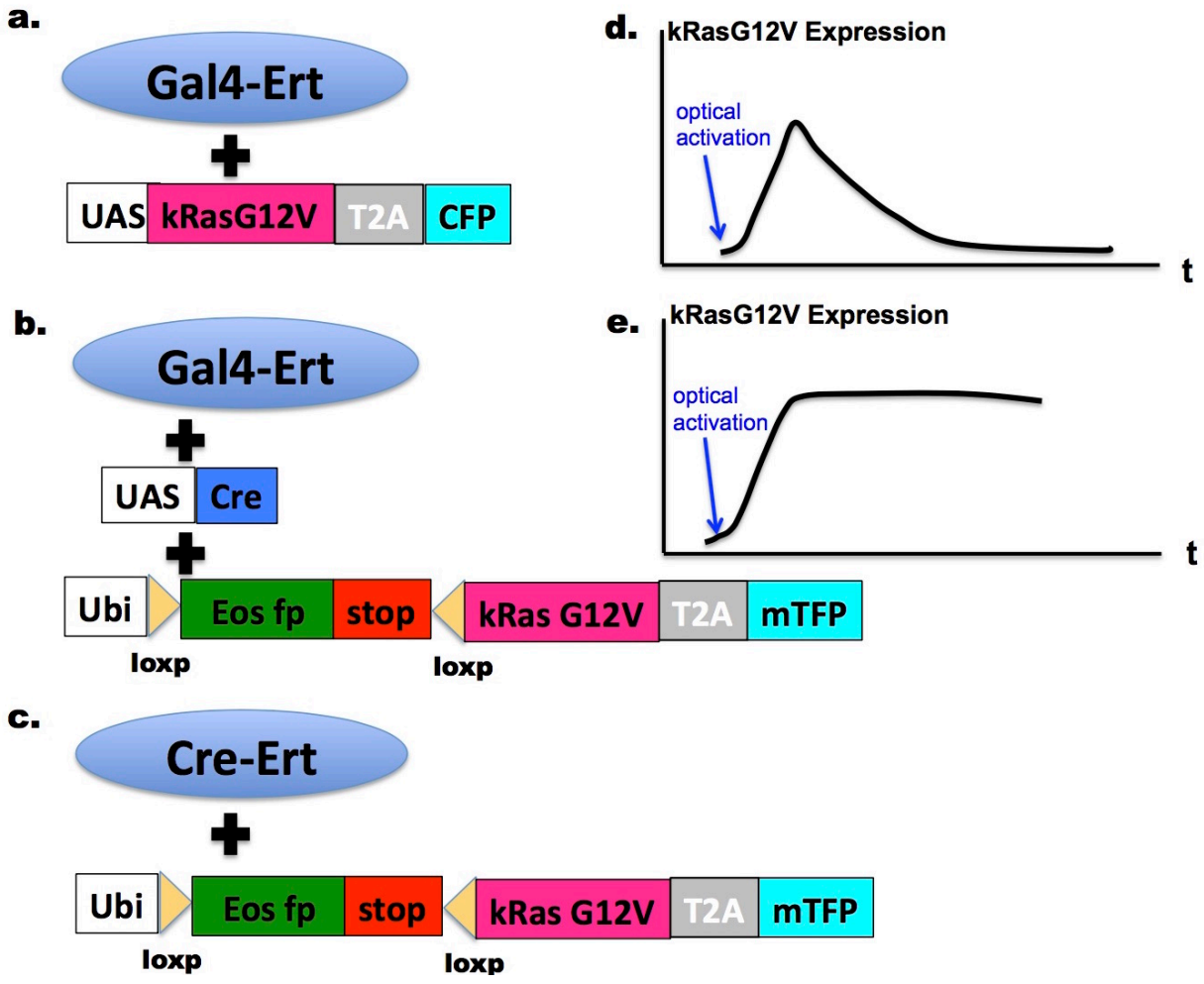

Figure 19. Two systems controlling kRasG12V expression in transient and permanent manner. (a.) Transient expression (d.) of kRasG12V was induced by injecting the uas:kRasG12V-T2A-CFP plasmid into Gal4-ert embryos at one-cell stage, and treated by either cyclofen or caged cyclofen uncaging. (b, c) For permanent activation (e.) of kRasG12V expression, uas:cre and ubi:loxp-Eosfp-stop-loxp-kRasG12V-T2A-mTFP plasmids were co-injected into Gal4-ert embryos(b), or alternatively, ubi:loxp-Eosfp-stop-loxp-kRasG12V-T2A-mTFP plasmid was injected into Cre-ert embryos at one-cell stage. Cyclofen or caged cyclofen uncaging later turned on kRasG12V expression permanently.

injected embryos expressed Eos, a photo-switchable fluorescent protein (Fig. 20b1), but not CFP (Fig. 20b2) in many muscle fiber cells. However, incubating in 2uM cyclofen for 2 hours

substantially activated the expression of CFP (Fig. 20c2), which also co-localized with Eos expression very well (Fig. 20c1). Although CFP expression implied successful induction of kRasG12V, it was still not a direct evidence of kRasG12V expression. Therefore, we performed *in situ* hybridization to directly probe kRasG12V mRNA expression with and without cyclofen activation (Fig. 20d1, d2). Indeed, kRasG12V mRNA could only be detected in embryos treated with cyclofen (Fig. 20d2), but not in embryos without cyclofen treatment (Fig. 20d1).

After we effectively demonstrated activating kRasG12V expression by native cyclofen, next we tested controlling the oncogenic expression with light. Again, uas:kRasG12V-T2A-CFP plasmid was injected into Gal4-ert embryo at one-cell stage. Healthy embryos expressing Eos were selected and incubated in 4uM caged cyclofen for 2 hours at 24hpf before they were briefly rinsed and transferred into the E3 medium. For the uncaging group, 2-minute UV illumination was applied with a benchtop UV lamp (~365nm). Control embryos were kept in E3 medium after pre-incubation with caged cyclofen. All manipulations were conducted in complete darkness expect UV illumination. As shown in Fig. 21, injected embryos treated with caged cyclofen without UV illumination expressed only Eos, but no CFP (Fig. 21b1, b2). But UV uncaging activated expression of CFP that again co-localized with Eos expression (Fig. 21c1, c2), implying successful induction of kRasG12V expression by photon illumination. Another side advantage of employing Eos [217] in UV uncaging was that Eos could converse itself from green fluorescence to red upon UV (~390nm) exposure. As presented in Fig. 21(a1, a2), Eos fluorescent protein was switched from green to red only in the region that was exposed to UV illumination. This color conversion served a perfect label for cells in which expression of kRasG12V was induced via UV uncaging.

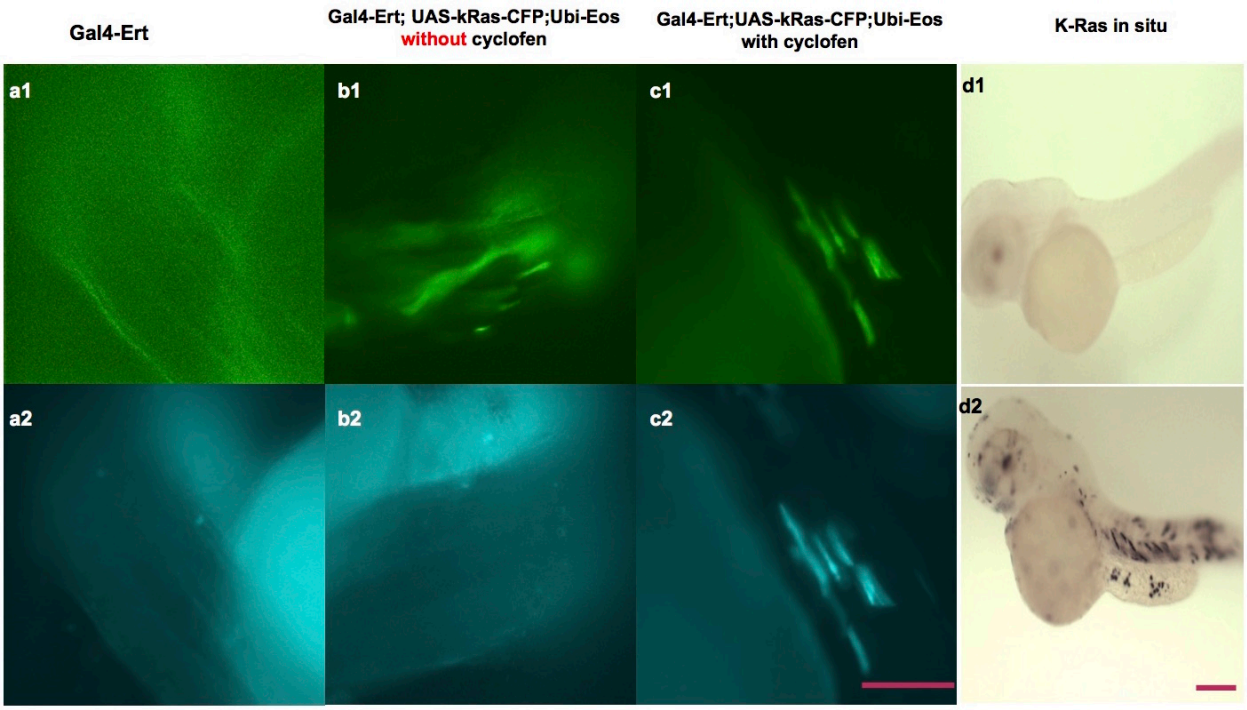

Figure 20. K-RasG12V induction by native cyclofen. Compared to non-injected Gal4-ert embryos (**a1,a2**), injecting UAS:K-Ras-T2A-CFP;Ubi:Eos plasmid into Gal4-ert embryos generated Eos protein(**b1**), but no CFP(**b2**). However, treating with 2uM cyclofen at 1dpf (day post fertilization) activated expression of CFP(**c2**). K-Ras induction together with CFP expression was confirmed by K-Ras mRNA *in situ* hybridization. Human K-Ras mRNA was transcribed only in embryos treated by cyclofen(**d2**) without detectable leakage(**d1**). Scale bar: 100μm

3.4.2 Delineating patterns of transient and permanent expression of kRasG12V

As previously stated, the two systems we developed were designed to transiently and permanently activate kRasG12V expression. We investigated dynamic patterns of both systems by tracking the expression of fluorescent proteins as well as the expression of mRNA (Fig. 22). For the transient system, about 200 picoliter of uas:kRasG12V-T2A-CFP plasmid (25ng/uL) mixed with tol2 mRNA (100ng/uL) was injected into Gal4-ert embryos at one-cell stage. Permanent activation was attained by co-injecting uas:cre (25ng/uL) and ubi:loxp-Eosfp-stop-

loxp-kRasG12V-T2A-mTFP (25ng/uL) plasmids into Gal4-ert embryos together with tol2 mRNA(100ng/uL) at one-cell stage. 2uM cyclofen was added for 24 hours to activate both systems at 24hpf. Then we looked at Eos, CFP, mTFP expression changes over two weeks (Fig. 22a, b). The images showed stable Eos expression in both systems over time. However, a clear decrease of CFP after less than a week was observed in the transient system (Fig. 22a). In contrast, mTFP expression stayed fairly stable in the permanent system (Fig. 22b). Additionally, we quantitatively analyzed the ratio of fluorescent intensities (CFP/Eos, mTFP/Eos) over 50 embryos in each system. The marked drop of CFP/Eos ratio in the transient system was clear after one day and continued to rapidly descend in the first week (Fig. 22c). On the other hand, cyclofen activation on Cre/Loxp system allowed stable value of mTFP/Eos ratio over two weeks (Fig. 22d). The similar measurements on the ratio of mRNA expression (kRasG12V/Eos) were examined by RT-PCR (Fig. 22e, f). Injected embryos were treated with 2uM cyclofen at 24hpf for 24 hours (12 hours for embryos collected at 36hpf), and RT-PCR was performed on embryos collected at 36hpf, 2dpf, 3dpf, 4dpf, 5dpf and 7dpf. Results showed a gradual decrease of kRas/Eos ratio at mRNA level over a week. However, in the permanent system, in contrast to an initial ratio around 0.6 at 1dpf, the ratio of kRas/Eos mRNA increased after 24 hours and was kept as high as 1 over a week. All these results reflected similar patterns to fluorescent quantifications, validating the optical control of two different expression systems.

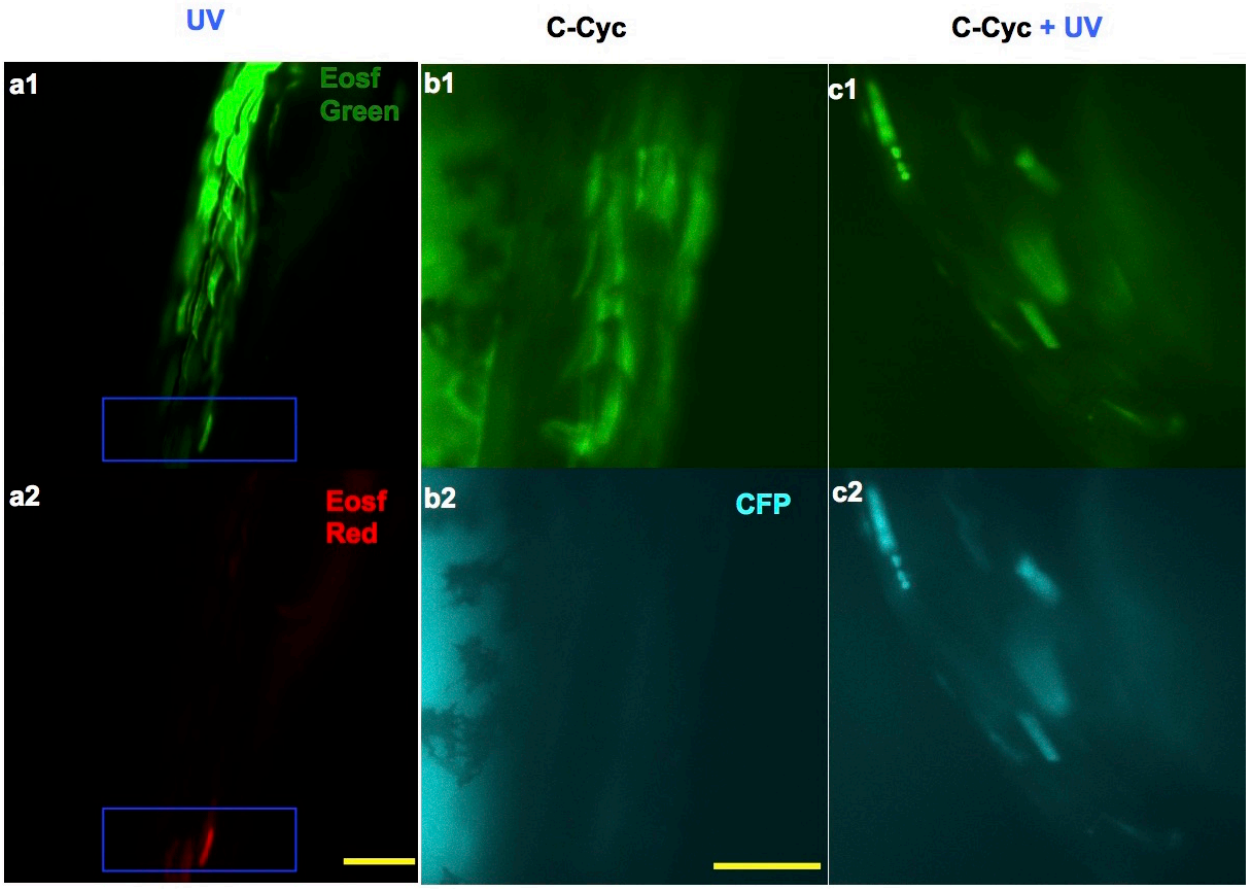

Figure 21. K-Ras induction by UV uncaging. (a1, a2)Eos protein, a light switchable fluorescent protein, serves as uncaging marker. Eos green turned into red after UV illumination (blue squared region). Gal4-ert embryos injected with UAS:K-Ras-T2A-CFP;Ubi:Eos were treated with caged cyclofen (c-Cyc) and showed no CFP expression(**b1, b2**). However, 2min UV uncaging activated the expression of CFP (**c1, c2**). Scale bar: 100μm

3.4.3 Much higher rigidity of cre-ert in controlling kRasG12V expression compared to native cre

As a side concern, we found co-injecting UAS:Cre; Ubi:Eos and Ubi:loxp-Eos-loxp-K-Ras-T2A-mTFP plasmids into Gal4-ert embryos exhibited leaking activity of cre. Minor expression of mTFP could be detected the next day after co-injection even without the cyclofen treatment (Fig.

23a1, a2). Nonetheless, the ratio of mTFP/Eos significantly increased once 2uM cyclofen was introduced for 2 hours at 24hpf, in comparison to those untreated with cyclofen (Fig. 23d.). The minor and basal leakage of cre activity from uas:cre was not so surprised since the leaky issue has been reported in previous reports within different species including mice and fish [218-220]. Despite the basal leakage, the system still allowed for a relatively productive control on kRasG12V induction (Fig. 23d). In light of the challenge that might rise in photon uncaging, we further exploited an alternative approach to achieve permanent activation of kRasG12V, in a much more rigid manner. As demonstrated in Fig.19c, ubi:loxp-Eosfp-stop-loxp-kRasG12V-T2A-mTFP plasmid was injected into Cre-ert embryos at one-cell stage. Healthy embryos expressing Eos were selected and incubated in 4uM caged cyclofen for 2 hours at 24hpf following a brief rinsing in the E3 medium. Some embryos were kept in the darkness to develop, while others were selected for 2min UV uncaging. Embryos were then covered with aluminum foil and transferred into a culturing incubator for imaging next day. The results showed that incubation in caged cyclofen without UV uncaging failed to activate mTFP expression (Fig. 23b1, b2), which indicated both non-existence of activity leakage from cre-ert and caged cyclofen. On the other hand, 2 min UV uncaging successfully turned on mTFP expression (Fig. 23c1, c2). Allover, we demonstrated here that two approaches were tested in controlling the permanent induction of kRasG12V expression. Concerning the basal leaking activity of uas:cre and its possible pitfall of adopting optical tool in the control system, a more rigid approach utilizing cre-ert showed better promise in spatiotemporally activating kRasG12V expression in the live zebrafish.

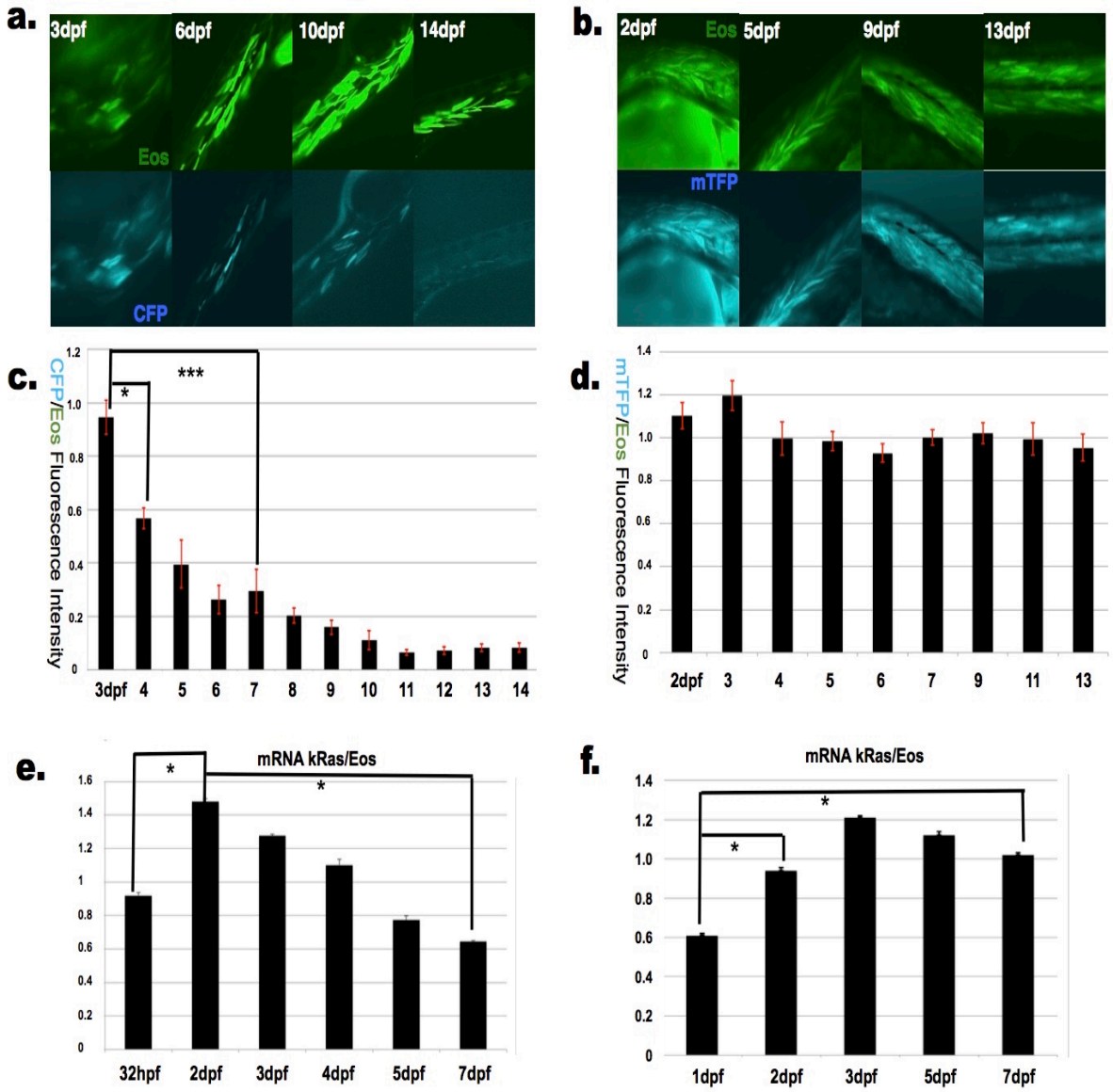

Figure 22. Maintenance of K-Ras over time after transient and permanent cyclofen activation. (**a.**) Transient K-Ras induction was achieved by injecting UAS:K-Ras-T2A-CFP; Ubi:Eos plasmid into Gal4-ert embryos followed by transient cyclofen treatment. (**b.**) Permanent induction was introduced by co-injecting UAS:Cre; Ubi:Eos and Ubi:loxp-Eos-loxp-K-Ras-T2A-mTFP plasmids into Gal4-ert embryos. Quantitative measurements of kRas maintenance showed gradual decrease of K-Ras expression in transient induction(**c, e.**), but constant K-Ras expression in permanent induction (**d, f.**).

3.4.4 Tumor induction by transient and permanent expression of kRasG12V

After we validated the tool we developed, we further tested the possibilities of inducing tumor in various conditions. Firstly, transient activation of kRasG12V was driven by 2-hour cyclofen incubation or caged cyclofen uncaging at 24hpf in gal4-ert embryos injected with uas:kRasG12V-T2A-CFP plasmid at one-cell stage. Healthily developing embryos at 3dpf were selected for further observations. No appreciable tumorigenesis was detected in early embryogenesis till 10dpf (data not shown), and those embryos were transferred to fish facility to continue grow. After six months, representative fish were taken out for imaging and pathological analysis. We found normally developed fish (Fig. 24a) with visible expression of Eos (Fig. 24b), but no more CFP (Fig. 24c). H&E staining also showed normal tissue structure (Fig. 24d, e).

Since a very short pulse of kRasG12V induction failed to induce tumor, we tried introducing periodic kRasG12V activation by treating the fish in 2uM cyclofen for 24 hours every five days till the fish reached one-month old. In this case, several fish bearing tumor were seen after 6 months (Fig. 24f). Similarly, the fish were analyzed by fluorescent imaging as well as H&E staining. Among those fish, we detected both Eos and CFP expression (Fig. 24g,h), and tumor cells were strongly revealed by H&E staining (Fig. 24i,j).

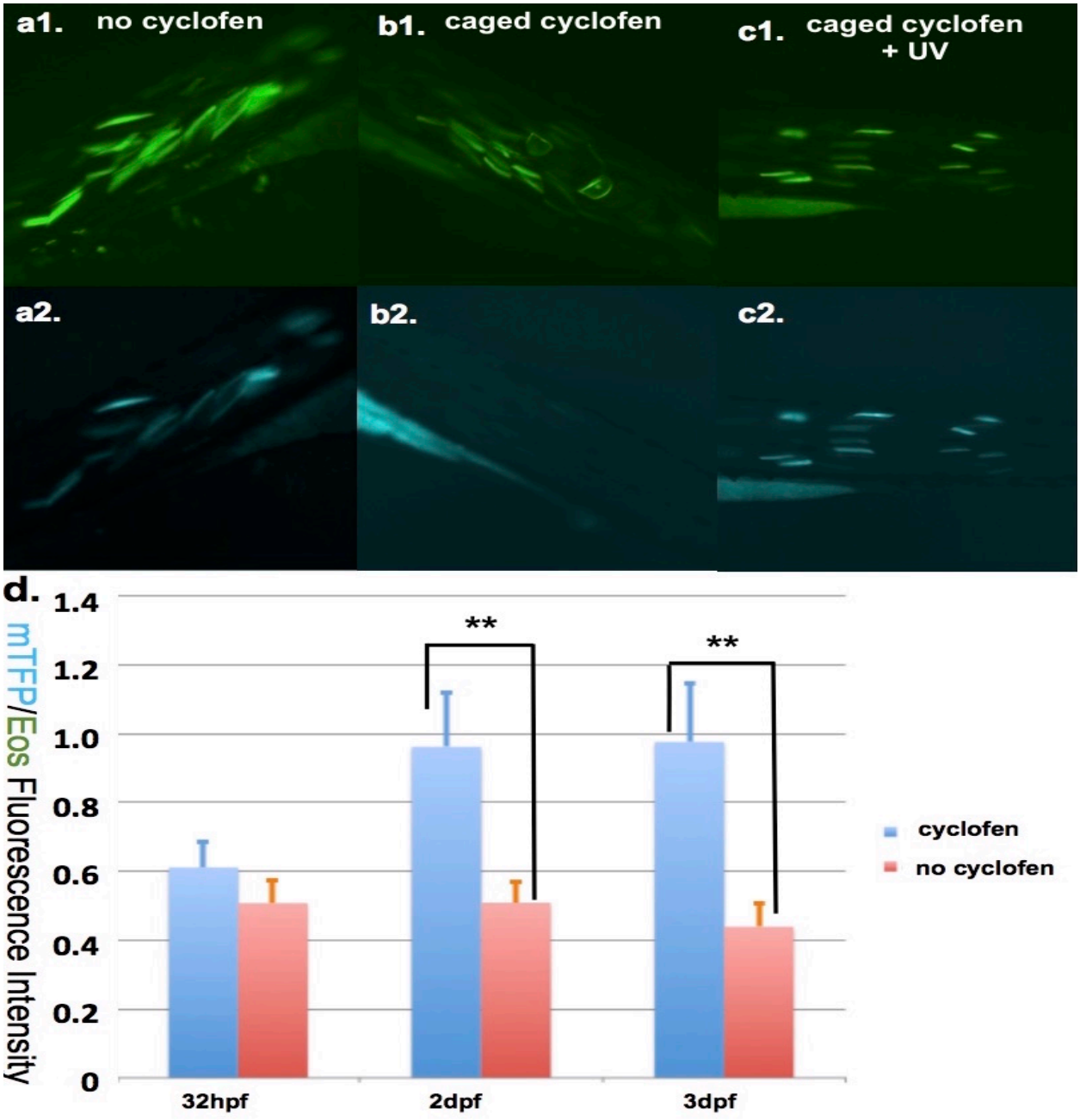

Figure 23. Basal leakage of cre activity and much higher rigidity of Cre-ert. (a1, a2) Leakage of mTFP expression was detected at 2dpf after co-injecting UAS:Cre; Ubi:Eos and Ubi:loxp-Eos-loxp-K-Ras-T2A-mTFP plasmids into Gal4-ert embryos even without cyclofen treatment. Although mTFP expression could be enhanced by cyclofen, basal leakage still exhibited (d.). However, injecting ubi:loxp-Eosfp-stop-loxp-kRasG12V-T2A-mTFP plasmid into ubi:cre-ert embryos showed no detectable mTFP expression after caged cyclfoen treatment without uncaging (b1,b2), while UV uncaging effectively turned on mTFP expression (c1,c2).

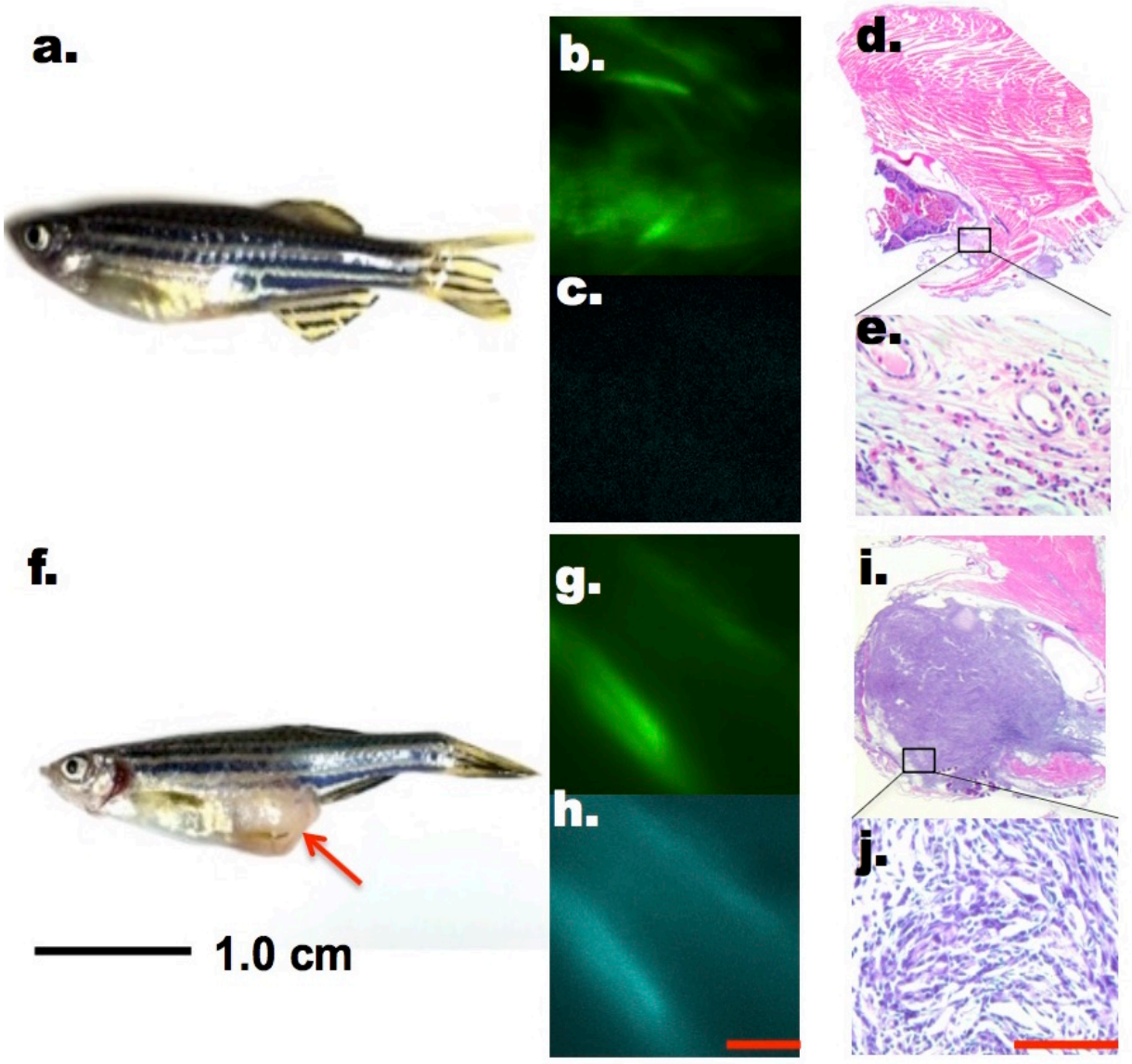

Figure 24. Tumorigenic phenotype of fish treated with one-time and periodic cyclofen induction. In the transient system, cyclofen was administered only one time at 1dpf (**a., b., c., d., e.**) or every five days for 24 hours (**f., g., h., i., j.**). In the 6-month old fish, one-time induction showed no CFP (**c.**) while CFP still existed in the fish periodically treated with cyclofen (**h.**). Tumor was observed in some fish periodically treated with cyclofen (**f.**). H&E staining showed distinct cancerous phenotypes in those fish (**i., j.**).

In parallel to transient activation of kRasG12V, we also investigated tumor development caused by permanent expression of kRasG12V. Gal4-ert embryos were co-injected with uas:cre and ubi:loxp-Eosfp-stop-loxp-kRasG12V-T2A-mTFP plasmids together with tol2 mRNA at one-cell stage. One day later, healthy embryos expressing Eos were selected, and some embryos were treated with cyclofen for 2 hours or caged cyclfoen uncaging. All treated embryos together with control were attentively cared and monitored. Tumorigenic phenotypes in some embryos could be readily observed at 5dpf (Fig. 25a). Tumorigenic embryos indicated by strong mTFP expression were taken for H&E staining (Fig. 25b, c). Furthermore, instead of gal4-ert embryos, we did the similar activation of kRasG12V expression in gal4-ert embryos with loss of p53 gene function. And this indeed promoted tumorigenesis in embryos at an early developmental stage (Fig. 25d, e, f, g).

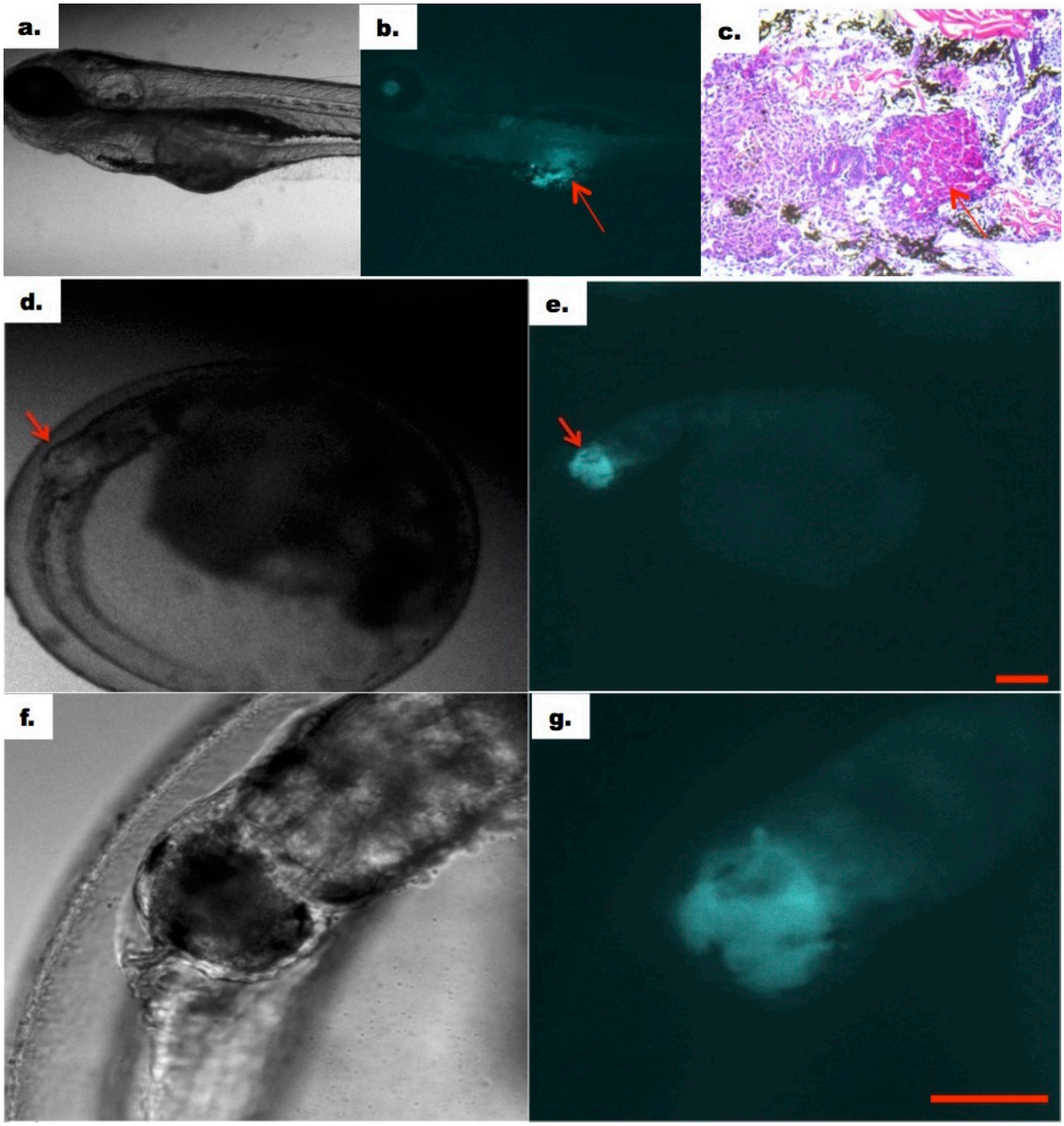

Figure 25. Permanent K-Ras induction in both wild type and p53 mutant embryos. Permanent induction of K-RasG12V at the early embryonic stage in gal4-ert embryos (**a., b., c.**) and in gal4-ert; p53-/- embryos (**d., e., f., g.**) showed tumorigenic phenotypes caused by K-Ras activation. Scale bar: 100μm

3.4.5 Characterizing the correlation between tumorigenesis probability and kRasG12V expression level

Thus far, we showed that induction of kRasG12V expression in early developing embryos, not always, but in some cases, did lead to tumor growth. An interesting and radically important question is what kept certain fish, but not the other from getting tumor, even the oncogene was turned on permanently in all the fish. An initial and forthright thought was to link tumorigenic rate to oncogenic expression level, in particular, the number of cells activated of kRasG12V expression. To elucidate the correlation, here we only focused on permanent activation of kRasG12V since transient activation had been observed to diminish shortly and had been less efficient in causing tumorigenesis.

In this experiment, we injected ubi:loxp-Eosfp-stop-loxp-kRasG12V-T2A-mTFP plasmid together with the tol2 mRNA into Cre-ert embryos at one-cell stage. Compared to co-injection of uas:cre and ubi:loxp-Eosfp-stop-loxp-kRasG12V-T2A-mTFP plasmids, this approach turned out to be more tightly controlled by optical activation (data not shown). Permanent expression of kRasG12V was activated at 24hpf by either cyclofen or caged cyclofen uncaging. Only healthily developed embryos at 3dpf were selected for continuing analysis, and tumorigenesis rates were measured since after till 8dpf. First of all, activation of kRasG12V, either by native cyclofen or caged cyclofen uncaging, resulted in significant increase of tumorigenesis (Fig. 26 a, c), which was implied by our earlier observations. Moreover, we split embryos into two subgroups after cyclofen activation according to the number of cells they carried at 3pdf. We found the group with more than 50 mTFP-expressing cells at 3dpf resulted in a much higher tumorigenic rate than the group with less than 50 mTFP-expression cells at 3dpf (Fig. 26 b, d).

a.

8dpf Fish	Cyclofen	No Cyclofen	Caged Cyclofen +UV	Caged Cyclofen
Tumorigenic Rate	21/95	4/99	18/35	3/22

b.

mTFP Expressing Cell Number	>50 cells	<50cells
Tumorigenic Rate	11/27	6/68

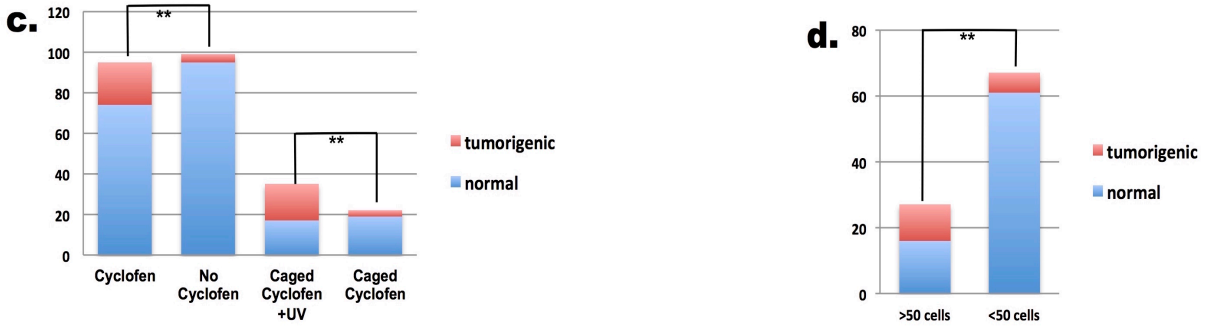

Figure 26. Statistics of early tumorigenesis in embryos manipulated in different conditions. Ubi:cre-ert embryos injected with ubi:loxp-Eos-stop-loxp-kRas-T2A-mTFP plasmid were split into cyclofen, no cyclofen, caged cyclofen +UV and caged cyclofen groups. Tumorigenic rates were measured for each group from 3dpf to 8dpf (**a,b**). For cyclofen group, embryos were binned into two sub-groups based on mTFP expression level within individual embryo at 3dpf, and tumorigenic rates were measured for each sub-group (**c,d**) (** $p<0.01$).

3.4.6 Optical activation and labeling of kRasG12V expression in a small group of cells in the zebrafish embryo

The fundamental challenge of understanding cancer initiation and evolution lies in the difficulties looking into the very early tumorigenic event in single cells. Lastly, we aimed to prove that, with the tool we developed, one would be able to activate oncogenic expression in a small number of cells without limitation to cell or tissue types. Again, we injected ubi:loxp-Eosfp-stop-loxp-kRasG12V-T2A-mTFP plasmids together with tol2 mRNA into Cre-ert embryos at one-cell stage. Embryos expressing Eos was selected at 24hpf, and some of them

were incubated in 4uM caged cyclofen for 2 hours in complete darkness. Then some embryos were moved to microscopic stage for UV uncaging after they were briefly rinsed in the E3 medium for 2 minutes.

A Lumencor LED UV light (~396nm) connected to a Nikon microscope served as the light source for uncaging. Localized activation of kRasG12V was achieved by tuning an iris, which focalized the illumination area to only a group of cells (Fig. 27c). Before UV illumination, Eos stayed in green form and no Eos red fluorescence was detected (Fig. 27a, b). However, substantial Eos green fluorescence was switched to red form (Fig. 27d, e), and conversion only happened in cells that were illuminated (Fig. 27f). This conversion served as a great marker for cells in which expression of kRasG12V was activated.

Following UV uncaging, embryos were put back in the E3 medium and grew at 28°C. 15 hours later, embryos were taken out for imaging. And indeed, only in cells with label of Eos red fluorescence showed mTFP expression, which indicated successful activation of kRasG12V in those cells (Fig. 27g, h, i). Although in this instance, activation of kRasG12V in a small number of cells has not generated tumor in Cre-ert embryos, our method demonstrated a powerful tool of manipulating oncogenic expression in a small number of cells in live zebrafish embryos. Further work will use the tool to understand exactly how some oncogenic mutations in a single cell leads to tumor, and on the fortunate side, why most oncogenic mutations in a single cell are not able to do so.

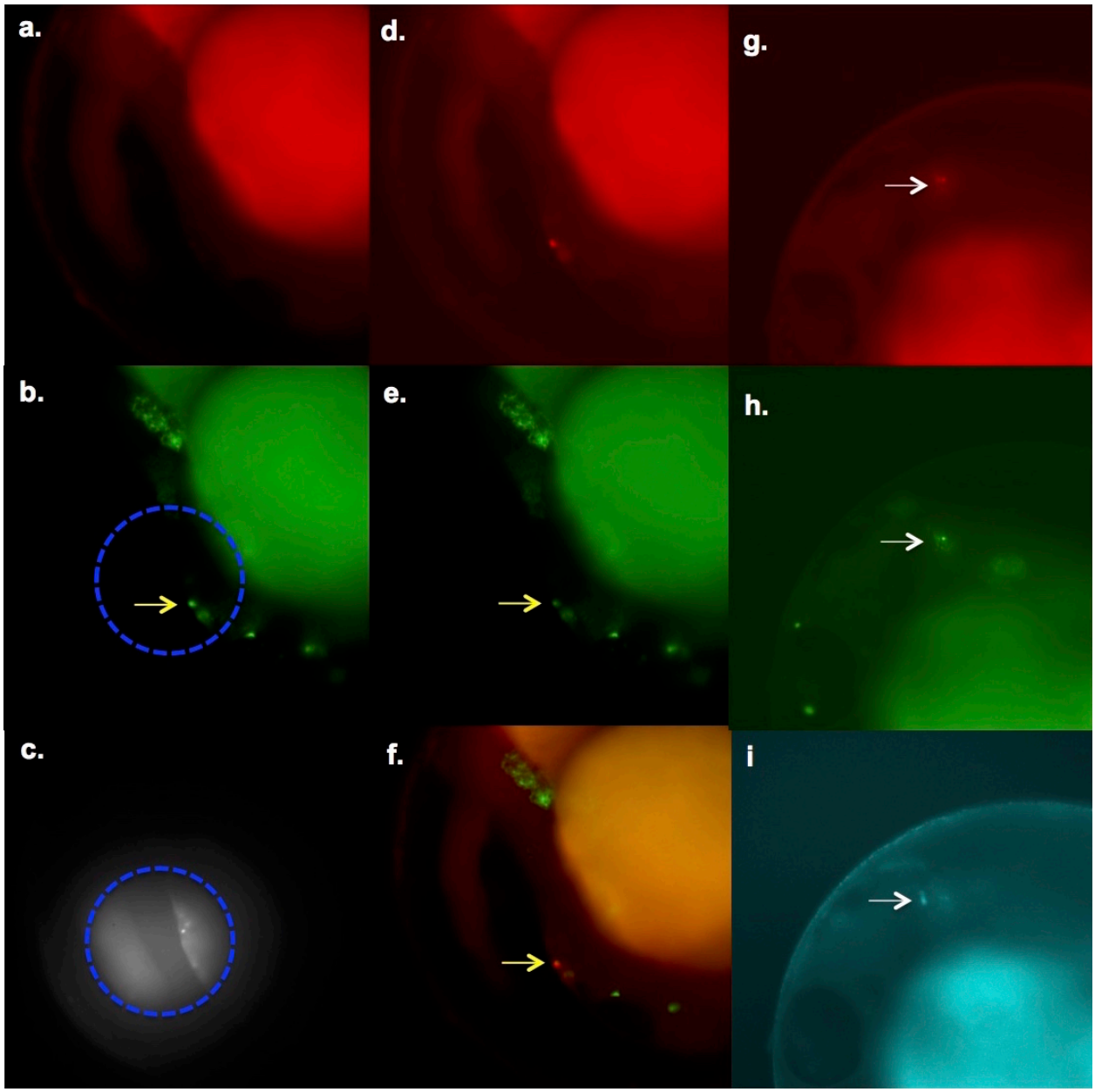

Figure 27. K-RasG12V activation and tracking in a small group of cells within a live zebrafish embryo. A 1dpf embryo was incubated in 3uM caged cyclofen for 3 hours under dark condition, and then transferred into the E3 medium before it was put on microscopic stage for uncaging. 2 minute UV (~400nm) was introduced to uncage the caged molecule at selected region (**b., c.**). Eos fluorescent protein expression was imaged before (**a., b., c.**) and after (**d., e., f.**) UV illumination. UV uncaging significantly converted most of Eos protein from green to red (**a., d.**), and overlay image (**f.**) showed Eos conversion was specifically limited to cells exposed to light. 24 hours later, the same embryo was imaged for oncogene expression (**g., h., i.**). K-RasG12V activation indicated by mTFP expression (**i.**, see arrow) co-localized with Eos red fluorescence, but was not seen in other cells only expressing Eos green fluorescence.

3.5 DISSCUSION

In this work, we demonstrated a powerful optical tool to activate oncogenic expression in a live zebrafish. Combining myriad advantages of imaging cancer in the zebrafish[194, 221-224], this technique could be utilized in generating cancer models to understand cancer initiation and evolution. Current theories of cancer evolution believe cancer derives from mutations of proto-oncogenes or tumor suppressor genes that lead to clonal expansion[20, 225-231]. In recent years, more and more studies[232-234] focus on interpreting cancer progression from evolutionary perspectives. Clearer explanation of cancer initiation and evolution requires more sophisticated approaches to look at cellular alternations in single cells from early tumorigenic stage. The optical tool we developed allows a robust control of activating oncogenic expression at high spatiotemporal resolution that could reach a small group of cells. We found that a short pulse of kRasG12V expression in embryos without additional oncogenic predispositions usually failed to cause cancer. This can be explained because cancer is usually induced by more than one oncogenic mutation[235, 236]. Such a short time of kRasG12V activation might not be enough to drive further oncogenic shocks. Reasonably, periodic and permanent activation of kRasG12V expression both increased tumorigenic rates. Since the incidence of mutation in a specific cell depends on its mutation rate and its numbers of mitoses, periodic and permanent activation could possibly promote the probability of sequential mutations within transformed cells.

Although we found a basal activity leakage from uas:cre expression which has otherwise been reported in many other studies. On the other hand, cyclofen has proven effective to significantly enhance mTFP expression regardless of minor expression leakage. Therefore, to a certain extent,

this approach could be still credited as a valid inducible system to control kRasG12V expression. Detectable leaking expression of mTFP has been induced from uas:cre, while no kras or CFP leakage is observed from uas:kras-T2A-CFP within the live organism. This, on the contrary, implies relatively tight expression control driven by the uas promoter. Expression of mTFP has consequently been signified because the loxp sequences are highly sensitive to even a small amount of cre protein that leaks from uas:cre element. Additionally, in light of possible perplexities that could be caused by even a minor leaking activity of cre, we adapt another more restrictive component to photo-activate kRasG12V. A ubi:cre-ert fish line demonstrates much better and tighter control of kRasG12V induction via UV uncaging. Furthermore, adding the loss of p53 together with permanent activation of kRasG12V substantially promoted tumorigenesis even in early developing embryos. All these observations comply with conventional theories of cancer initiation[237-241].

Profiling the correlation between tumorigenic rate and the number of kRasG12V expressing cells in an individual zebrafish revealed a highly correlative connection. This is not so surprising either, given that more initial oncogenic activation increases the probability of driving further mutations. An interesting question to ask shall help test the theory of “bad luck” in cancer. Is the possibility of cancer arising from a specific tissue simply proportional to its stem cells’ division numbers? The tool demonstrated here could be implemented to induce an initial kRasG12V expression in tissues with different capabilities of stem cell divisions. Then one will be able to find out whether an initial oncogenic mutation in tissue with higher stem cell division is more susceptible to developing cancer. Yet, a caution shall be noted that different species and organs might respond to a certain oncogenic mutation such as kRasG12V differently[242, 243]. In this

case, the oncogenes need to be carefully chosen to test the mathematical “bad luck” theory. On the other hand, our technique will be extremely helpful to evaluate how different organs and tissues respond to the same oncogenic induction differently in terms of tumor formation. More importantly, successful demonstration of activating and labeling kRasG12V expression in a small number of cells by photons makes this technique extremely powerful to study early initiation and evolution of cancer. For example, this will be significantly helpful to look at how microenvironments promote or halt cancer progression at an early stage[244-246], and solve many other recent controversies such as dependences of tumor development on stem cell division rate[191] and cellular migration activities[247]. Ultimately, the march toward investigating and understanding cancer initiation would lead to developing novel and effective barriers to, and treatments for cancer.

CHAPTER FOUR:

CONCLUSIONS AND FUTURE DIRECTIONS

This dissertation reviews the rising field of introducing optical tools to understanding complex biological networks, which could otherwise not be possibly investigated by conventional approaches. Enabling light control over physiological molecules provides an unprecedented spatiotemporal resolution, often times in noninvasive ways. Leading researches over the past years have substantially demonstrated the power of optogenetic tools in manipulating neuronal activities. Free from physical contact and invasion, *in vivo* neuronal manipulation and activity recording can be achieved via optogenetics by genetically engineering photo-responding proteins in live organisms [143, 248, 249]. In addition to light sensitive proteins such as photoreceptors, chemical and genetic approaches now enable light-sensitivity with a protein of interest, by whose nature is not so [250]. Those efforts have greatly expanded the realm of which subjects could be investigated by optical tools. Besides its huge popularity and powerful capability in studying neuroscience, optical control of biological processes could also be extremely helpful to reveal fundamental problems in other fields of study. My work, which has been elaborated in this dissertation, applies optical manipulations on retinoic acid photo-isomerization to reveal its controversial role in hindbrain patterning; and on photo-uncaging to initiate oncogenic expression in the live zebrafish.

Photo-isomerization of active all-trans RA and inactive 13-cis RA yields a quantitative, spatiotemporal control of RA activity in a developing zebrafish embryo. With the optical control at such a high spatial resolution, we are able to specifically isomerize RA in selected cells of different fates. We have shown that in an embryo of which native RA synthesis is inhibited, one is only able to observe rescue of hindbrain development later if all-trans RA is released in cells that are destined to develop into head. In contrast, activation of all-trans RA in cells that will

develop into tail fails to render rescue of normal rhombomere patterning. What we have reported here clarifies and augments the long-controversial claiming to retinoic acid's playing role as a morphogen in vertebrate patterning. After all, the retinoic acid activity we have perturbed here would not be considered from endogenous regulation. It has been demonstrated that measuring endogenous retinoic acid in live developing embryos is extremely challenging due to retinoic acid's low quantity in the cells. Nonetheless, a recent tool has attempted at profiling endogenous RA gradient via genetically encoded fluorescent probes [251]. Regardless of concerns on accuracy, this approach serves as another great example of how optically physiological sensor could facilitate our understanding of complex biological networks.

A more interesting and unresolved question rises in our project that developing embryos at early stage could still obtain partial hindbrain rescue when a very short pulse of RA exposure is given. This unexpected phenomenon even happens with embryos at one-cell stage when cellular RA binding proteins would not be expected, let alone the existence of RA synthesizing enzymes. All observations so far hint a relatively strong sequestration of early RA pulse within the developing embryos via certain mysterious binding molecules. However, rescue of hindbrain disappears when the RA pulse is administrated before fertilization indicates that the binding molecules are not readily available before sperms come in. Defined methods are required to reveal what molecules are responsible for early RA sequestration. In the fact that binding molecules are highly likely to be certain proteins, one possible approach is to tag retinoic acid-binding proteins by photo-labeling the proteins [252]. Then antibodies targeting retionic acid conjugated protein could help pull down the photo-labeled complex. The complex comprising the target proteins could then be further assayed on a gel and by mass-spectrometry. Actually we have made

substantial efforts to pin down the proteins by this way. Unfortunately, no consistent results yielded so far. This could be due to a very low level of RA, or a foul specificity of the antibody we chose, or simply bad efficiency of photoaffinity labeling. Besides the endeavors to disseminate exact proteins that bind to an early pulse of RA, characterizing spatial the distribution of RA after early sequestration would also avail to investigate the phenomenon. To this extent, other indirect means may come forth by, for example, using a carbon 14 retinoic acid as a radioactive tracer. The radiolabeled retinoic acid, imaged by positron emission tomography could reveal how the RA pulse is spatially sequestered within developing embryo [253]. Another possible alternative without complicate labeling invites a recent technology based on fluorescence lifetime imaging microscopy and phasor analysis [254]. This novel tool developed by the lab of Schilling. T takes advantage of native auto-fluoresces displayed in certain cellular metabolites and their noises in developing systems. In this way, endogenous and externally introduced retinoic acid could be nicely delineated in a live embryo.

The second project presents a powerful tool to control oncogenic induction in a live zebrafish via photon uncaging. We have successfully built two different systems to transiently and permanently induce a human oncogene, kRasG12V's expression in a live zebrafish. In addition, we have shown how florescent reporters could help label transformed cells. Tumorigenesis under various conditions has been assayed and has been correlated to numbers of transformed cells in individual fish. Howbeit, the effort stated here serves as an important and powerful platform to further and advance our exploration. Ongoing tasks include testing oncogenic induction in different tissue types with the stable ubi:loxp-eosf-stop-loxp-kRasG12V-T2A-mTFP line we made, as well as achieving oncogenic activation from a single cell that is most likely to raise

tumor. We have already shown that by crossing ubi:loxp-eosf-stop-loxp-kRasG12V-T2A-mTFP fish with ubi:cre-ert fish, one is able to activate kRasG12V expression globally with cyclofen treatment (Fig. 28). More statistics and analysis will be collected on the stable, homologous ubi:cre-ert; ubi:loxp-eosf-stop-loxp-kRasG12V-T2A-mTFP line.

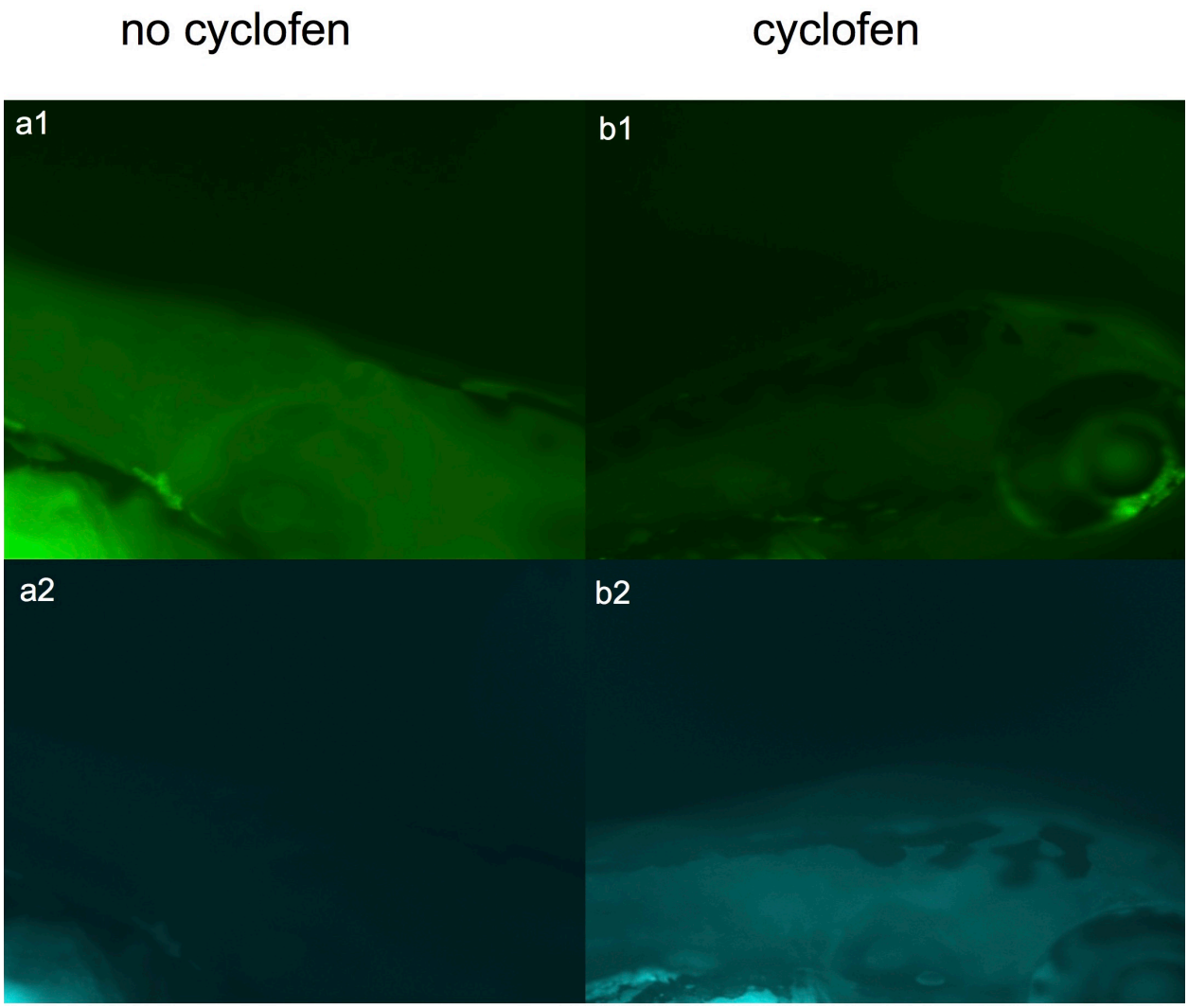

Figure 28. Global induction of kRasG12V expression in the heterozygous ubi:cre-ert; ubi:loxp-eosf-stop-loxp-kRasG12V-T2A-mTFP embryo. Embryos produced by crossing ubi:cre-ert and ubi: loxp-eosf-stop-loxp-kRasG12V-T2A-mTFP fish were treated with or without 2uM cyclofen at 24hpf for 4 hours. Cyclofen treatments activated mTFP expression that indicated oncogene induction (b1, b2), while control group only exhibited Eos expression (a1, a2).

According to our current observations, kRasG12V induction in a small number of cells, or for a short period of time in wild type background is not likely to cause tumor. We will probably need to elicit additional cancer-promoting agents such as immune-deficiency [255] or loss of tumor suppressors [204]. Once an adept inducible cancer model has been validated, one will be able to answer many standing puzzles of how cancer evolves from a single cell origin. Furthermore, the model we developed here will also be extremely valuable to test anti-cancer theories. A recent discovery has found the existence of multiple copies of a tumor-suppressor gene, TP53, might offer elephants great armor to fight cancer [256]. Therefore, one foreseeing example will call for inquest into whether and how up-regulating expression of certain tumor-suppressor genes could effectively prevent cancer. Another benefit stemming from the technique would be testing anti-cancer molecules, which could promisingly restrain or eliminate transformed cells at the initial stage. Overall, the development and validation of our technology that exploits optical tool in controlling cancer initiation from single cells in live animal could render an unprecedented feasibility and resolution on investigating cancer evolution theories and promoting cancer therapies and prevention strategies.

REFERENCES:

1. Rouault, H. and V. Hakim, *Different Cell Fates from Cell-Cell Interactions: Core Architectures of Two-Cell Bistable Networks*. Biophysical Journal, 2012. **102**(3): p. 417-426.
2. Francois, P. and V. Hakim, *Design of genetic networks with specified functions by evolution in silico*. Proceedings of the National Academy of Sciences of the United States of America, 2004. **101**(2): p. 580-585.
3. Turing, A.M., *The Chemical Basis of Morphogenesis*. Philosophical Transactions of the Royal Society of London Series B-Biological Sciences, 1952. **237**(641): p. 37-72.
4. Wolpert, L., *Citation-Classic - Positional Information and the Spatial Pattern of Cellular-Differentiation*. Current Contents/Life Sciences, 1986(3): p. 19-19.
5. Porcher, A. and N. Dostatni, *The Bicoid Morphogen System*. Current Biology, 2010. **20**(5): p. R249-R254.
6. Eldar, A., et al., *Self-enhanced ligand degradation underlies robustness of morphogen gradients*. Developmental Cell, 2003. **5**(4): p. 635-646.
7. Rhinn, M. and P. Dolle, *Retinoic acid signalling during development*. Development, 2012. **139**(5): p. 843-858.
8. Avantaggiato, V., et al., *Retinoic acid induces stage-specific repatterning of the rostral central nervous system*. Developmental Biology, 1996. **175**(2): p. 347-357.
9. Durston, A.J., et al., *Retinoic Acid Causes an Anteroposterior Transformation in the Developing Central Nervous-System*. Nature, 1989. **340**(6229): p. 140-144.

10. Bayha, E., et al., *Retinoic Acid Signaling Organizes Endodermal Organ Specification along the Entire Antero-Posterior Axis*. Plos One, 2009. **4**(6).

11. Franceschi, R.T., *Retinoic Acid - Morphogen or More Mysteries*. Nutrition Reviews, 1992. **50**(1): p. 19-20.

12. Noji, S., et al., *Retinoic Acid Induces Polarizing Activity but Is Unlikely to Be a Morphogen in the Chick Limb Bud*. Nature, 1991. **350**(6313): p. 83-86.

13. Green, J.B.A., *Retinoic Acid - the Morphogen of the Main Body Axis*. Bioessays, 1990. **12**(9): p. 437-439.

14. Lampert, J.M., et al., *Provitamin A conversion to retinal via the beta,beta-carotene-15,15 '-oxygenase (bcox) is essential for pattern formation and differentiation during zebrafish embryogenesis*. Development, 2003. **130**(10): p. 2173-2186.

15. White, R.J., et al., *Complex regulation of cyp26a1 creates a robust retinoic acid gradient in the zebrafish embryo*. Plos Biology, 2007. **5**(11): p. 2522-2533.

16. Pennimpede, T., et al., *The Role of CYP26 Enzymes in Defining Appropriate Retinoic Acid Exposure during Embryogenesis*. Birth Defects Research Part a-Clinical and Molecular Teratology, 2010. **88**(10): p. 883-894.

17. Helms, J., C. Thaller, and G. Eichele, *Relationship between Retinoic Acid and Sonic Hedgehog, 2 Polarizing Signals in the Chick Wing Bud*. Development, 1994. **120**(11): p. 3267-3274.

18. Maves, L. and C.B. Kimmel, *Dynamic and sequential patterning of the zebrafish posterior hindbrain by retinoic acid*. Developmental Biology, 2005. **285**(2): p. 593-605.

19. Hanahan, D. and R.A. Weinberg, *Hallmarks of cancer: the next generation*. Cell, 2011. **144**(5): p. 646-74.

20. Nowell, P.C., *The clonal evolution of tumor cell populations*. Science, 1976. **194**(4260): p. 23-8.

21. Bonnet, D. and J.E. Dick, *Human acute myeloid leukemia is organized as a hierarchy that originates from a primitive hematopoietic cell*. Nature Medicine, 1997. **3**(7): p. 730-737.

22. Lawson, D.A. and O.N. Witte, *Stem cells in prostate cancer initiation and progression*. Journal of Clinical Investigation, 2007. **117**(8): p. 2044-2050.

23. Tysnes, B.B. and R. Bjerkvig, *Cancer initiation and progression: Involvement of stem cells and the micro environment*. Biochimica Et Biophysica Acta-Reviews on Cancer, 2007. **1775**(2): p. 283-297.

24. Morton, C.L. and P.J. Houghton, *Establishment of human tumor xenografts in immunodeficient mice*. Nature Protocols, 2007. **2**(2): p. 247-250.

25. Talmadge, J.E., et al., *Murine models to evaluate novel and conventional therapeutic strategies for cancer*. American Journal of Pathology, 2007. **170**(3): p. 793-804.

26. Speicher, D.W., *Proteome analysis : interpreting the genome*. 1st ed. 2004, Amsterdam ; Boston: Elsevier. xvii, 375 p.

27. Spiller, D.G., et al., *Measurement of single-cell dynamics*. Nature, 2010. **465**(7299): p. 736-745.

28. Magde, D., W.W. Webb, and E. Elson, *Thermodynamic Fluctuations in a Reacting System - Measurement by Fluorescence Correlation Spectroscopy*. Physical Review Letters, 1972. **29**(11): p. 705-&.

29. Charier, S., et al., *Reactant concentrations from fluorescence correlation spectroscopy with tailored fluorescent probes. An example of local calibration-free pH measurement*. Journal of the American Chemical Society, 2005. **127**(44): p. 15491-15505.

30. Weiss, M., et al., *Anomalous subdiffusion is a measure for cytoplasmic crowding in living cells*. Biophysical Journal, 2004. **87**(5): p. 3518-3524.

31. El-Sherif, A.A. and M.M. Shoukry, *Equilibrium investigation of complex formation reactions involving copper(II), nitrilo-tris(methyl phosphonic acid) and amino acids, peptides or DNA constitutents. The kinetics, mechanism and correlation of rates with complex stability for metal ion promoted hydrolysis of glycine methyl ester*. Journal of Coordination Chemistry, 2006. **59**(14): p. 1541-1556.

32. Berthoumieux, H., L. Jullien, and A. Lemarchand, *Response to a temperature modulation as a signature of chemical mechanisms*. Physical Review E, 2007. **76**(5).

33. Schoen, I., H. Krammer, and D. Braun, *Hybridization Kinetics Is Different Inside Cells*. Biophysical Journal, 2010. **98**(3): p. 12A-12A.

34. Lemarchand, A., et al., *Chemical Mechanism Identification from Frequency Response to Small Temperature Modulation*. Journal of Physical Chemistry A, 2012. **116**(33): p. 8455-8463.

35. Guo, M.H., Y.F. Xu, and M. Gruebele, *Temperature dependence of protein folding kinetics in living cells*. Proceedings of the National Academy of Sciences of the United States of America, 2012. **109**(44): p. 17863-17867.

36. Mettetal, J.T., et al., *The frequency dependence of osmo-adaptation in Saccharomyces cerevisiae*. Science, 2008. **319**(5862): p. 482-484.

37. Shimizu, T.S., Y.H. Tu, and H.C. Berg, *A modular gradient-sensing network for chemotaxis in Escherichia coli revealed by responses to time-varying stimuli*. Molecular Systems Biology, 2010. **6**.

38. Dhumpa, R. and M.G. Roper, *Temporal gradients in microfluidic systems to probe cellular dynamics: a review*. Anal Chim Acta, 2012. **743**: p. 9-18.

39. Tomida, T., et al., *The temporal pattern of stimulation determines the extent and duration of MAPK activation in a Caenorhabditis elegans sensory neuron*. Sci Signal, 2012. **5**(246): p. ra76.

40. Toettcher, J.E., et al., *The promise of optogenetics in cell biology: interrogating molecular circuits in space and time*. Nat Methods, 2011. **8**(1): p. 35-8.

41. Couture, O., et al., *Ultrasound internal tattooing*. Med Phys, 2011. **38**(2): p. 1116-23.

42. Petit, M., et al., *X-ray photolysis to release ligands from caged reagents by an intramolecular antenna sensitive to magnetic resonance imaging*. Angew Chem Int Ed Engl, 2011. **50**(41): p. 9708-11.

43. Geva-Zatorsky, N., et al., *Fourier analysis and systems identification of the p53 feedback loop*. Proc Natl Acad Sci U S A, 2010. **107**(30): p. 13550-5.

44. Ntziachristos, V., *Going deeper than microscopy: the optical imaging frontier in biology*. Nature Methods, 2010. **7**(8): p. 603-614.

45. Wang, L.H.V. and S. Hu, *Photoacoustic Tomography: In Vivo Imaging from Organelles to Organs*. Science, 2012. **335**(6075): p. 1458-1462.

46. Pawlicki, M., et al., *Two-Photon Absorption and the Design of Two-Photon Dyes*. Angewandte Chemie-International Edition, 2009. **48**(18): p. 3244-3266.

47. Bochet, C.G., *Photolabile protecting groups and linkers*. Journal of the Chemical Society-Perkin Transactions 1, 2002(2): p. 125-142.

48. Klan, P., et al., *Photoremovable Protecting Groups in Chemistry and Biology: Reaction Mechanisms and Efficacy*. Chemical Reviews, 2013. **113**(1): p. 119-191.

49. Mayer, G. and A. Heckel, *Biologically active molecules with a "light switch"*. Angewandte Chemie-International Edition, 2006. **45**(30): p. 4900-4921.

50. Specht, A., et al., *Photochemical tools to study dynamic biological processes*. Hfsp Journal, 2009. **3**(4): p. 255-264.

51. Fortin, D.L., et al., *Photochemical control of endogenous ion channels and cellular excitability*. Nature Methods, 2008. **5**(4): p. 331-338.

52. Pasparakis, G., et al., *Harnessing photochemical internalization with dual degradable nanoparticles for combinatorial photo-chemotherapy*. Nature Communications, 2014. **5**.

53. Gug, S., et al., *Molecular Engineering of Photoremovable Protecting Groups for Two-Photon Uncaging*. Angewandte Chemie-International Edition, 2008. **47**(49): p. 9525-9529.

54. Sebej, P., et al., *Fluorescein Analogues as Photoremovable Protecting Groups Absorbing at 520 nm*. Journal of Organic Chemistry, 2013. **78**(5): p. 1833-1843.

55. Majjigapu, J.R.R., et al., *Release and report: A new photolabile caging system with a two-photon fluorescence reporting function*. Journal of the American Chemical Society, 2005. **127**(36): p. 12458-12459.

56. Gagey, N., et al., *Two-photon uncaging with fluorescence reporting: Evaluation of the o-hydroxycinnamic platform*. Journal of the American Chemical Society, 2007. **129**(32): p. 9986-9998.

57. Stegmaier, P., J.M. Alonso, and A. del Campo, *Photoresponsive Surfaces with Two Independent Wavelength-Selective Functional Levels*. Langmuir, 2008. **24**(20): p. 11872-11879.

58. Kotzur, N., et al., *Wavelength-Selective Photoactivatable Protecting Groups for Thiols*. Journal of the American Chemical Society, 2009. **131**(46): p. 16927-16931.

59. So, P.T.C., et al., *Two-photon excitation fluorescence microscopy*. Annual Review of Biomedical Engineering, 2000. **2**: p. 399-429.

60. Riggsbee, C.W. and A. Deiters, *Recent advances in the photochemical control of protein function*. Trends in Biotechnology, 2010. **28**(9): p. 468-475.

61. Hahn, M.E. and T.W. Muir, *Photocontrol of Smad2, a multiphosphorylated cell-signaling protein, through caging of activating phosphoserines*. Angewandte Chemie-International Edition, 2004. **43**(43): p. 5800-5803.

62. De Rosa, L., et al., *Semi-Synthesis of Labeled Proteins for Spectroscopic Applications*. Molecules, 2013. **18**(1): p. 440-465.

63. Lemke, E.A., et al., *Control of protein phosphorylation with a genetically encoded photocaged amino acid*. Nat Chem Biol, 2007. **3**(12): p. 769-72.

64. Wu, N., et al., *A genetically encoded photocaged amino acid*. J Am Chem Soc, 2004. **126**(44): p. 14306-7.

65. Gautier, A., et al., *Genetically Encoded Photocontrol of Protein Localization in Mammalian Cells*. Journal of the American Chemical Society, 2010. **132**(12): p. 4086-+.

66. Gautier, A., A. Deiters, and J.W. Chin, *Light-Activated Kinases Enable Temporal Dissection of Signaling Networks in Living Cells*. Journal of the American Chemical Society, 2011. **133**(7): p. 2124-2127.

67. Li, H., J.M. Hah, and D.S. Lawrence, *Light-mediated liberation of enzymatic activity: "Small Molecule" caged protein equivalents*. Journal of the American Chemical Society, 2008. **130**(32): p. 10474-+.

68. Kala, A., et al., *The synthesis of tetra-modified RNA for the multidimensional control of gene expression via light-activated RNA interference*. Nature Protocols, 2014. **9**(1): p. 11-20.

69. Hemphill, J., et al., *Genetically Encoded Light-Activated Transcription for Spatiotemporal Control of Gene Expression and Gene Silencing in Mammalian Cells*. Journal of the American Chemical Society, 2013. **135**(36): p. 13433-13439.

70. Sauers, D.J., et al., *Light-Activated Gene Expression Directs Segregation of Co-cultured Cells in Vitro*. Acs Chemical Biology, 2010. **5**(3): p. 313-320.

71. Yamaguchi, S., et al., *Light-activated gene expression from site-specific caged DNA with a biotinylated photolabile protection group*. Chemical Communications, 2010. **46**(13): p. 2244-2246.

72. Tang, X., et al., *Regulating gene expression in human leukemia cells using light-activated oligodeoxynucleotides*. Nucleic Acids Research, 2008. **36**(2): p. 559-569.

73. Dmochowski, I.J., *Light-activated oligonucleotides for controlling gene expression*. Abstracts of Papers of the American Chemical Society, 2007. **234**.

74. Obara, P.A., et al., *PWA-diureasils organic-inorganic hybrids. Photochromism and effect of the organic chain length*. Optical Materials, 2015. **46**: p. 64-69.

75. Jin, M., et al., *Photochromism-based detection of volatile organic compounds by W-doped TiO2 nanofibers*. Journal of Colloid and Interface Science, 2011. **362**(1): p. 188-193.

76. Zhang, G.J. and J.N. Yao, *Photochromism of inorganic/organic ultra-thin films*. Advances in Optical Data Storage Technology, 2005. **5643**: p. 79-87.

77. Bouas-Laurent, H. and H. Durr, *Organic photochromism*. Pure and Applied Chemistry, 2001. **73**(4): p. 639-665.

78. Hampp, N., *Bacteriorhodopsin as a photochromic retinal protein for optical memories*. Chemical Reviews, 2000. **100**(5): p. 1755-1776.

79. Bhoo, S.H., et al., *Bacteriophytochromes are photochromic histidine kinases using a biliverdin chromophore*. Nature, 2001. **414**(6865): p. 776-779.

80. Scheerer, P., et al., *Light-Induced Conformational Changes of the Chromophore and the Protein in Phytochromes: Bacterial Phytochromes as Model Systems*. Chemphyschem, 2010. **11**(6): p. 1090-1105.

81. Drepper, T., et al., *Lights on and action! Controlling microbial gene expression by light*. Applied Microbiology and Biotechnology, 2011. **90**(1): p. 23-40.

82. Xu, L., et al., *Spatiotemporal manipulation of retinoic acid activity in zebrafish hindbrain development via photo-isomerization*. Development, 2012. **139**(18): p. 3355-62.

83. Callaway, E.M. and R. Yuste, *Stimulating neurons with light*. Current Opinion in Neurobiology, 2002. **12**(5): p. 587-592.

84. Bartels, E., N.H. Wassermann, and B.F. Erlanger, *Photochromic activators of the acetylcholine receptor*. Proc Natl Acad Sci U S A, 1971. **68**(8): p. 1820-3.

85. Banghart, M.R., M. Volgraf, and D. Trauner, *Engineering light-gated ion channels*. Biochemistry, 2006. **45**(51): p. 15129-41.

86. Gorostiza, P. and E.Y. Isacoff, *Optical switches for remote and noninvasive control of cell signaling*. Science, 2008. **322**(5900): p. 395-9.

87. Kramer, R.H., D.L. Fortin, and D. Trauner, *New photochemical tools for controlling neuronal activity*. Curr Opin Neurobiol, 2009. **19**(5): p. 544-52.

88. Hausser, M., *Optogenetics: the age of light*. Nat Methods, 2014. **11**(10): p. 1012-4.

89. Deisseroth, K., *Optogenetics*. Nat Methods, 2011. **8**(1): p. 26-9.

90. Miesenbock, G., *The Optogenetic Catechism*. Science, 2009. **326**(5951): p. 395-399.

91. Chudakov, D.M., et al., *Fluorescent proteins and their applications in imaging living cells and tissues*. Physiol Rev, 2010. **90**(3): p. 1103-63.

92. Miyawaki, A., et al., *Fluorescent indicators for Ca2+ based on green fluorescent proteins and calmodulin*. Nature, 1997. **388**(6645): p. 882-887.

93. Van, T.N.N. and M.C. Morris, *Fluorescent Sensors of Protein Kinases: From Basics to Biomedical Applications*. Fluorescence-Based Biosensors: From Concepts to Applications, 2013. **113**: p. 217-274.

94. Zhang, F., et al., *The Microbial Opsin Family of Optogenetic Tools*. Cell, 2011. **147**(7): p. 1446-1457.

95. Livet, J., et al., *Transgenic strategies for combinatorial expression of fluorescent proteins in the nervous system*. Nature, 2007. **450**(7166): p. 56-+.

96. Garner, J.N., B. Joshi, and R. Jagus, *Characterization of rainbow trout and zebrafish eukaryotic initiation factor 2 alpha and its response to endoplasmic reticulum stress and IPNV infection*. Developmental and Comparative Immunology, 2003. **27**(3): p. 217-231.

97. Hadjieconomou, D., et al., *Flybow: genetic multicolor cell labeling for neural circuit analysis in Drosophila melanogaster*. Nature Methods, 2011. **8**(3): p. 260-U111.

98. Hampel, S., et al., *Drosophila Brainbow: a recombinase-based fluorescence labeling technique to subdivide neural expression patterns (vol 8, pg 253, 2011)*. Nature Methods, 2015. **12**(9): p. 893-893.

99. Hampel, S., et al., *Drosophila Brainbow: a recombinase-based fluorescence labeling technique to subdivide neural expression patterns*. Nature Methods, 2011. **8**(3): p. 253-U102.

100. Wachsman, G., R. Heidstra, and B. Scheres, *Distinct Cell-Autonomous Functions of RETINOBLASTOMA-RELATED in Arabidopsis Stem Cells Revealed by the Brother of Brainbow Clonal Analysis System*. Plant Cell, 2011. **23**(7): p. 2581-2591.

101. Gupta, V. and K.D. Poss, *Clonally dominant cardiomyocytes direct heart morphogenesis*. Nature, 2012. **484**(7395): p. 479-U102.

102. Hipfner, D.R. and S.M. Cohen, *Connecting proliferation and apoptosis in development and disease*. Nature Reviews Molecular Cell Biology, 2004. **5**(10): p. 805-815.

103. Favaloro, B., et al., *Role of Apoptosis in disease*. Aging-Us, 2012. **4**(5): p. 330-349.

104. Sakaue-Sawano, A., et al., *Visualizing spatiotemporal dynamics of multicellular cell-cycle progression*. Cell, 2008. **132**(3): p. 487-498.

105. Sugiyama, M., et al., *Illuminating cell-cycle progression in the developing zebrafish embryo*. Proceedings of the National Academy of Sciences of the United States of America, 2009. **106**(49): p. 20812-20817.

106. Abe, T., et al., *Visualization of cell cycle in mouse embryos with Fucci2 reporter directed by Rosa26 promoter*. Development, 2013. **140**(1): p. 237-246.

107. Kuranaga, E., *Beyond apoptosis: caspase regulatory mechanisms and functions in vivo*. Genes to Cells, 2012. **17**(2): p. 83-97.

108. Li, F., et al., *Apoptotic Caspases Regulate Induction of iPSCs from Human Fibroblasts*. Cell Stem Cell, 2010. **7**(4): p. 508-520.

109. Ai, H.W., et al., *Fluorescent protein FRET pairs for ratiometric imaging of dual biosensors*. Nature Methods, 2008. **5**(5): p. 401-403.

110. Bardet, P.L., et al., *A fluorescent reporter of caspase activity for live imaging*. Proceedings of the National Academy of Sciences of the United States of America, 2008. **105**(37): p. 13901-13905.

111. Wu, B., et al., *Modern fluorescent proteins and imaging technologies to study gene expression, nuclear localization, and dynamics*. Current Opinion in Cell Biology, 2011. **23**(3): p. 310-317.

112. Ben-Ari, Y., et al., *The life of an mRNA in space and time*. Journal of Cell Science, 2010. **123**(10): p. 1761-1774.

113. Wachter, R.M. and S.J. Remington, *Sensitivity of the yellow variant of green fluorescent protein to halides and nitrate*. Current Biology, 1999. **9**(17): p. R628-R629.

114. Jayaraman, S., et al., *Mechanism and cellular applications of a green fluorescent protein-based halide sensor*. Journal of Biological Chemistry, 2000. **275**(9): p. 6047-6050.

115. Barondeau, D.P., et al., *Structural chemistry of a green fluorescent protein Zn biosensor*. Journal of the American Chemical Society, 2002. **124**(14): p. 3522-3524.

116. Hanson, G.T., et al., *Investigating mitochondrial redox potential with redox-sensitive green fluorescent protein indicators*. Journal of Biological Chemistry, 2004. **279**(13): p. 13044-13053.

117. Dooley, C.T., et al., *Imaging dynamic redox changes in mammalian cells with green fluorescent protein indicators*. Journal of Biological Chemistry, 2004. **279**(21): p. 22284-22293.

118. Palm, G.J., et al., *The structural basis for spectral variations in green fluorescent protein*. Nature Structural Biology, 1997. **4**(5): p. 361-365.

119. Brejc, K., et al., *Structural basis for dual excitation and photoisomerization of the Aequorea victoria green fluorescent protein*. Proceedings of the National Academy of Sciences of the United States of America, 1997. **94**(6): p. 2306-2311.

120. Miesenbock, G., D.A. De Angelis, and J.E. Rothman, *Visualizing secretion and synaptic transmission with pH-sensitive green fluorescent proteins*. Nature, 1998. **394**(6689): p. 192-195.

121. Chudakov, D.M., et al., *Photoswitchable cyan fluorescent protein for protein tracking*. Nature Biotechnology, 2004. **22**(11): p. 1435-1439.

122. Clapham, D.E., *Calcium signaling*. Cell, 2007. **131**(6): p. 1047-1058.

123. Berridge, M.J., *Neuronal calcium signaling*. Neuron, 1998. **21**(1): p. 13-26.

124. Miyawaki, A., *Fluorescence imaging of physiological activity in complex systems using GFP-based probes*. Current Opinion in Neurobiology, 2003. **13**(5): p. 591-596.

125. Nakai, J., M. Ohkura, and K. Imoto, *A high signal-to-noise Ca2+ probe composed of a single green fluorescent protein*. Nature Biotechnology, 2001. **19**(2): p. 137-141.

126. Akerboom, J., et al., *Optimization of a GCaMP Calcium Indicator for Neural Activity Imaging*. Journal of Neuroscience, 2012. **32**(40): p. 13819-13840.

127. Warp, E., et al., *Emergence of Patterned Activity in the Developing Zebrafish Spinal Cord*. Current Biology, 2012. **22**(2): p. 93-102.

128. Reynaud, E.G., et al., *Light sheet-based fluorescence microscopy: more dimensions, more photons, and less photodamage*. Hfsp Journal, 2008. **2**(5): p. 266-275.

129. Ahrens, M.B., et al., *Whole-brain functional imaging at cellular resolution using light-sheet microscopy*. Nature Methods, 2013. **10**(5): p. 413-+.

130. Panier, T., et al., *Fast functional imaging of multiple brain regions in intact zebrafish larvae using Selective Plane Illumination Microscopy*. Frontiers in Neural Circuits, 2013. **7**.

131. Kralj, J.M., et al., *Optical recording of action potentials in mammalian neurons using a microbial rhodopsin*. Nature Methods, 2012. **9**(1): p. 90-U130.

132. Zhu, P.X., et al., *High-resolution optical control of spatiotemporal neuronal activity patterns in zebrafish using a digital micromirror device*. Nature Protocols, 2012. **7**(7): p. 1410-1425.

133. Szobota, S. and E.Y. Isacoff, *Optical Control of Neuronal Activity*. Annual Review of Biophysics, Vol 39, 2010. **39**: p. 329-348.

134. Yamanaka, A., T. Tsunematsu, and M. Tominaga, *Optical Control of Orexin/Hypocretin Neuronal Activity*. Journal of Physiological Sciences, 2009. **59**: p. 521-521.

135. Arenkiel, B.R., et al., *In vivo light-induced activation of neural circuitry in transgenic mice expressing channelrhodopsin-2*. Neuron, 2007. **54**(2): p. 205-218.

136. Fenno, L., O. Yizhar, and K. Deisseroth, *The Development and Application of Optogenetics*. Annual Review of Neuroscience, Vol 34, 2011. **34**: p. 389-412.

137. Tye, K.M. and K. Deisseroth, *Optogenetic investigation of neural circuits underlying brain disease in animal models*. Nature Reviews Neuroscience, 2012. **13**(4): p. 251-266.

138. Abilez, O.J., et al., *Multiscale Computational Models for Optogenetic Control of Cardiac Function*. Biophysical Journal, 2011. **101**(6): p. 1326-1334.

139. Arrenberg, A.B., et al., *Optogenetic Control of Cardiac Function*. Science, 2010. **330**(6006): p. 971-974.

140. Bruegmann, T., et al., *Optogenetic control of heart muscle in vitro and in vivo*. Nature Methods, 2010. **7**(11): p. 897-U45.

141. Stroh, A., et al., *Tracking Stem Cell Differentiation in the Setting of Automated Optogenetic Stimulation*. Stem Cells, 2011. **29**(1): p. 78-88.

142. Oh, E., et al., *Substitution of 5-HT1A Receptor Signaling by a Light-activated G Protein-coupled Receptor*. Journal of Biological Chemistry, 2010. **285**(40): p. 30825-30836.

143. Airan, R.D., et al., *Temporally precise in vivo control of intracellular signalling*. Nature, 2009. **458**(7241): p. 1025-1029.

144. Dequeant, M.L. and O. Pourquie, *Segmental patterning of the vertebrate embryonic axis*. Nat Rev Genet, 2008. **9**(5): p. 370-82.

145. Niederreither, K. and P. Dolle, *Retinoic acid in development: towards an integrated view*. Nat Rev Genet, 2008. **9**(7): p. 541-53.

146. Ross, S.A., et al., *Retinoids in embryonal development*. Physiol Rev, 2000. **80**(3): p. 1021-54.

147. Diez del Corral, R., et al., *Opposing FGF and retinoid pathways control ventral neural pattern, neuronal differentiation, and segmentation during body axis extension*. Neuron, 2003. **40**(1): p. 65-79.

148. Sirbu, I.O. and G. Duester, *Retinoic-acid signalling in node ectoderm and posterior neural plate directs left-right patterning of somitic mesoderm*. Nat Cell Biol, 2006. **8**(3): p. 271-7.

149. Vermot, J., et al., *Retinoic acid controls the bilateral symmetry of somite formation in the mouse embryo*. Science, 2005. **308**(5721): p. 563-6.

150. Vermot, J. and O. Pourquie, *Retinoic acid coordinates somitogenesis and left-right patterning in vertebrate embryos*. Nature, 2005. **435**(7039): p. 215-20.

151. White, R.J., et al., *Complex regulation of cyp26a1 creates a robust retinoic acid gradient in the zebrafish embryo*. PLoS Biol, 2007. **5**(11): p. e304.

152. Grandel, H., et al., *Retinoic acid signalling in the zebrafish embryo is necessary during pre-segmentation stages to pattern the anterior-posterior axis of the CNS and to induce a pectoral fin bud*. Development, 2002. **129**(12): p. 2851-65.

153. Niederreither, K., et al., *Embryonic retinoic acid synthesis is essential for early mouse post-implantation development*. Nature Genetics, 1999. **21**(4): p. 444-448.

154. Blum, N. and G. Begemann, *Retinoic acid signaling controls the formation, proliferation and survival of the blastema during adult zebrafish fin regeneration*. Development, 2012. **139**(1): p. 107-16.

155. Kikuchi, K., et al., *Retinoic Acid Production by Endocardium and Epicardium Is an Injury Response Essential for Zebrafish Heart Regeneration*. Developmental Cell, 2011. **20**(3): p. 397-404.

156. Armstrong, J.L., C.P. Redfern, and G.J. Veal, *13-cis retinoic acid and isomerisation in paediatric oncology--is changing shape the key to success?* Biochem Pharmacol, 2005. **69**(9): p. 1299-306.

157. Elstner, E., et al., *Ligands for peroxisome proliferator-activated receptorgamma and retinoic acid receptor inhibit growth and induce apoptosis of human breast cancer cells in vitro and in BNX mice*. Proc Natl Acad Sci U S A, 1998. **95**(15): p. 8806-11.

158. Costaridis, P., et al., *Endogenous retinoids in the zebrafish embryo and adult*. Dev Dyn, 1996. **205**(1): p. 41-51.

159. Maden, M., et al., *The distribution of endogenous retinoic acid in the chick embryo: implications for developmental mechanisms*. Development, 1998. **125**(21): p. 4133-44.

160. Begemann, G., et al., *Beyond the neckless phenotype: influence of reduced retinoic acid signaling on motor neuron development in the zebrafish hindbrain*. Dev Biol, 2004. **271**(1): p. 119-29.

161. Neveu, P., et al., *A caged retinoic acid for one- and two-photon excitation in zebrafish embryos*. Angew Chem Int Ed Engl, 2008. **47**(20): p. 3744-6.

162. Allenby, G., et al., *Retinoic acid receptors and retinoid X receptors: interactions with endogenous retinoic acids*. Proc Natl Acad Sci U S A, 1993. **90**(1): p. 30-4.

163. Westerfield, M., *The Zebrafish Book: A guide for the laboratory use of zebrafish (Danio rerio)*. 4th ed. 2000, Eugene: University of Oregon Press.

164. Kawakami, K., et al., *A transposon-mediated gene trap approach identifies developmentally regulated genes in zebrafish*. Dev Cell, 2004. **7**(1): p. 133-44.

165. Meng, A., et al., *Promoter analysis in living zebrafish embryos identifies a cis-acting motif required for neuronal expression of GATA-2*. Proc Natl Acad Sci U S A, 1997. **94**(12): p. 6267-72.

166. Prince, V.E., et al., *Zebrafish hox genes: expression in the hindbrain region of wild-type and mutants of the segmentation gene, valentino*. Development, 1998. **125**(3): p. 393-406.

167. Hauptmann, G. and T. Gerster, *Regulatory gene expression patterns reveal transverse and longitudinal subdivisions of the embryonic zebrafish forebrain*. Mech Dev, 2000. **91**(1-2): p. 105-18.

168. Oxtoby, E. and T. Jowett, *Cloning of the zebrafish krox-20 gene (krx-20) and its expression during hindbrain development*. Nucleic Acids Res, 1993. **21**(5): p. 1087-95.

169. Sun, Z. and N. Hopkins, *vhnf1, the MODY5 and familial GCKD-associated gene, regulates regional specification of the zebrafish gut, pronephros, and hindbrain*. Genes Dev, 2001. **15**(23): p. 3217-29.

170. Herbomel, P., B. Thisse, and C. Thisse, *Ontogeny and behaviour of early macrophages in the zebrafish embryo*. Development, 1999. **126**(17): p. 3735-45.

171. Herrgen, L., et al., *Multiple embryo time-lapse imaging of zebrafish development*. Methods Mol Biol, 2009. **546**: p. 243-54.

172. Bempong, D.K., I.L. Honigberg, and N.M. Meltzer, *Separation of 13-cis and all-trans retinoic acid and their photodegradation products using capillary zone electrophoresis and micellar electrokinetic chromatography (MEC)*. J Pharm Biomed Anal, 1993. **11**(9): p. 829-33.

173. Carmichael, C., M. Westerfield, and Z.M. Varga, *Cryopreservation and in vitro fertilization at the zebrafish international resource center*. Methods Mol Biol, 2009. **546**: p. 45-65.

174. Maves, L. and C.B. Kimmel, *Dynamic and sequential patterning of the zebrafish posterior hindbrain by retinoic acid*. Dev Biol, 2005. **285**(2): p. 593-605.

175. Stafford, D. and V.E. Prince, *Retinoic acid signaling is required for a critical early step in zebrafish pancreatic development*. Curr Biol, 2002. **12**(14): p. 1215-20.

176. Sharma, M.K., et al., *A cellular retinoic acid-binding protein from zebrafish (Danio rerio): cDNA sequence, phylogenetic analysis, mRNA expression, and gene linkage mapping*. Gene, 2003. **311**: p. 119-128.

177. Sharma, M.K., et al., *Differential expression of the duplicated cellular retinoic acid-binding protein 2 genes (crabp2a and crabp2b) during zebrafish embryonic development*. Gene Expression Patterns, 2005. **5**(3): p. 371-379.

178. Kohei, H., T. Hitomi, and O. Tomomi, *Cell tracking using a photoconvertible fluorescent protein*. Nature Protocols, 2006. **1**: p. 960-967.

179. Dong, D., et al., *Distinct roles for cellular retinoic acid-binding proteins I and II in regulating signaling by retinoic acid*. J Biol Chem, 1999. **274**(34): p. 23695-8.

180. Bernstein, P.S., et al., *Photoaffinity labeling of retinoic acid-binding proteins*. Proc Natl Acad Sci U S A, 1995. **92**(3): p. 654-8.

181. Ong, D.E., et al., *Epididymal retinoic acid-binding protein*. Biochim Biophys Acta, 2000. **1482**(1-2): p. 209-17.

182. Goldbeter, A., D. Gonze, and O. Pourquie, *Sharp developmental thresholds defined through bistability by antagonistic gradients of retinoic acid and FGF signaling*. Dev Dyn, 2007. **236**(6): p. 1495-508.

183. Cairns, J., *Mutation selection and the natural history of cancer*. Nature, 1975. **255**(5505): p. 197-200.

184. Crespi, B. and K. Summers, *Evolutionary biology of cancer*. Trends Ecol Evol, 2005. **20**(10): p. 545-52.

185. Pleasance, E.D., et al., *A comprehensive catalogue of somatic mutations from a human cancer genome*. Nature, 2010. **463**(7278): p. 191-6.

186. Stratton, M.R., P.J. Campbell, and P.A. Futreal, *The cancer genome*. Nature, 2009. **458**(7239): p. 719-24.

187. Kanwal, R. and S. Gupta, *Epigenetic modifications in cancer*. Clin Genet, 2012. **81**(4): p. 303-11.

188. DeGregori, J., *Evolved tumor suppression: why are we so good at not getting cancer?* Cancer Res, 2011. **71**(11): p. 3739-44.

189. Greaves, M. and C.C. Maley, *Clonal evolution in cancer*. Nature, 2012. **481**(7381): p. 306-13.

190. Ma, Q.C., C.A. Ennis, and S. Aparicio, *Opening Pandora's Box--the new biology of driver mutations and clonal evolution in cancer as revealed by next generation sequencing*. Curr Opin Genet Dev, 2012. **22**(1): p. 3-9.

191. Tomasetti, C. and B. Vogelstein, *Cancer etiology. Variation in cancer risk among tissues can be explained by the number of stem cell divisions*. Science, 2015. **347**(6217): p. 78-81.

192. Stratton, M.R., *Exploring the genomes of cancer cells: progress and promise*. Science, 2011. **331**(6024): p. 1553-8.

193. Gonzalez, C., *Drosophila melanogaster: a model and a tool to investigate malignancy and identify new therapeutics*. Nat Rev Cancer, 2013. **13**(3): p. 172-83.

194. White, R., K. Rose, and L. Zon, *Zebrafish cancer: the state of the art and the path forward*. Nature Reviews Cancer, 2013. **13**(9): p. 624-636.

195. Potts, M.B. and S. Cameron, *Cell lineage and cell death: Caenorhabditis elegans and cancer research*. Nat Rev Cancer, 2011. **11**(1): p. 50-8.

196. Heyer, J., et al., *Non-germline genetically engineered mouse models for translational cancer research*. Nat Rev Cancer, 2010. **10**(7): p. 470-80.

197. Coffey, D.S., *Understanding the cancer biology universe: enigmas, context and future prospects*. Cancer Biol Ther, 2002. **1**(5): p. 564-7.

198. Casas-Selves, M. and J. Degregori, *How cancer shapes evolution, and how evolution shapes cancer*. Evolution (N Y), 2011. **4**(4): p. 624-634.

199. Feng, Y., et al., *Live imaging of innate immune cell sensing of transformed cells in zebrafish larvae: parallels between tumor initiation and wound inflammation*. PLoS Biol, 2010. **8**(12): p. e1000562.

200. Kajita, M., et al., *Filamin acts as a key regulator in epithelial defence against transformed cells*. Nature Communications, 2014. **5**.

201. Feil, R., et al., *Ligand-activated site-specific recombination in mice*. Proc Natl Acad Sci U S A, 1996. **93**(20): p. 10887-90.

202. Brocard, J., et al., *Spatio-temporally controlled site-specific somatic mutagenesis in the mouse*. Proc Natl Acad Sci U S A, 1997. **94**(26): p. 14559-63.

203. Langenau, D.M., et al., *Myc-induced T cell leukemia in transgenic zebrafish*. Science, 2003. **299**(5608): p. 887-90.

204. Berghmans, S., et al., *tp53 mutant zebrafish develop malignant peripheral nerve sheath tumors*. Proc Natl Acad Sci U S A, 2005. **102**(2): p. 407-12.

205. Nguyen, A.T., et al., *An inducible kras(V12) transgenic zebrafish model for liver tumorigenesis and chemical drug screening*. Dis Model Mech, 2012. **5**(1): p. 63-72.

206. Weger, B.D., et al., *A chemical screening procedure for glucocorticoid signaling with a zebrafish larva luciferase reporter system*. J Vis Exp, 2013(79).

207. Le, X., et al., *A novel chemical screening strategy in zebrafish identifies common pathways in embryogenesis and rhabdomyosarcoma development*. Development, 2013. **140**(11): p. 2354-64.

208. Howe, K., et al., *The zebrafish reference genome sequence and its relationship to the human genome*. Nature, 2013. **496**(7446): p. 498-503.

209. de Grouchy, J., *Cancer and the evolution of species: a ransom*. Biomedicine, 1973. **18**(1): p. 6-8.

210. Armitage, P. and R. Doll, *The age distribution of cancer and a multi-stage theory of carcinogenesis*. Br J Cancer, 1954. **8**(1): p. 1-12.

211. Rozhok, A.I. and J. DeGregori, *Toward an evolutionary model of cancer: Considering the mechanisms that govern the fate of somatic mutations*. Proc Natl Acad Sci U S A, 2015. **112**(29): p. 8914-21.

212. Mosimann, C., et al., *Ubiquitous transgene expression and Cre-based recombination driven by the ubiquitin promoter in zebrafish*. Development, 2011. **138**(1): p. 169-77.

213. Peterson, S.M. and J.L. Freeman, *RNA isolation from embryonic zebrafish and cDNA synthesis for gene expression analysis*. J Vis Exp, 2009(30).

214. Kawakami, K., *Tol2: a versatile gene transfer vector in vertebrates*. Genome Biol, 2007. **8 Suppl 1**: p. S7.

215. Rosen, J.N., M.F. Sweeney, and J.D. Mably, *Microinjection of zebrafish embryos to analyze gene function*. J Vis Exp, 2009(25).

216. Moore, J.L., et al., *Fixation and decalcification of adult zebrafish for histological, immunocytochemical, and genotypic analysis*. Biotechniques, 2002. **32**(2): p. 296-8.

217. McKinney, S.A., et al., *A bright and photostable photoconvertible fluorescent protein*. Nature Methods, 2009. **6**(2): p. 131-133.

218. Reinert, R.B., et al., *Tamoxifen-Induced Cre-loxP Recombination Is Prolonged in Pancreatic Islets of Adult Mice*. Plos One, 2012. **7**(3).

219. Kyrkanides, S., et al., *Transcriptional and posttranslational regulation of Cre recombinase by RU486 as the basis for an enhanced inducible expression system*. Molecular Therapy, 2003. **8**(5): p. 790-795.

220. Okuyama, T., et al., *Controlled Cre/loxP Site-Specific Recombination in the Developing Brain in Medaka Fish, Oryzias latipes*. Plos One, 2013. **8**(6).

221. Ignatius, M.S. and D.M. Langenau, *Fluorescent Imaging of Cancer in Zebrafish*. Zebrafish: Disease Models and Chemical Screens, 3rd Edition, 2011. **105**: p. 437-459.

222. Tobia, C., et al., *Zebrafish embryo as a tool to study tumor/endothelial cell cross-talk*. Biochimica Et Biophysica Acta-Molecular Basis of Disease, 2013. **1832**(9): p. 1371-1377.

223. Shive, H.R., *Zebrafish Models for Human Cancer*. Veterinary Pathology, 2013. **50**(3): p. 468-482.

224. Liu, S. and S.D. Leach, *Zebrafish Models for Cancer*. Annual Review of Pathology: Mechanisms of Disease, Vol 6, 2011. **6**: p. 71-93.

225. Brentnall, T.A., et al., *Mutations in the P53 Gene - an Early Marker of Neoplastic Progression in Ulcerative-Colitis*. Gastroenterology, 1994. **107**(2): p. 369-378.

226. Maley, C.C., et al., *The combination of genetic instability and clonal expansion predicts progression to esophageal adenocarcinoma*. Cancer Research, 2004. **64**(20): p. 7629-7633.

227. Beerenwinkel, N., et al., *Genetic progression and the waiting time to cancer*. Plos Computational Biology, 2007. **3**(11): p. 2239-2246.

228. Heppner, G.H. and F.R. Miller, *The cellular basis of tumor progression*. International Review of Cytology - a Survey of Cell Biology, Vol 177, 1998. **177**: p. 1-56.

229. Wang, E., et al., *Cancer systems biology in the genome sequencing era: Part 2, evolutionary dynamics of tumor clonal networks and drug resistance*. Seminars in Cancer Biology, 2013. **23**(4): p. 286-292.

230. Crespi, B. and K. Summers, *Evolutionary biology of cancer*. Trends in Ecology & Evolution, 2005. **20**(10): p. 545-552.

231. Nagy, J.D., *The ecology and evolutionary biology of cancer: A review of mathematical models of necrosis and tumor cell diversity*. Mathematical Biosciences and Engineering, 2005. **2**(2): p. 381-418.

232. Michor, F., Y. Iwasa, and M.A. Nowak, *Dynamics of cancer progression*. Nature Reviews Cancer, 2004. **4**(3): p. 197-205.

233. DeGregori, J., *Evolved Tumor Suppression: Why Are We So Good at Not Getting Cancer?* Cancer Research, 2011. **71**(11): p. 3739-3744.

234. Maley, C.C. and B.J. Reid, *Natural selection in neoplastic progression of Barrett's esophagus*. Seminars in Cancer Biology, 2005. **15**(6): p. 474-483.

235. Tomasetti, C., et al., *Only three driver gene mutations are required for the development of lung and colorectal cancers*. Proceedings of the National Academy of Sciences of the United States of America, 2015. **112**(1): p. 118-123.

236. Hornsby, C., K.M. Page, and I.P. Tomlinson, *What can we learn from the population incidence of cancer? Armitage and Doll revisited*. Lancet Oncol, 2007. **8**(11): p. 1030-8.

237. Vinall, R.L., et al., *Initiation of prostate cancer in mice by Tp53(R270H): evidence for an alternative molecular progression*. Disease Models & Mechanisms, 2012. **5**(6): p. 914-920.

238. Knudsen, B.S. and V. Vasioukhin, *Mechanisms of Prostate Cancer Initiation and Progression*. Advances in Cancer Research, Vol 109, 2010. **109**: p. 1-50.

239. Grizzi, F., et al., *Cancer initiation and progression: an unsimplifiable complexity*. Theoretical Biology and Medical Modelling, 2006. **3**.

240. Whitehead, R.H., J. Weinstock, and J.L. Joseph, *The Development of Models of Cancer Initiation and Progression Using Conditionally Immortalized Colonic Mucosal Cells*. Gastroenterology, 1995. **108**(4): p. A552-A552.

241. Heim, S., B. Johansson, and F. Mertens, *Genetic Mechanisms in Tumor Initiation and Progression .12. Constitutional Chromosome Instability and Cancer Risk*. Mutation Research, 1989. **221**(1): p. 39-51.

242. Nguyen, D.X., P.D. Bos, and J. Massague, *Metastasis: from dissemination to organ-specific colonization*. Nat Rev Cancer, 2009. **9**(4): p. 274-84.

243. Bertram, J.S., *The molecular biology of cancer*. Mol Aspects Med, 2000. **21**(6): p. 167-223.

244. Polyak, K., I. Haviv, and I.G. Campbell, *Co-evolution of tumor cells and their microenvironment*. Trends in Genetics, 2009. **25**(1): p. 30-38.

245. Hu, M. and K. Polyak, *Microenvironmental regulation of cancer development*. Current Opinion in Genetics & Development, 2008. **18**(1): p. 27-34.

246. Quail, D.F. and J.A. Joyce, *Microenvironmental regulation of tumor progression and metastasis*. Nature Medicine, 2013. **19**(11): p. 1423-1437.

247. Waclaw, B., et al., *A spatial model predicts that dispersal and cell turnover limit intratumour heterogeneity*. Nature, 2015. **525**(7568): p. 261-+.

248. Aravanis, A.M., et al., *An optical neural interface: in vivo control of rodent motor cortex with integrated fiberoptic and optogenetic technology*. Journal of Neural Engineering, 2007. **4**(3): p. S143-S156.

249. Kravitz, A.V. and A.C. Kreitzer, *Optogenetic manipulation of neural circuitry in vivo*. Current Opinion in Neurobiology, 2011. **21**(3): p. 433-439.

250. Gautier, A., et al., *How to control proteins with light in living systems*. Nature Chemical Biology, 2014. **10**(7): p. 533-541.

251. Shimozono, S., et al., *Visualization of an endogenous retinoic acid gradient across embryonic development*. Nature, 2013. **496**(7445): p. 363-+.

252. Bernstein, P.S., et al., *Photoaffinity-Labeling of Retinoic Acid-Binding Proteins*. Proceedings of the National Academy of Sciences of the United States of America, 1995. **92**(3): p. 654-658.

253. Sandell, J., *Carbon-14 radiosynthesis of the benzofuran derivative and beta-amyloid plaque neuroimaging positron emission tomography radioligand AZD4694*. Journal of Labelled Compounds & Radiopharmaceuticals, 2013. **56**(6): p. 321-324.

254. Zhang, L., et al., *Noise drives sharpening of gene expression boundaries in the zebrafish hindbrain*. Molecular Systems Biology, 2012. **8**.

255. Huang, W.C., et al., *Treatment of Glucocorticoids Inhibited Early Immune Responses and Impaired Cardiac Repair in Adult Zebrafish*. PLoS One, 2013. **8**(6): p. e66613.

256. Abegglen, L.M., et al., *Potential Mechanisms for Cancer Resistance in Elephants and Comparative Cellular Response to DNA Damage in Humans*. JAMA, 2015. **314**(17): p. 1850-60.